ABSTRACT

The United States Environmental Protection Agency is currently in the process of adding or lowering the maximum contaminant levels of many organic compounds, including trihalomethanes (THMs). As a result, many water treatment facilities are expected to consider the use of processes such as ozone oxidation and granular activated carbon (GAC) adsorption. Since these processes are quite expensive, accurate design of these systems for the removal of humic substances, the precursors of THMs, is essential.

This work examined the effects of bench scale coagulation, ozonation, and biodegradation processes on the adsorption of aquatic humic substances obtained from a swamp lake in southeastern Virginia. The equilibrium adsorption behavior was described by dividing each humic mixture into several fictive components and ideal adsorbed solution theory (IAST) was then used to find the Freundlich parameters and initial concentration of each component. IAST was found to provide adequate descriptions of humic substance adsorption, even though many assumptions in the model were not considered to be valid for humic solutions. This multicomponent adsorption model was used to show that compositional changes were responsible for increased adsorbability upon coagulation and for decreased

i

adsorbability upon ozonation and biostabilization. Unfortunately, systematic changes in the IAST parameters were not found to occur with increasing ozone dose, thereby implying that accurate prediction and design of combined ozone and GAC systems may be difficult. However, a normalized adsorption isotherm showed some promise in this regard although the technique may not be applicable to kinetic systems.

External mass transfer characteristics of humic solutions were examined with a mini-column adsorber. The free liquid diffusion coefficient was found to increase upon coagulation while no significant changes were observed after ozonation and biostabilization. Internal mass transfer characteristics were examined with a pore and surface diffusion model. The overall mass transfer rate was found to increase after coagulation and after ozonation and biostabilization. However, tests with three different ozone doses showed no change in mass transfer rates with ozone dose. In addition, the techniques used in this work were not found to be capable of describing the mechanism of humic substance diffusion.

ACKNOWLEDGMENTS

As with any report of this type, the work and ideas presented here represent the combined effort and help from many others who certainly deserve plenty of credit. Firstly, I would like to extend my appreciation to my advisor, Dr. Fran DiGiano, for his guidance in helping me understanding much of the theory and significance of the results presented here. In addition, a tremendous amount of help was provided by Joachim Fettig, who showed me how to set up all of the laboratory experiments, how to use all of the computer models, and how to interpret and understand the results. The guidance of these two shows throughout this work and, without them, a work of this nature would not have been produced.

I also received helpful comments from several others during the course of this project. Many suggestions were recently provided by the remaining members of my committee, Drs. Phil Singer and Casey Miller, whom I would like to thank for the time they put into reading the previous draft of this report and for providing their input. Significant amounts of insight were provided by Joe Pedit, especially in regard to the computational methods used by the adsorption models. Additional thanks are extended to Emery Kong for his help in setting up many of the experiments performed in

It is my hope that work such as this will not only help eliminate the THM problem but will also help in the continued effort to eliminate all causes of cancer. For this reason, I have dedicated this work to the memory of my grandmother, Dorothy Scott, and Georgiana's mother, Verna Marie Ference, both of whom succumbed to this awful disease at an early age.

TABLE OF CONTENTS

CHAPTER 1

INTRODUCTION

Research in the area of humic substances has steadily increased since their implication in the formation of trihalomethanes (THMs) during chlorination in drinking water treatment (Rook, 1974). After a subsequent investigation found THMs to be prevalent in treated waters on a nationwide basis (Symons, et al., 1975), the United States Congress enacted legislation that amended the Safe Drinking Water Act to include a maximum contaminant level (MCL) for THMs at 0.10 mg/l (Code of Federal Regulations, 1986a). Presently, the United States Environmental Protection Agency (EPA) is reviewing the addition of many organic contaminants to the regulatory listing and plans to consider lowering the THM standard in 1990 (Cook and Schnare, 1986).

These current and proposed regulations require the removal of THMs and THM precursors in order to reduce human health risks. Granular activated carbon (GAC) adsorbers are considered to be very effective in removing many synthetic organic chemicals and, as noted in the Code of Federal Regulations (1986b), are suitable for the removal of THM precursors. Therefore, the addition of MCLs to regulate more organic contaminants and the potential lowering of the THM standard implies an increased demand for the use of GAC

1

adsorbers. The lower THM standard will also result in increased demand for alternatives to chlorine oxidation, such as ozone, and for the improvement of the coagulation process to better remove the humic precursors of THMs. The understanding of how the coagulation and ozonation processes affect the adsorption of humic substances is required since these processes typically precede GAC adsorbers in water treatment systems. In addition, the large cost of processes such as ozonation and GAC adsorption requires the ability to optimally design the combination of processes such as ozonation and GAC adsorption for humic substance removal.

OBJECTIVES

This research was aimed at examining the effects of alum coagulation and the subsequent treatments of ozonation and biodegradation on the adsorption behavior of aquatic humic materials. In addition, current modeling methods were tested to determine their applicability to humic substance adsorption in bench scale systems and to search for a quantitative relationship between the amount of ozone applied and humic substance adsorbability.

CHAPTER 2

BACKGROUND

HUMIC SUBSTANCES

Humic substances are widely prevalent in natural aquatic systems and may represent up to 80% of the dissolved organic materials present in lake waters. These materials primarily represent biodegradation products of dead plant matter such as leaves, and bark leachates such as lignins. These products are generally formed in soils and subsequently reach aquatic systems by runoff or groundwater movement. In their review of humic substances in lake waters, Steinberg and Muenster (1985) also add that aquatic humic substances are formed by the degradation of dead algal and bacterial matter and, as a result, are more aliphatic in nature than soil humic materials.

Although little is known about the structure of humic materials, significant progress has been made in understanding the role of humic substances in the aquatic environment. Prakash and MacGregor (1983) note that humic materials play a significant role in global carbon cycles and are considered to benefit aquatic biological systems by stimulating processes associated with cellular metabolism. In addition, dissolved humics are known to bind with heavy

metals and pesticides (Carter and Suffet, 1982), thereby reducing short term toxicity.

Progress has also been made in understanding the molecular nature of humic materials. A review of several lake waters by Steinberg and Muenster (1985) reveals that aquatic humic substances have elemental compositions (by weight) in the range of 43-55% carbon, 35-50% oxygen, 3-6% hydrogen, and small amounts of nitrogen, phosphorous, sulfur, chlorine, and ash components. Oxidation studies have further indicated the presence of highly substituted aromatic rings interconnected by short aliphatic chains and have also indicated the presence of fused aromatic and other cyclic components (Liao, et al., 1982). Potentiometric titrations by Narkis and Rebhun (1977) with two commercial humic acids and a peat fulvic acid indicated the presence of carboxylic and phenolic functional groups. Several authors have proposed humic structures (Christman and Ghassemi, 1966; Dragunov, 1961) even though they exist in a multitude of different species within any given system. Thus, the best representation (shown in Figure 2-1) appears to be the one presented by Trussell and Umphres (1978) where humic substances are represented as an "amorphous mass of polyhetero condensate with certain functional groups protruding from its surface."

The physical nature of humic molecules is also becoming better understood. Molecular weight distributions obtained from ultrafiltration and gel permeation chromatography (GPC)

4
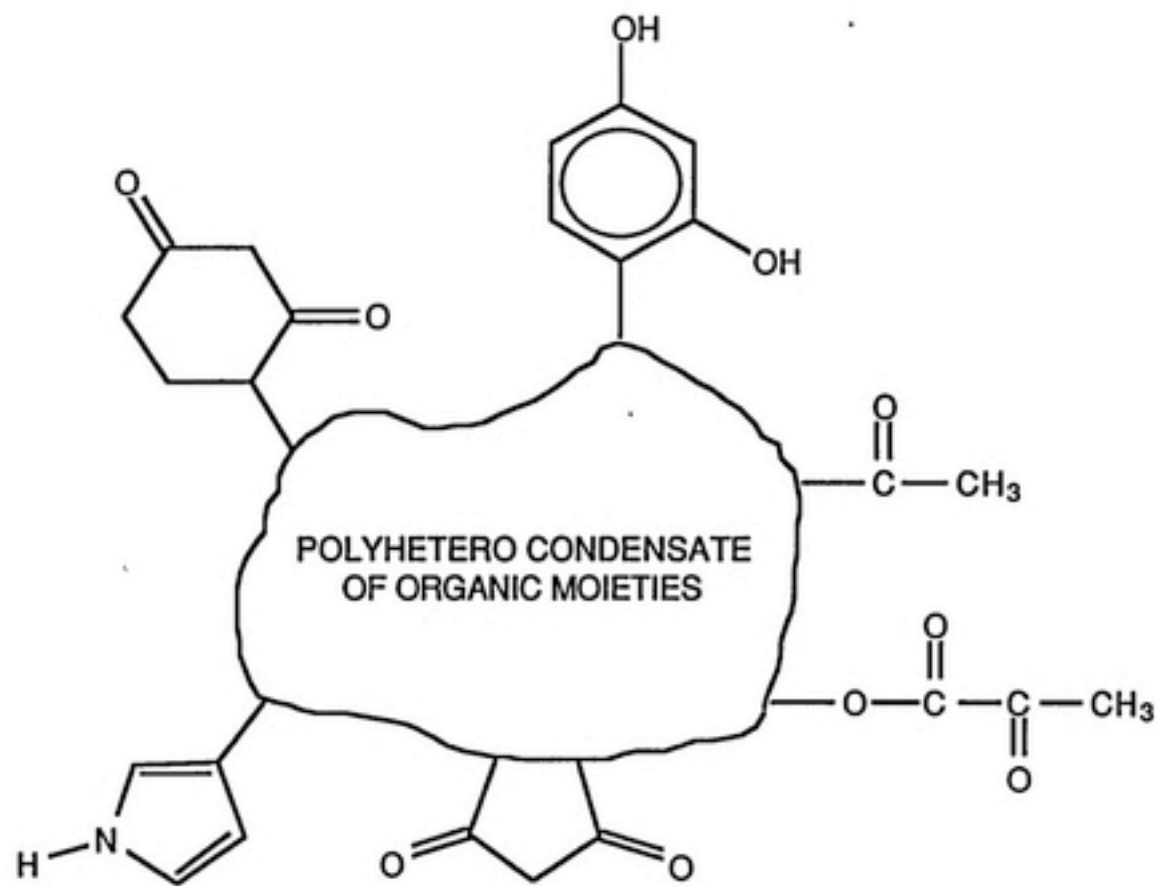
FIGURE 2-1: A MODEL HUMIC COMPOUND (AFTER TRUSSELL AND UMPHRES, 1978)

reveal a wide range of molecular sizes from molecular weights < 1000 to > 50,000 (Lienhard and Sontheimer, 1979; Summers, 1986; Anderson, et al., 1986; Flögstad and Ödegaard, 1985). In addition, Ghosh and Schnitzer (1980) modeled soil humic molecules in a manner similar to the way that polymers are modeled. Therefore, a solution of humic substances should be considered as a mixture of weak polyelectrolytes covering a wide range of molecular sizes.

HUMIC SUBSTANCES AND HUMAN HEALTH

Humic substances have received a great deal of attention since Rook (1974) first linked them with the formation of chloroform and other trihalomethanes (THMs) upon chlorination at the water treatment plant in Rotterdam, the Netherlands. Several studies subsequently found THMs in finished waters throughout the state of North Carolina (Singer, et al., 1981) and throughout the United States (Symons, et al., 1975). Shortly after Rook's discovery, several researchers found chloroform to be carcinogenic to mice and rats, the results of which suggested that a maximum of 252 out of 300,000 annual cancer deaths could be attributed to the drinking of chlorinated waters (Tardiff, 1977). In addition, epidemiological studies by Cragle, et al. (1985), and by Cantor, et al. (1985), found statistically significant relationships between the drinking of chlorinated waters and cancer of the colon and bladder,

respectively, for several age groups and several areas of the country.

Other health concerns noted for humic materials are the formation of chlorination byproducts other than the THMs (Norwood, et al., 1981; Johnson and Randtke, 1983) and the ability of humic substances to complex with metals and pesticides (as reviewed by Prakash and MacGregor, 1983). The health implications of these matters are largely unknown, a troubling problem since Fleischacker and Randtke (1983) pointed out that THMs represent a small fraction of the chlorinated byproducts in drinking waters.

The information provided about THMs in the mid 1970's quickly received strong legislative attention. The Safe Drinking Water Act (SDWA), originally passed in 1974, was amended to include a maximum contaminant level (MCL) of 0.10 mg/l for total THMs (Code of Federal Regulations, 1986a). Currently, the United States Environmental Protection Agency (USEPA) is in the process of phasing in new MCLs for many organic contaminants and plans to revise the THM standard to a lower level in 1990 (Cook and Schnare, 1986).

The Code of Federal Regulations (1986b) also lists a set of "generally available methods" that may be used to meet the THM standard. Water suppliers are further required to use higher cost approaches if the generally available methods are found to be unsuccessful. Among the methods listed for handling the THM problem are the uses of

7

coagulation prior to chlorination, ozonation, and activated
carbon adsorption to remove THM precursors. As a result of
the expected lowering of the THM standard, many facilities
are expected to make use of these options.

ACTIVATED CARBON ADSORPTION OF HUMIC SUBSTANCES

Activated Carbon

The understanding of humic substance adsorption onto
activated carbon requires the knowledge of both adsorbent
and adsorbate properties. For this research, the adsorbates
were aquatic humic materials, the properties of which were
discussed above, while the adsorbent was activated carbon,
the characteristics of which will be described from reviews
provided by Smisek and Cerny (1970) and by Mattson and Mark
(1971).

Activated carbons are produced from sources such as
coke, carbonized shells, and crushed charcoal by subjecting
them to an activating gas such as steam. The resulting
material is generally considered to be comprised of
microcrystallites of trigonally bonded carbon in
turbostratic layers. The turbostratic structure is subtly
different from the lattice structure of graphite in that the
layers are not linked together.

The microcrystallites are interconnected by
tetragonally bonded carbon crosslinks and are randomly

oriented within a given particle, thereby creating the openings known as pores. The porous nature of a given carbon is determined by the source material and the activation process. All activated carbons contain a wide variety of pore diameters which, as noted by Summers (1986), have been categorized into three size ranges known as micropores (r_p < 1 nm), mesopores (1 nm < r_p < 25 nm), and macropores (r_p > 25 nm). The distributions of pore volume and surface area with respect to these pore sizes are important characteristics of an activated carbon. The micropores typically contain a range of 50 - 80 % of the total surface area of a carbon particle while as much as 98% of the total surface area can be found in pores with r_p < 10 nm.

The microcrystallites are also subject to forming surface functional groups as a result of reactions with the activating gas. The nature of the groupings depends on both the activating gas and the activation process itself. For instance, activation at high temperatures with carbon dioxide (CO_2) yields basic surface oxides while activation at low temperatures with oxygen (O_2) produces acidic surface oxides.

Therefore, when considering the adsorption of humic materials, one must consider the physical and chemical interactions between the activated carbon and the adsorbing molecules. The pore structure of an activated carbon can effectively exclude large molecules from adsorbing ·at

interior adsorption sites while interactions between humic functional groups and surface functional groups can also hinder or favor the adsorption process. These physical and chemical interactions are notably apparent in the literature of humic substance adsorption.

Adsorption of Humic Substances

Humic substance adsorption has been shown to be strongly influenced by the distribution of carbon pore sizes. In experiments with nine different activated carbons, Lee, et al. (1981), showed that those carbons having the largest pore sizes adsorbed the most humic material. Weber, et al. (1983), made the same observation with three different carbons. These results were taken as evidence that humic substances may be physically excluded from many adsorption sites by pore constrictions smaller than many humic molecules.

Further evidence of this nature of humic substance adsorption was also provided by Lee, et al. (1981), when they separated a humic solution into various molecular weight fractions and found better adsorbability for smaller molecules than for larger molecules. In addition, their work showed a strong correlation between the adsorption capacity of the < 1000 MW fraction and the volume in pores with radii < 70 Å while the adsorption capacity of the > 50,000 MW fraction correlated well with the volume in

pores with radii < 400 Å. Preferential adsorption of lower MW fractions has also been observed by McCreary and Snoeyink (1980) and Summers (1986).

Interestingly, polymer scientists have found adsorption capacities to increase with molecular size (Fleer and Lyklema, 1983) although these results were observed with nonporous adsorbents. Similarly, adsorption capacities for humic materials were observed to increase with molecular weight for adsorption on kaolin clay (Manos and Tsai, 1980) as well as on a synthetic resin (Mantoura and Riley, 1975). Summers (1986) hypothesized that the adsorption of humics, being similar to the adsorption of polymers, should also indicate increased capacities for larger molecules on activated carbon when pore size limitations are accounted for. By combining estimated humic molecule radii from the work of Cornel, et al. (1986b), with pore surface area distributions from his own work, Summers was able to present isotherms showing little effect of molecular size on humic adsorbability. Thus, the molecular size dependence of adsorption observed with the activated carbon work noted earlier was shown to be due to the exclusion effect.

Ionic strength and pH conditions have been observed to have a profound influence on humic substance adsorption (Weber, et al., 1983; McCreary and Snoeyink, 1980). Changes in these conditions can alter adsorbability by altering charge densities on the GAC surface and around humic functional groups. In the most complete study to date on

11
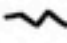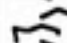
the subject, Randtke and Jepsen (1982) observed significantly increased adsorbability with the addition of monovalent cations (K^+, Na^+) and an even more pronounced increase in adsorbability with the addition of divalent cations (Ca^{2+}, Mg^{2+}). The study also found increased adsorption capacities with decreasing pH and found anion concentrations to have no effect on adsorption capacities.

These results were attributed to three possible mechanisms: (1) cation-adsorbate interactions in solution (such as the shielding and neutralization of humic functional groups); (2) cation-adsorbate interactions in the adsorbed phase (similar to those of the solution phase although a negative surface charge would create a greater concentration of cations in the adsorbed phase thereby enhancing the effects); and (3) interactions between cations and the surface that could reduce electrostatic repulsions between the surface and humic molecule or form surface-cation-adsorbate complexes.

However, Summers (1986) found that the GAC used in the above study was positively charged at pH values below 10.0 and observed the same effects. Therefore, any adsorption mechanism depending on attraction between cations and a negatively charged surface must be ruled out. As a result of his findings, Summers concluded that the enhanced adsorption caused by cations must be due to cation-adsorbate interactions in the solution phase.

The enhanced adsorbability caused by cations may be explained by considering that humic molecules behave similarly to polymeric molecules. Polymer science indicates that the most thermodynamically stable form of an uncharged macromolecule is that of the random coil (Atkins, 1982). When the macromolecule contains negatively charged substituents, as humic molecules do, electrostatic repulsions force the configuration to become more linear. When the concentration of cations such as sodium is increased, electrostatic repulsions are reduced due to the accumulation of cations around the negatively charged functional groups. Therefore, the macromolecule is allowed to adjust to a more coiled and compact nature that allows increased penetration into the microporous structure of the activated carbon.

Observations of this phenomenon were made by Ghosh and Schnitzer (1980) who used surface pressure and viscosity measurements to imply decreased molecular size with increased ionic strength and decreasing pH. Figure 2-2 shows their proposed configurations and shows that the configuration of humic molecules is more linear under natural conditions. Similar observations were made by Cornel, et al. (1986b), when studying the effects of ionic strength and pH on the film diffusivities of humic substances. As expected, their results show increased diffusion rates with increased ionic strength and decreased

FULVIC ACID										
	ELECTROLYTE CONC'N (M)					pH				
	0.001	0.005	0.010	0.050	0.100	2.0	3.5	6.5		9.5
LOW CONC'N										
HIGH CONC'N										
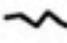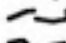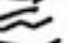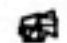
HUMIC ACID									
	ELECTROLYTE CONC'N (M)					pH			
	0.001	0.005	0.010	0.050	0.100			6.5	8.0	9.5
LOW CONC'N									
HIGH CONC'N									

FIGURE 2-2: EFFECT OF IONIC STRENGTH AND pH ON HUMIC STRUCTURE
(AFTER GHOSH AND SCHNITZER, 1980)

pH. These considerations show, once again, the importance of pore size in relation to molecular size.

Effects of Coagulation on Humic Substance Adsorption

Several studies have been performed to understand the effect of alum coagulation on humics adsorption. Semmens, et al. (1986), found improved GAC filter performance with coagulation and attributed this result to lower influent concentrations and the removal of larger organics during coagulation. In addition, coagulation was found to increase adsorption capacity in isotherm studies by Randtke and Jepsen (1981) and Lee, et al. (1981). However, Jodellah (1985) found inconsistent results with various humic solutions and concluded that the effect of alum coagulation on humic adsorption was system specific.

Several reasons may be considered for the general improvement in adsorbability observed with coagulation. Randtke and Jepsen (1981) proposed that better adsorbing aluminum-humic complexes were responsible. However, Lee, et al. (1981), and Weber, et al. (1983), observed decreased adsorbability when alum was added to an aluminum concentration similar to that remaining after coagulation. The results obtained by Jodellah (1985) showed that alteration of the molecular size distribution by alum coagulation, not the simple addition of aluminum ions, was the most likely explanation for the observed results. Alum

concentrations that caused complete destabilization and
sedimentation revealed a compositional change towards
domination by smaller molecules. However, in cases where
complete destabilization did not take place, the
distribution of sizes was dominated by larger molecules
formed by aggregation. Therefore, as long as alum
coagulation causes complete destabilization, improvement
should be observed for humic substance adsorption.

Effects of Ozonation on Humic Substance Adsorption

Ozonation followed by activated carbon has received a
considerable amount of attention because of the ability of
ozone to break down organics into readily biodegradable
substances and because of the ability of activated carbon
filters to support biological growth. Thus, the activated
carbon process becomes capable of removing organics by
adsorption or by biodegradation, thereby increasing the
length of time that a carbon filter can be run until all of
the adsorption sites are exhausted.

Humic substance removals with ozone and GAC has
produced mixed results. Zabel (1985), in reviewing British
treatment plants, determined that ozonation provided little
benefit for the GAC process, even after conventional
treatment. Glaze, et al. (1981), found that GAC columns
receiving waters pretreated with ozone were outperformed by
GAC columns receiving non-ozonated waters in terms of

removing THM precursor material. This group also found that the GAC filters receiving ozonated water provided better removals than those not receiving ozonated water after the filters had reached exhaustion. Maloney, et al. (1985), found that pre-ozonation increased DOC removal in GAC beds although the same group (Neukrug, et al., 1984) determined that the extra removals were not always cost effective.

While bench scale work with adsorption isotherms generally indicate reduced adsorption capacities after ozonation of humic substances (Hubele, 1984; Chen, et al., 1987; Glaze, et al., 1986), there have been exceptions. Benedek, et al. (1980), and Somiya, et al. (1986) revealed insignificant changes in adsorbability while Kaastrup (1985) found significant increases in adsorbability. These apparently contradictory results are explained by the fact that ozonation reduces the average molecular size of a mixture (indicating increased adsorbability) and also creates highly polar end products (indicating decreased adsorbability due to increased hydrophilicity). The combination of these two effects may be different for different sources of humic material.

The increased biodegradability of humic substances after ozonation has been documented by Stephenson, et al. (1979), Yamada, et al. (1986), and DeWaters (1987). Hubele (1984) observed that the isotherm of an ozonated humic mixture shifted towards increased adsorbability after the mixture was biostabilized. This result would tend to

indicate the biodegradation of the highly polar species produced by ozonation.

Summary

The removal of humic substances by activated carbon has been shown to be a function of system conditions. The process is limited both physically (i.e., by size exclusion from pores) and chemically (i.e., humic functional group interactions between the solvent and the adsorbent surface), although at this stage the physical limitations seem to apply much more heavily when considering humic substance adsorption. In any event, one must obtain a thorough knowledge of system conditions before characterizing the adsorption of humic material.

MODELING HUMIC SUBSTANCE ADSORPTION

As demand increases for the use of activated carbon filters due to tighter control of THMs and other disinfection byproducts, the need for accurate predictive models to aid in design also increases. Modeling of humic substance adsorption has been somewhat limited. It is often applied to carbon columns with fairly sophisticated kinetic approaches although, for lack of better knowledge, humic solutions have been considered as single solutes. Examples of this approach are the analyses of batch and column rate

18

data with the homogeneous surface diffusion model (HSDM), developed by Crittenden and Weber (1978), that used the Freundlich equation to describe the isotherms of humic materials (Lee, et al., 1983; Kaastrup, 1985; Jodellah, 1985; Summers, 1986).

However, isotherm results have shown that humic solutions are multicomponent in nature (Weber, et al., 1983) and attempts have been made to model humic mixtures as such. Multicomponent equilibrium models, such as the ideal adsorbed solution theory (IAST, Radke and Prausnitz, 1972) and the simplified version of IAST known as the simplified competitive adsorption model (SCAM, DiGiano, et al., 1978) were shown to describe humic substance adsorption after dividing the humic mixture into a set of three fictitious components (Frick and Sontheimer, 1983). This approach has been extended to kinetic simulations by Crittenden, et al. (1987b), who used IAST to describe a synthetic mixture as a set of hypothetical components and then incorporated the multicomponent equilibrium condition into a pore and surface diffusion model to describe subsequent column performance. Fettig and Sontheimer (1987) used SCAM to describe humic mixtures as three pseudo-components and obtained surface diffusion coefficients from batch rate data and a multicomponent surface diffusion model. In addition to providing better descriptions of isotherm data, other advantages to modeling humic solutions as multicomponent systems may become apparent when attempts are made to model

competitive adsorption between humic materials and toxic
pollutants.

CHAPTER 3

EXPERIMENTAL PROCEDURES

PREPARATION OF HUMIC SOLUTIONS

Raw water was obtained from Lake Drummond, Virginia, on January 27, 1986. This lake, part of the Great Dismal Swamp in southeastern Virginia, is highly colored, low in pH and alkalinity, and serves as one of the water sources for the city of Chesapeake, Virginia. Werdehoff (1986) found that raw water from Lake Drummond had an elemental composition (by weight) of 55.7% carbon, 4.3% hydrogen, 31.6% oxygen, 0.9% nitrogen, 1.5% ash, 6% dry loss. In addition, a study by Liao, et al. (1982), identified many products of potassium permanganate ($KMnO_4$) oxidation and hydrolysis of Lake Drummond humic and fulvic acids in order to postulate functional group characteristics. Of the identified oxidation products, benzenecarboxylic acids were found to be most abundant, followed by aliphatic dibasic acids, furancarboxylic acids, aliphatic monobasic acids, (carboxyphenyl)glyoxylic acids, and aliphatic tribasic acids. These groups were also identified as hydrolysis products although the order of abundance changed to aliphatic dibasic acids, benzenecarboxylic acids, aliphatic monobasic acids, aliphatic tribasic acids, furancarboxylic

22

acids, and (carboxyphenyl)glyoxylic acids. These results led to the hypothesis that the humic material in Lake Drummond consists of single ring aromatic structures having three to six alkyl, carboxylic, ketone, or hydroxyl substituent groups; short aliphatic carbon chains connecting these structures; and polycyclic ring structures.

After being returned to Chapel Hill, the raw water was filtered through 1.0 μm honeycomb filters to remove leaves and sediment prior to further treatment. This pre-filtered water was then stored in a cool, dark storage area for future use.

Experiments using this water were conducted over the course of two separate time periods. The first set of experiments was conducted from February through April of 1986 and will be referred to as the 1986 data set. The second set of observations was made from April through July of 1987 and will be referred to as the 1987 data set. The results of these two data sets will be shown individually due to possible changes in the composition of the pre-filtered raw water between February, 1986, and April, 1987.

For both sets of data, alum coagulation was the first stage of treatment. Jar tests were performed to find the optimal alum dose for coagulation at a pH of 6.5, the coagulation pH reportedly used by the city of Chesapeake in their water treatment plant. The results, shown in Figure 3-1 as percent UV-254 absorbance removed as a function of alum dose, revealed a sharp increase in removal
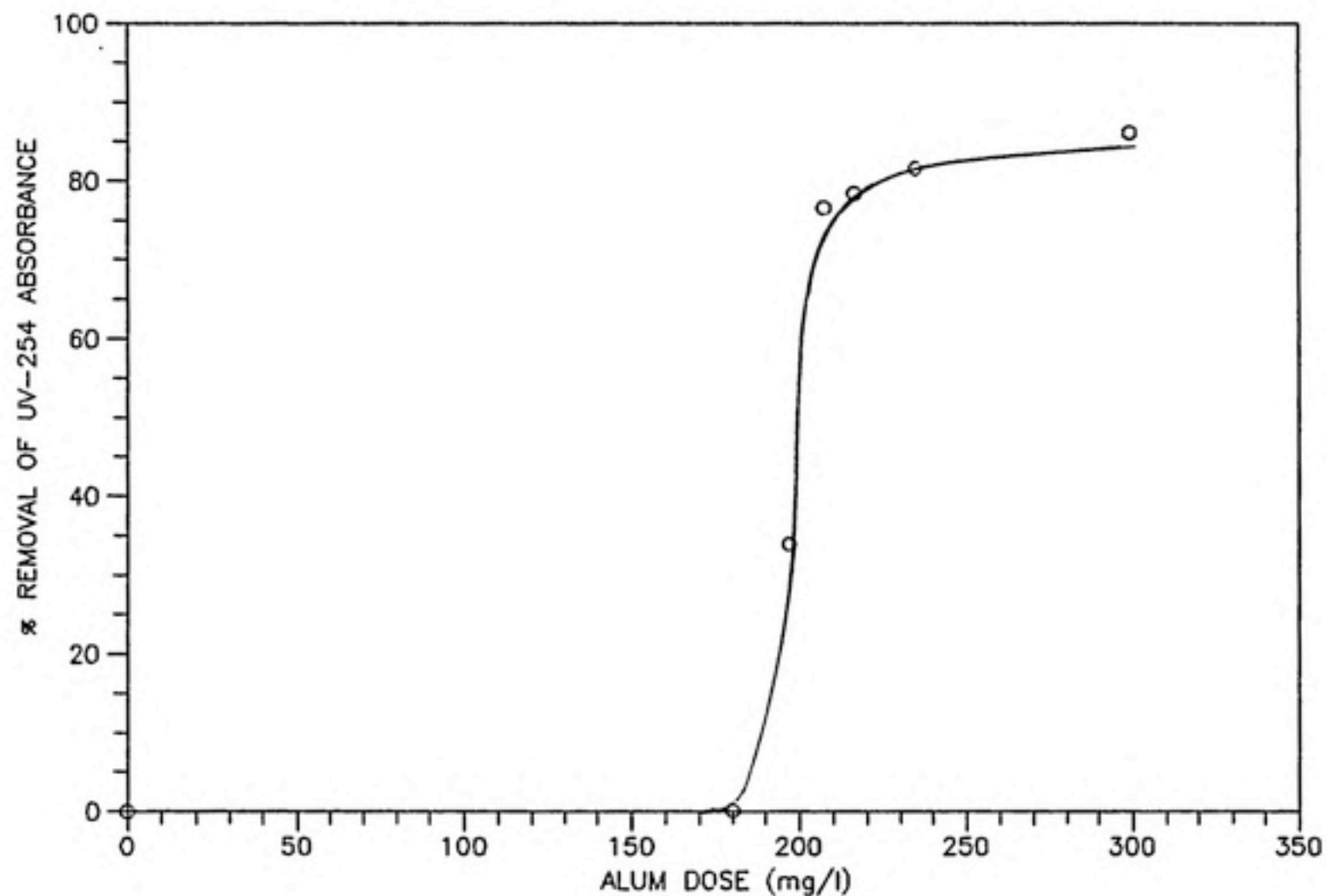
FIGURE 3-1: JAR TEST RESULTS FOR LAKE DRUMMOND HUMIC MATERIAL. THE SHARP INCREASE IN HUMIC SUBSTANCE REMOVAL OVER A SMALL INCREASE IN ALUM DOSAGE MAY BE INDICATIVE OF STOICHIOMETRIC INTERACTIONS BETWEEN HYDROLIZED ALUMINUM AND CARBOXYLIC ACID GROUPS ON THE HUMIC SUBSTANCE MOLECULES.

at alum doses in the vicinity of 200-210 mg/l as
$Al_2(SO_4)_3 \cdot 18 \, H_2O$. This type of removal has been previously
observed for humic and fulvic acids (Randtke and Jepsen,
1981; Babcock and Singer, 1979; Narkis and Rebhun, 1977) and
may be a result of stoichiometric reactions between the
hydrolysis product of alum and the carboxylic acid
functional groups on the humic molecules.

As a result of the jar tests, coagulation was performed
at a pH of 6.5 and an alum dose of 200-210 mg/l for both
data sets. The coagulation procedure involved pH adjustment
of 3 liter samples of the pre-filtered water from 4.3 to 6.5
by the addition of 2.4×10^{-2} M sodium carbonate (Na_2CO_3)
followed by simultaneous addition of a 3 g/l alum solution
and the Na_2CO_3 solution. The addition step was performed at
high mixing intensity and was immediately followed by
flocculation for forty minutes at 30 revolutions per minute.
The flocculated samples were allowed to settle overnight and
were then vacuum filtered with 0.45 μm membrane filters.
For both experimental runs, the filtrate solutions were
combined in a 5 gal glass carboy and stored in a
refrigerator for the prevention of biodegradation.

The coagulation stage was followed by treatment with
ozone (O_3) and biodegradation. Batch ozonation was used for
the 1986 data set, wherein the coagulated sample (buffered
with NaH_2PO_4 and Na_2HPO_4 to give a pH of 7.0) was combined
with an equal volume of distilled, deionized (DDI) water
(buffered with NaH_2PO_4 to give a pH of 4.5) that had been

25

ozonated to a concentration of 25 mg O_3/l. The ozonated sample was then placed in the reservoir of a recycle batch reactor (Figure 3-2), the column of which was previously seeded with return activated sludge from the Chapel Hill Wastewater Treatment Plant. The solution was recycled until no further reduction in TOC was observed (the condition for biostabilization) and was then stored in a refrigerator.

The solutions from the 1987 data set were ozonated with a semi-batch operation where ozone was bubbled through the coagulated solution. The ozonation system, depicted in Figure 3-3, utilized two circuits for the determination of apparent ozone dose (AOD). The actual ozonation procedure was as follows:

1. The ozone generator was turned on with ozone carried directly to the vent. The generator was allowed to run for at least 15 minutes in order to reach stabilization.

2. All four gas washing bottles were filled with 500 ml of 40 g/l potassium iodide (KI).

3. The flow of ozone was directed to the secondary circuit for a specified time period (2-3 minutes) and allowed to react with the KI solutions.

4. The ozone flow was switched to the primary circuit to allow reaction with the coagulated solution. Unreacted ozone flowed from the reactor to the gas washing bottles to react with the KI solutions. This step was also carried out at a specified time period, depending on the desired ozone dose.

5. During Step 4, the gas washing bottles from the secondary circuit were emptied, rinsed, refilled with KI solution, and placed back on the circuit.
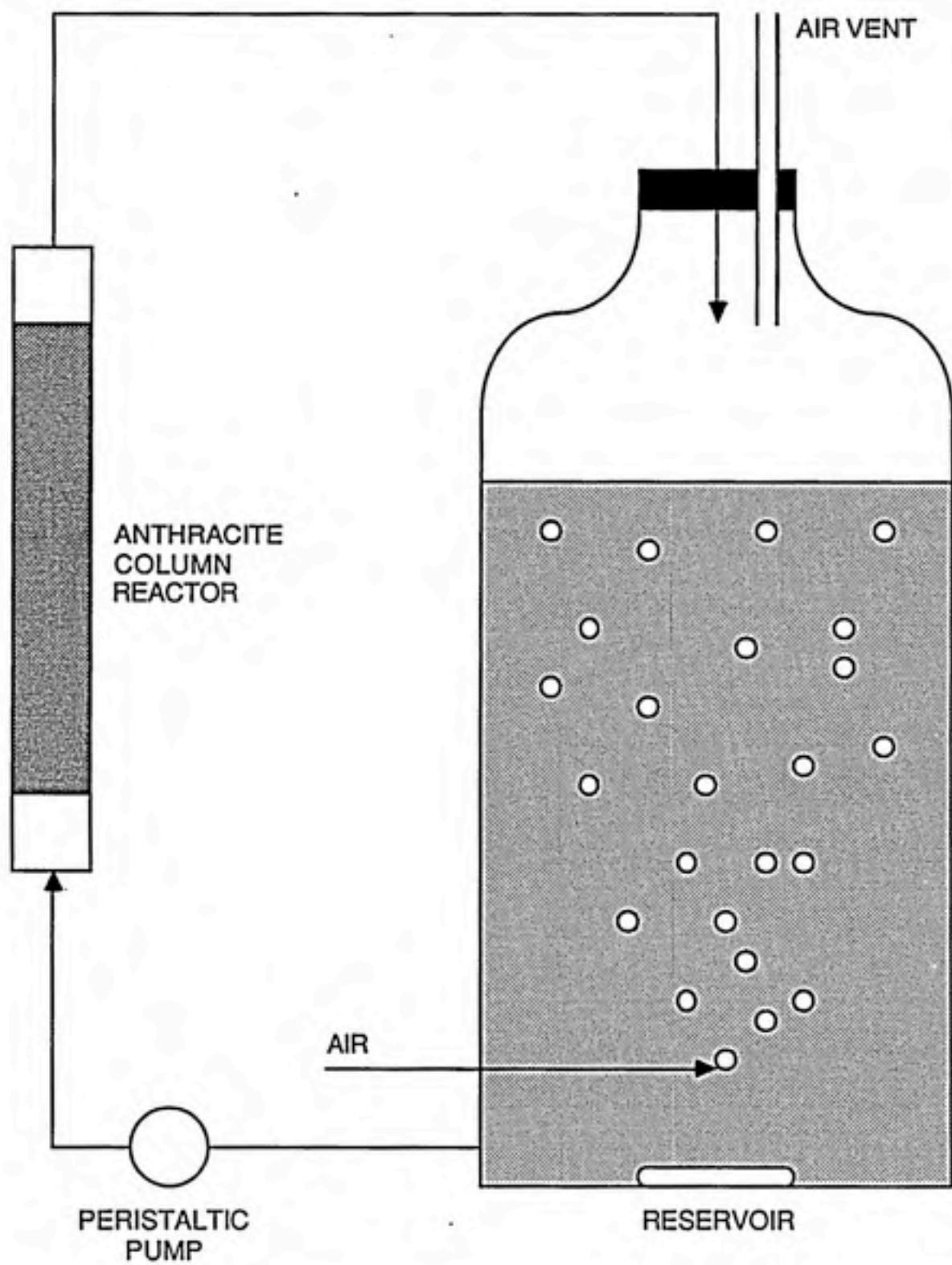
FIGURE 3-2:   SCHEMATIC OF BIOLOGICAL RECYCLE REACTOR
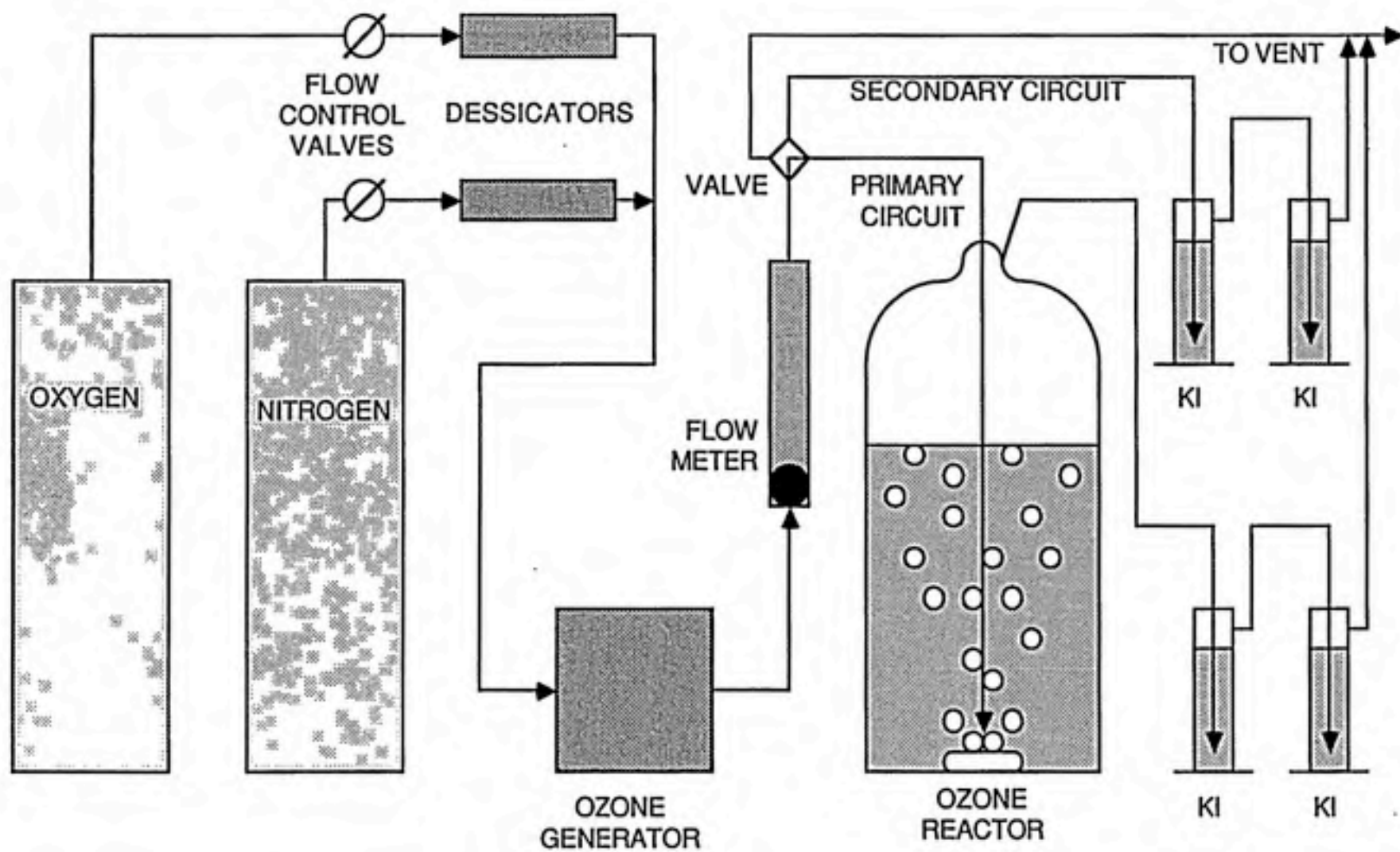
FIGURE 3-3: SEMI-BATCH OZONATION APPARATUS

6. After the specified time period of Step 4, the ozone was redirected to the secondary circuit for the same time period as Step 3.

7. The gas flow was switched to vent and the ozone generator was turned off. The oxygen tank was then shut off and the nitrogen tank was opened. Nitrogen was allowed to pass through the system for at least 15 minutes to purge any residual ozone out of the system.

8. The nitrogen was then allowed to pass through the primary circuit for 2 hours to strip unreacted ozone from the solution.

During Steps 7 and 8, the Iodometric Method (Standard Methods, 1975) was used to determine the amount of ozone reacted in the secondary circuit before and after ozone contact with the primary circuit. The ozone generation rates were calculated from the amount of ozone reacted by the following equation:

$$r_G = ([O_3]_{KI} \cdot V_{KI}) / t \qquad\qquad (3-1)$$

where r_G is the ozone generation rate, $[O_3]_{KI}$ is the amount of ozone reacted in the KI solution, V_{KI} is the volume of the KI solution, and t is the time period for which the ozone was passed through the KI solution.

After purging the primary circuit with nitrogen, the same method was used to determine the amount of ozone reacted with the KI solutions in the exhaust stream. Thus, the ozone exhaust rate was calculated as follows:

$$r_E = ([O_3]_{KI} \cdot V_{KI}) / t \qquad\qquad (3-2)$$

where r_E is the rate of ozone delivery through the exhaust from the reactor. The amount of ozone depleted in the reactor was then calculated from

$$[O_3]_R = [(r_{G,avg} - r_E) \cdot t] / V_R \qquad (3-3)$$

where $[O_3]_R$ is the amount of ozone reacted in the humic solution, $r_{G,avg}$ is the average of the generation rates calculated before and after ozonation of the humic solution, and V_R is the volume of the humic solution in the reactor. The AOD was calculated by dividing $[O_3]_R$ by the TOC of the coagulated humic mixture prior to ozonation.

Using the above procedure, three batches of the coagulated solution were ozonated at three separate ozone dosages by varying the time of ozonation. After ozonation, the samples were biostabilized the same way as those of the 1986 data set with the exception that the bacterial seed was obtained from the effluent of a laboratory GAC column using ozonated humics as the adsorbate (DeWaters, 1987).

Prior to refrigeration and subsequent testing, all of the above samples received 6.5 mM of Na^+ from the addition of phosphate buffer (575.5 mg/l NaH_2PO_4 and 118.3 mg/l Na_2HPO_4) and the samples from the 1987 data set received 5 mg/l of sodium azide (NaN_3). The buffer was added to maintain a pH of 6.5 during the testing while the NaN_3 was added to inhibit biological growth in experiments performed on samples that were ozonated and not biostabilized. Tests

30

showed that this dose of NaN_3 was not enough to prevent bacterial removal over 7 days in these samples. Thus, adsorption results will not be reported for ozonated and non-biostabilized humic mixtures. However, NaN_3 was added to the other solutions from the 1987 data set to maintain consistency as the ozonated and non-biodegraded solutions were intended for comparisons with the rest of the solutions from that data set.

ANALYSIS OF HUMIC SOLUTIONS

All of the solutions described above were characterized by total organic carbon (TOC) content, a useful measure of the concentration of unknown organic mixtures. Samples from the 1986 data set were analyzed with a Beckman Model 915-B TOC Analyzer. The Beckman analyzer uses high temperature catalysis for combustion of organics to carbon dioxide (CO_2) and measures total carbon (TC) with an infrared (IR) detector. Potassium hydrogen phthalate (KHP) was used to set up a linear calibration between the IR readout and TC. The manufacturer's specifications stated that the process resulted in a maximum error of ± 2% of full scale due to the linear assumption. In addition, the manufacturer reported a maximum error of repeatability of ± 2% of the full scale for TC > 5.0 mg/l and ± 4% of the full scale for TC < 5.0 mg/l. When using this instrument, all samples were brought to a pH of 2 with concentrated sulfuric acid (H_2SO_4) and purged with

nitrogen to remove inorganic carbon (IC) prior to analysis. This procedure would also remove volatile organic carbon (VOC) implying that the TOC referred to in this report is non-purgeable organic carbon.

The samples from the 1987 data set were analyzed with O. I. Corporation's Model 700 TOC Analyzer. Samples introduced into the OI 700 were automatically acidified with 5% phosphoric acid, purged to remove IC (as well as VOC), and analyzed to measure IC. After the purging step, sodium persulfate (100 g/l $Na_2S_2O_8$) was introduced to the sample in a 100°C reactor to oxidize the organics to CO_2. The CO_2 was subsequently purged to an IR detector and measured against a a linear KHP calibration to yield TOC (actually non-purgeable organic carbon). The specifications for this instrument indicate a ± 2% of full scale error as a result of the linear assumption and a ± 2% of full scale error of repeatability for sample concentrations greater than 0.002 mg/l.

Measurements made on all of the samples yielded the results posted in Table 3-1 and provide several insights. The results for both pre-filtered samples indicate that Lake Drummond is extremely high in organic content. In addition, the results indicate a loss of 8% TOC in the pre-filtered sample between early February, 1986, and early April, 1987. Some flocculation and sedimentation was observed to have occurred in the pre-filtered waters over the fourteen month storage period. Biodegradation could conceivably account

32

TABLE 3-1

TOC Concentrations of the Humic Mixtures Tested

Humic Mixture	$[O_3]_R$ (mg O_3/l)		TOC (mg/l)	
	1986	1987	1986	1987
Pre-Filtered	0.0	0.0	43.8	40.3
Coagulated	0.0	0.0	21.7	16.3
Ozone Dose #1 + Biostabilization	12.5	13.2	7.00	13.3
Ozone Dose #2 + Biostabilization	----	39.6	----	10.5
Ozone Dose #3 + Biostabilization	----	89.3	----	6.92

for some of the loss as well, although it is unknown as to whether this phenomenon actually took place.

The coagulation results showed a 50.5% TOC reduction in the 1986 data set and a 59.6% TOC reduction in the 1987 data set, even though both experiments utilized the same range of alum doses. The steepness of the curve for UV absorbance (a surrogate for TOC) versus alum dose in Figure 3-1 shows that it is extremely difficult to repeat the same TOC removal by coagulation in the alum dose region used. In addition, the TOCs for the coagulated mixtures allows the calculation of the AODs for each of the ozonation and biostabilization stages. The resulting AODs are posted in Table 3-2. For the ozonation performed in the 1986 data set, AOD was calculated based on the assumption that all of the ozone in the DDI water reacted with the TOC of the coagulated mixture. In addition, since equal volumes of the two solutions were combined, the initial TOC was 10.85 mg/l just prior to ozonation.

Table 3-3 lists the values of TOC obtained immediately after ozonation as well as the percent of coagulated TOC removed due to the ozonation steps and due to the combined ozonation and biostabilization steps. The results indicate that 33% - 40% of the TOC removed by ozonation and biostabilization was removed by the ozonation step in the 1987 data set while only 4% of the TOC removed by ozonation and biostabilization was removed by the ozonation step in the 1986 data set. This result indicates that the organics

34

TABLE 3-2

Apparent Ozone Doses (AODs) for the Various Ozonation Steps

Humic Mixture	$[O_3]_R$ (mg O_3/l)		AOD (mg O_3/mg TOC)	
	1986	1987	1986	1987
Ozone Dose #1	12.5	13.2	1.15	0.81
Ozone Dose #2	----	39.6	----	2.43
Ozone Dose #3	----	89.3	----	5.48

TABLE 3-3

TOC Removals Due to Ozonation and the Combined Treatments of Ozonation and Biostabilization

AOD (mg O_3/mg TOC)	Data Set	TOC After O_3 (mg/l)	TOC After O_3 and biostabilization (mg/l)	% TOC Removed by O_3	% TOC Removed by O_3 & Biostabilization
1.15	1986	10.7	7.00	1.4	35.5
0.81	1987	15.3	13.3	6.1	18.4
2.43	1987	13.9	10.5	14.7	35.6
5.48	1987	12.9	6.92	20.9	57.5

in the 1987 data set were much more readily oxidized by ozone to CO_2 as compared with organics in the 1986 data set. This observation may also be indicative of the removal of volatile ozonation products prior to TOC measurement in the solutions of the 1987 data set. These differences may be a result of buffer conditions since the phosphate buffer used in the 1986 data set may reduce the amount of radical $OH^{\bullet}$ reactions taking place due to the lower pH. Thus, the ozonation step in the 1986 data set may have been more selective than the ozonation step in the 1987 data set. Any additional differences in starting materials are noted in Table 3-4.

Based on literature reports of a linear relationship between ultraviolet absorbance at a wavelength of 254 nm (UV-254) and TOC (Edzwald, et al., 1985; Singer, et al., 1981), the possibility of using UV-254 as a surrogate for TOC was investigated for the 1986 data set. UV-254 was determined with a Varian Cary 219 Spectrophotometer and the results are posted in Table 3-5 along with comparisons between the percent removal of UV-254 and the percent removal of TOC for a given treatment stage. In addition, correlations between TOC and UV-254 are depicted in Figure 3-4 and are shown to be quite linear. However, the results posted in Table 3-5 and Figure 3-4 show that coagulation, as well as the combined treatments of ozonation and biostabilization, removed more UV-254 than TOC. These results imply that both treatment steps preferentially

37

TABLE 3-4

**Characteristics of the Coagulated Humic Solutions Prior to and
During Ozonation**

	1986	1987
TOC After Coagulation	10.9	16.3
% TOC Removed During Coagulation	50.5	59.6
Buffer During Ozonation	phosphate	none
Ozone Contact Method	batch	semi-batch

TABLE 3-5

UV-254 Values for the 1986 Humic Solutions and Comparisons Between UV-254 Removals and TOC Removals

Humic Mixture	UV-254 (m^{-1})	% UV-254 Removed from Previous Stage	% TOC Removed from Previous Stage
Pre-Filtered	144.6	----	----
Coagulated	47.8	66.9	50.5
Ozonated & Biostabilized	10.4	78.2	35.5
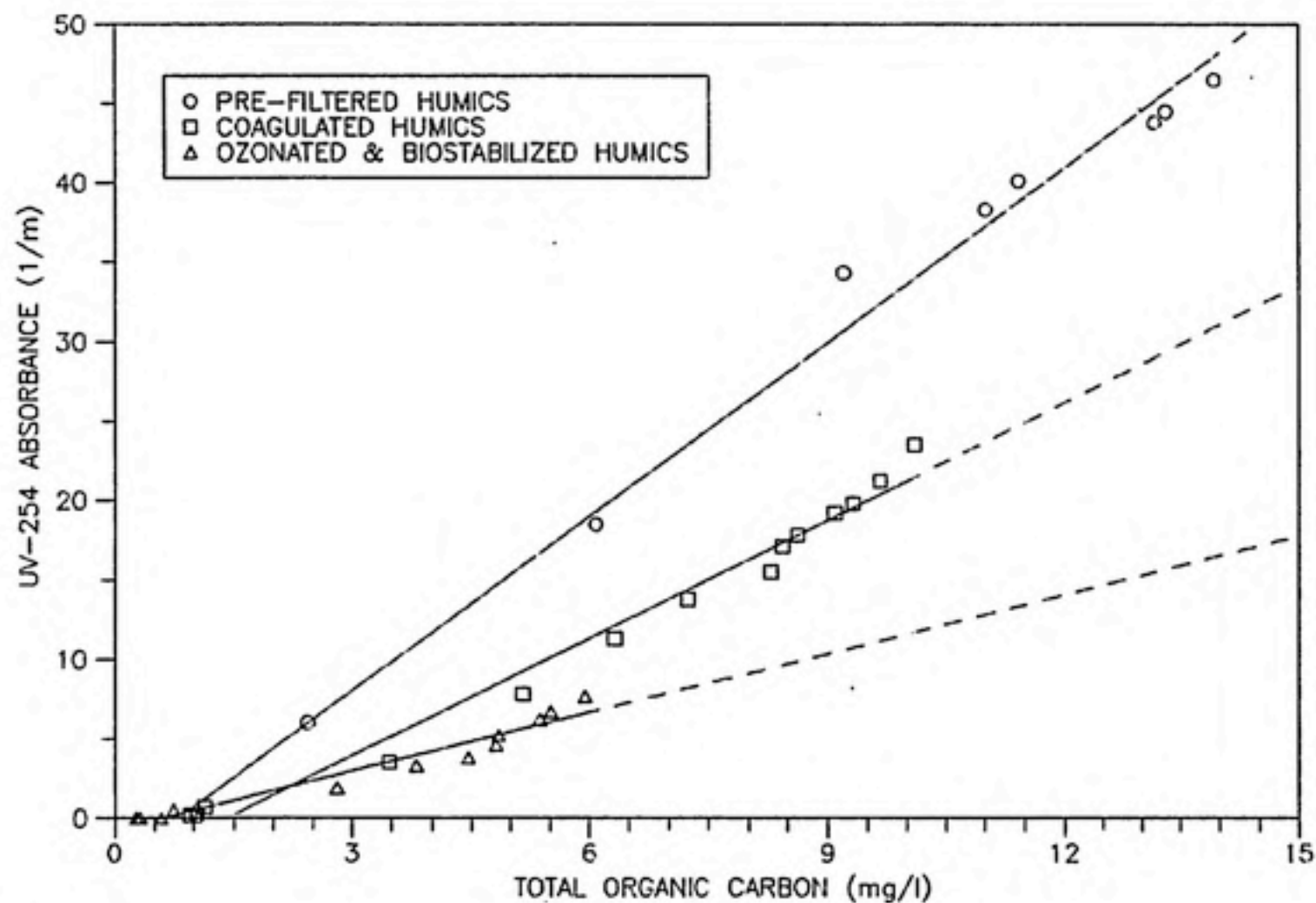
FIGURE 3-4: CORRELATION BETWEEN TOTAL ORGANIC CARBON AND UV-254 ABSORBANCE FOR THREE HUMIC MIXTURES TESTED FROM THE 1986 DATA SET. SOLID LINES INDICATE THE BEST LINEAR FIT TO THE OBSERVED DATA WHILE THE DASHED LINES INDICATE EXTRAPOLATIONS BEYOND THE OBSERVED DATA.

remove humic molecules that absorb ultraviolet light at a wavelength of 254 nm. Semmens and Field (1980) noted this result for coagulation and several investigators have made the same observation for ozonation (Sierka and Amy, 1985; Somiya, et al., 1986; Stephenson, et al., 1979). Decreases in UV-254 indicate the removal or oxidation of carbon-carbon double bonds and chromophoric groups such a -OH and $-NH_2$ (Anderson, et al., 1986) and, therefore, the results suggest that the chemical composition of humic mixtures are significantly changed by these treatments in comparison with organic content. Based on these results, one can conclude that the correlation between UV-254 and TOC is system specific and should be judiciously applied.

DETERMINATION OF EQUILIBRIUM ADSORPTION BEHAVIOR

Adsorption isotherms were determined for all humic solutions by using the bottle point method. This method can be carried out by using two different approaches. The first involves the addition of varying adsorbent doses to bottles containing a known volume and constant initial concentration of the solution of interest while the second consists of the addition of varying concentrations of the solution of interest to bottles containing a known and constant mass of adsorbent. The former approach is termed as the "constant C_o approach" while the latter is known as the "constant dose approach." For solutions containing only one adsorbate,

41

both approaches would yield the same isotherm. However, due to the heterogeneous nature of humic solutions, each approach yields a different result. In addition, the constant C_O approach yields isotherms that are dependent on the initial concentration, C_O, and the constant dose approach yields isotherms that are dependent on the adsorbent dose, D (Weber, et al., 1983). These divergent results are caused by competitive adsorption among the different humic species. However, any multicomponent equilibrium model can account for these dependencies and, as a result, the constant C_O approach was used for all isotherm studies. Another drawback to the bottle point method, as discussed by Wang (1986), is the possibility of overpredicting equilibria observed in adsorption columns. This was considered to be a result of the fact that the bottle point method approaches equilibrium from high to low concentration while columns approach equilibrium from low to high concentration.

In order to achieve sufficiently fast equilibration, powdered activated carbon (PAC) was used in the isotherm experiments. The PAC was prepared from Calgon F-400 granular activated carbon (GAC) by washing with DDI water in a Soxhlet Extractor, drying at 110°C, grinding to a 200/325 U.S. mesh size, and storing in bottles in an air-tight dessicator. This procedure, described by Randtke and Snoeyink (1983), was used to ensure that a representative sample of the "as received" GAC was used. Summers (1986)

showed that this carbon is positively charged below a pH of 10.0 and has a relatively small total surface area. In this manner, a batch of PAC was prepared for the 1986 data set and another batch was prepared for the 1987 data set.

The test solution was transferred in 100 ml aliquots to a total of 13 to 20 bottles containing a range of PAC doses from 5 mg/l to 4000 mg/l. The bottles, including a control bottle containing no PAC, were then placed on a tumbling apparatus for a period of 7 to 10 days at a temperature of 23°C. This equilibration time was determined to be adequate after tests showed little change in adsorption of humic material after 7 days based on measurements of UV-254. At the end of the equilibration period, the bottles were filtered with 0.45 μm membrane filters to remove PAC and the TOC of each sample was then measured. Table 3-6 provides a summary of this procedure to elucidate any differences between the 1986 and 1987 data sets.

DETERMINATION OF ADSORPTION RATE BEHAVIOR

Mini-Column Studies

The external mass transfer characteristics were determined through the use of a short, fixed-bed reactor known as a mini-column. A theoretical treatment of how the mini-column works is given in Chapter 4 as this section will be devoted to procedure only. Figure 3-5 shows a schematic

TABLE 3-6

**Methodology Differences Between the 1986
and 1987 Isotherm Studies**

	1986	1987
pH	6.5	6.5
$[Na^+]$ from Phosphate Buffer (mM)	6.5	6.5
Sodium Azide (mg/l)	0.0	5.0
# of Observations (Bottles)	12 - 13	20
Range of PAC Dosages (mg/l)	5 - 4000	5 - 4000
Equilibration Time (days)	7 - 10	7
Temperature (°C)	23 ± 2	23 ± 3
TOC Analyzer	Beckman	OI Corp.

EFFLUENT

MINI-
COLUMN

WASTE

CONSTANT
HEAD
RESERVOIR

FLOW
METER
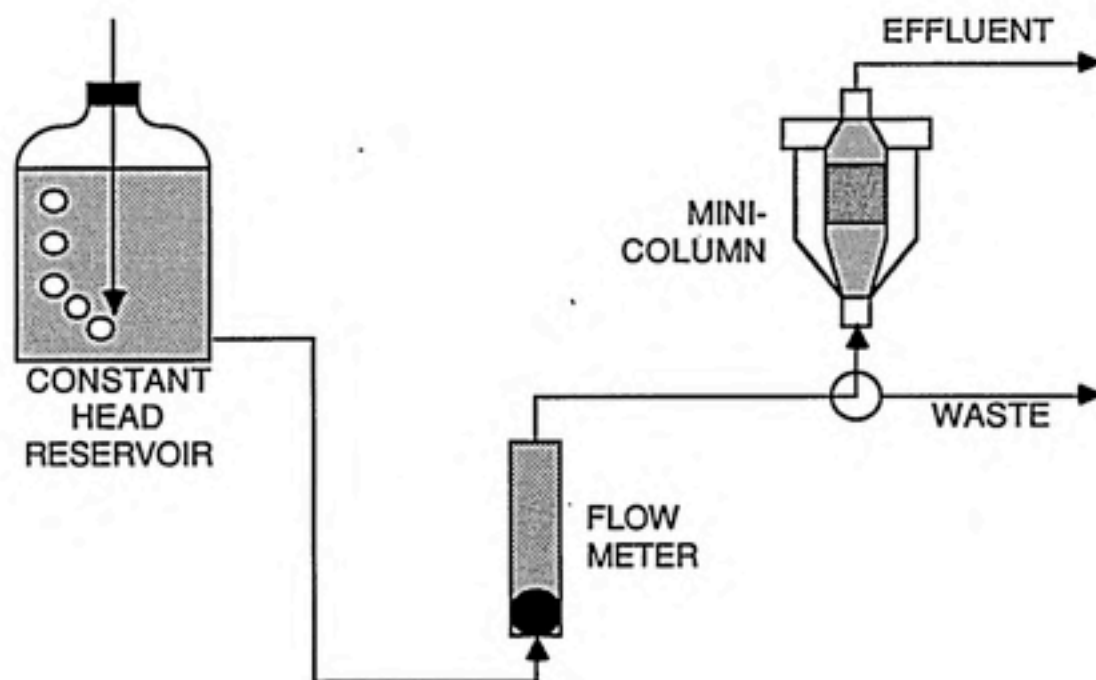
FIGURE 3-5a: SCHEMATIC OF MINI-COLUMN SETUP

GLASS
SUPPORT
MEDIA

GRANULAR
ACTIVATED
CARBON

GLASS
SUPPORT
MEDIA
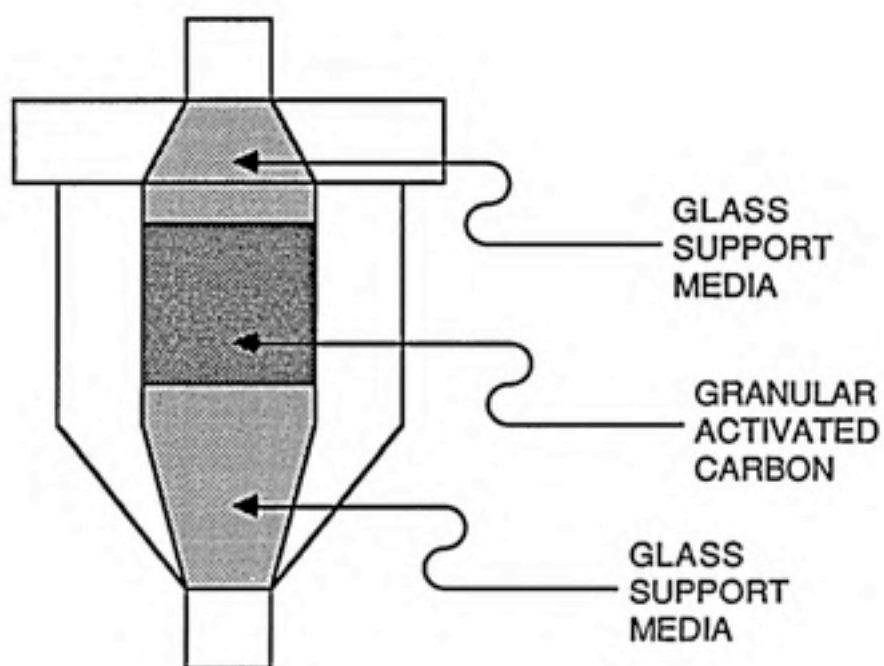
FIGURE 3-5b: BLOW-UP OF MINI-COLUMN PACKING MATERIAL

of the mini-column setup which was constructed on the basis of work done by Cornel, et al. (1986b), and Roberts, et al. (1985). The reactor, made of lucite, had an internal diameter of 2 cm and two stainless steel screens, separated by 5 cm, between which the bed was placed.

A single batch of 18/20 mesh GAC was prepared from "as received" F-400 GAC in the same manner as the isotherm PAC batches were prepared. Just prior to testing, a certain amount of GAC was weighed, placed in DDI water, brought to boiling, and immediately cooled to fill the pores with the DDI water.

In the meantime, the column was filled with DDI water and a GAC support material was placed in the column's cone of expansion. This support material was 3 mm glass beads for the 1986 data set and was changed to 18/20 mesh crushed glass tubing for the 1987 data set to better approximate the hydrodynamics of the carbon bed. The prepared GAC was then immersed in the column to form a layer over the glass support. This step was followed by the addition of glass beads or crushed glass to fill the column volume. The column was then sealed and the effluent tube was filled to capacity with DDI water.

A constant head reservoir was filled with the solution to be tested and 250 ml of solution were allowed to pass through the tubing and sent to waste just prior to the mini-column. Since the tubing was estimated to hold a volume of

80 ml, this step was considered necessary in order to provide undiluted solution through the entire tube.

A stopcock was opened at a time previously determined to be zero such that the test solution would begin to flow through the column. The flow meter was immediately checked to confirm a steady flow rate of 25 ml/min and, at a time of 30 seconds, sampling was begun such that samples were taken over the course of one minute each. A sample was considered to be taken at the midpoint of the time range covered by the sample (i.e., the sample taken from $t = 30$ seconds to $t = 90$ seconds was considered to be taken at 60 seconds). This procedure was halted after 10.5 minutes of run time and was immediately followed by verification of flow rate with a graduated cylinder. The temperature was recorded and the TOC of each sample was subsequently measured to yield average concentrations over the time range of each sample.

Batch Rate Studies

Internal diffusion rates of humic substances were determined in completely mixed batch reactors. Once again, the theory of determining internal diffusion rates will be discussed in Chapter 4, leaving this discussion to procedures only.

The batch rate tests employed an impeller constructed of polyvinylchloride (PVC) to provide the mixing. This impeller was designed from a similar device in use at the

labs of the Engler-Bunte Institute at the University of Karlsruhe, Federal Republic of Germany (Fettig, 1986). A GAC trap was located at the point of flow input to the impeller as shown in Figure 3-6. This method of GAC contact with the aqueous solution prevents break-up of carbon particles as is commonly observed in conventional batch stirring systems. In addition, the device provides a consistent hydrodynamic regime that should eliminate variability in external mass transfer limitations. The trap consisted of two stainless steel screens (to keep the GAC from entering the entire solution) and an outer wall made of PVC that was capable of being attached to the impeller. The tests utilized the same batch of GAC that was used in the mini-column and the GAC was prepared in the same manner (i.e., weighed, boiled in DDI water, and cooled to fill the pores). Twelve hours prior to testing, 3 liters of solution were transferred to a 4 liter glass beaker and the impeller, containing no GAC, was placed in the solution and attached to a motor which was immediately started. This step was run to examine the possibility of humic substance adsorption to PVC. After 11.5 hours, a 40 ml sample was taken from the beaker and analyzed for TOC. Comparisons between this value of TOC and the initial TOC showed, in all cases, adsorption on PVC as negligible. The GAC was prepared in the next half hour, transferred to the GAC trap one minute before start-up, and the trap was then attached to the impeller. The impeller was immersed in the test solution and attached to

GRANULAR
ACTIVATED
CARBON
TRAP

FLOW
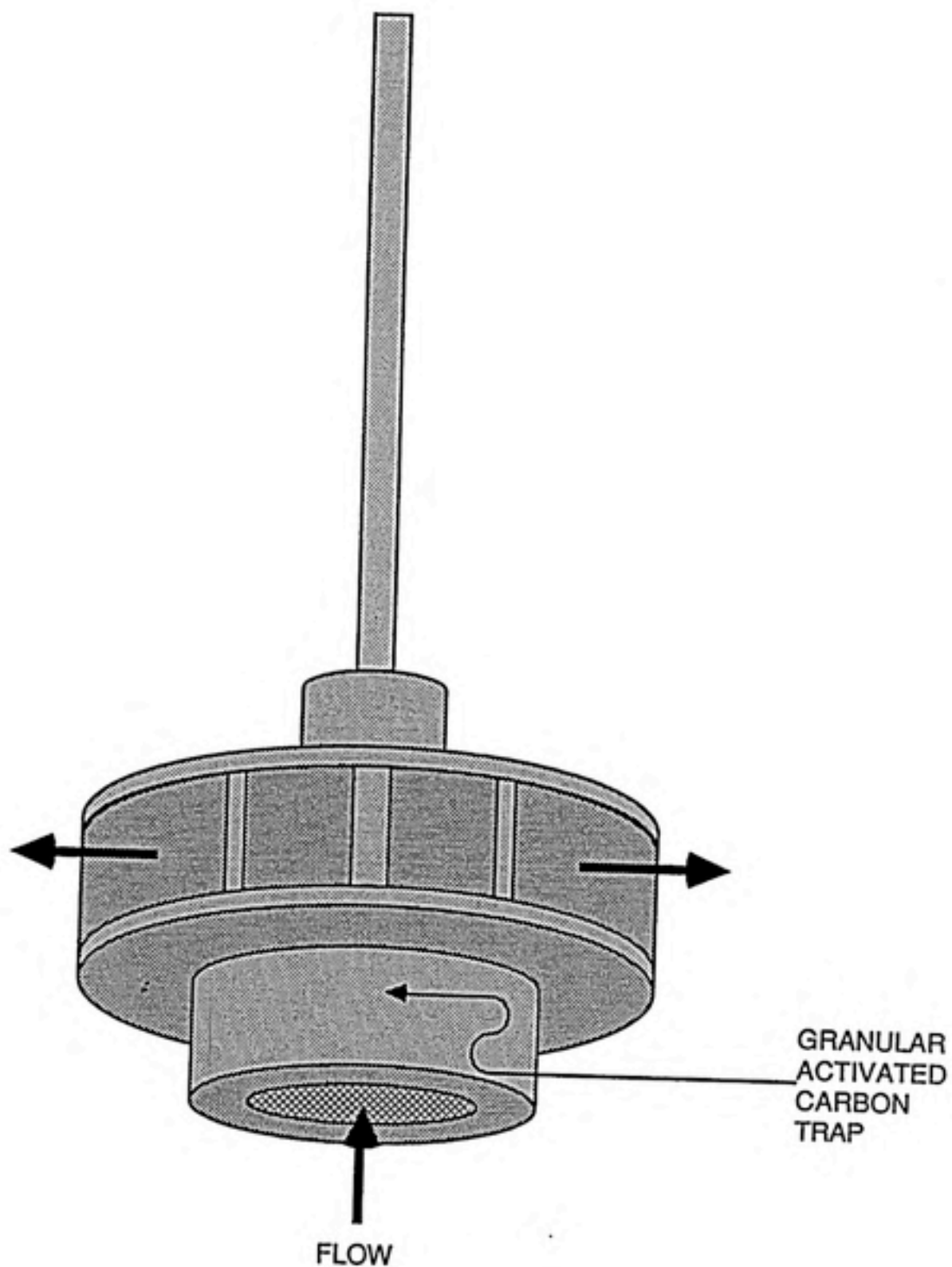
FIGURE 3-6: IMPELLER USED FOR BATCH RATE TEST

the motor which was immediately started. Samples were taken
at exponential intervals (i.e., short time intervals between
samples at the beginning of the run and long time intervals
near the end of the run) over a period of 190-225 hours and
were immediately analyzed for TOC. This sampling method
allowed a more accurate measurement of the larger change in
concentration with time at the beginning of the test.

CHAPTER 4

PROCEDURES FOR MODELING THE ADSORPTION OF UNKNOWN MIXTURES

ADSORPTION EQUILIBRIA

Ideal Adsorbed Solution Theory

Due to the heterogeneous nature of humic substance mixtures, the model to be used must be able to describe humic adsorption equilibria based on multicomponent adsorption theories. Frick and Sontheimer (1983) showed that such a description is possible by using ideal adsorbed solution theory (IAST) to model the adsorption isotherms of unknown mixtures when the mixtures were treated as a set of three pseudo-components (PCs). The IAST model performs a non-linear curve fitting routine to minimize deviations between observed and calculated results by systematically adjusting the appropriate adsorption parameters. The mathematical technique of this process will be shown below. Conceptually, this process reduces the complexity of humic solutions such that each PC may be considered as representative of a group of actual components having similar adsorbabilities. While an appealing approach, the limitations of extending IAST to model humic substance adsorption must also be understood.

IAST was first developed by Myers and Prausnitz (1965) to describe and predict the adsorption of gaseous mixtures on a thermodynamically consistent basis. Radke and Prausnitz (1972) then extended IAST to multisolute adsorption from dilute liquid solutions. As with any equilibrium process, a favorable change in free energy must accompany the adsorption of solutes from the bulk liquid phase to the adsorbed phase. This thermodynamic concept was incorporated with the following assumptions: (1) the solid phase is inert and has an identical specific surface area for all adsorbates, (2) the bulk liquid phase is a dilute solution obeying Henry's Law, and (3) the adsorbed phase is solvent free and forms an ideal solution obeying Raoult's Law when solutes adsorb simultaneously at constant temperature and spreading pressure.

Spreading pressure is defined as the change in interfacial tension between the solid and adsorbed phases resulting from the addition of solutes to a pure solvent system. Therefore, a constant spreading pressure implies that the interfacial tension must also be constant. Since the adsorbed phase is considered to be two dimensional, the interfacial tension is analogous to the three dimensional pressure of the ideal gas law. The assumption that the adsorbed phase is solvent free (see assumption 3 above) implies that the spreading pressure is equal to the interfacial tension and, therefore, spreading pressure is also analogous to three dimensional pressure.

The above assumptions lead to the following equation:

$$1/q_T = \sum_{i=1}^{N}(z_i/q^{\cdot}_i) \qquad (4\text{-}1)$$

Equation 4-1 relates the total amount of solute adsorbed, q_T, to the loadings, $q^{\cdot}_i$, that would occur if each of the N solutes were to adsorb singly from dilute solution at the same temperature and spreading pressure as the mixture. The mixture and single solute systems must be considered at the same temperature and spreading pressure since these two intensive variables set the equilibrium state of each solute. The total surface loading is defined as the sum of the individual solute loadings in the adsorbed phase mixture as follows:

$$q_T = \sum_{i=1}^{N}q_i \qquad (4\text{-}2)$$

Thus, q_i is the adsorbed phase concentration of solute i when solute i is adsorbed from the bulk liquid phase. The surface mole fraction, z_i, used in Equation 4-1 is defined as:

$$z_i = q_i/q_T \qquad \text{for i = 1 to N.} \qquad (4\text{-}3)$$

The assumptions made to arrive at Equation 4-1 seem somewhat reasonable for the bulk liquid phase. However, PAC and GAC are not inert materials as they contain many surface functional groups that are capable of reacting with solute functional groups (Mattson and Mark, 1971; Smisek and Cerny, 1970). In addition, the pore structure of activated carbons can effectively exclude larger solutes from interior adsorption sites (as evidenced by Lee, et al., 1981) thereby implying that an identical specific surface area is not available for all solutes.

For the adsorbed phase assumptions, a solute follows Raoult's Law only as z_i approaches 1, especially if the solute is significantly different from others in solution. Since, in this case, the adsorbing mixture is a natural humic solution containing a multitude of solutes, it would appear unlikely that any component would approach a mole fraction of unity in the adsorbed phase. Thus, humic solutions are highly unlikely to follow the assumption of an ideal adsorbed phase. In addition, some of the PAC or GAC functional groups could conceivably attract water (the solvent) into the adsorbed phase via such mechanisms as hydrogen bonding. Despite these drawbacks, IAST will be shown to work reasonably well for humic solutions adsorbing onto activated carbon.

At equilibrium, the chemical potential of the bulk liquid phase must equal the chemical potential of the adsorbed phase. As a result, the liquid phase concentration

54

of a given solute in the mixture can be determined from the liquid phase concentration of that solute when it adsorbs without competition at the same temperature and spreading pressure as the mixture. The equation is given by

$$c_i = z_i c^{\circ}_i \qquad \text{for } i = 1 \text{ to } N \qquad (4\text{-}4)$$

where c_i is the liquid phase concentration of solute i in the mixture when the liquid and adsorbed phases are at equilibrium. c°_i is the liquid phase concentration of solute i in a single solute system at equilibrium and z_i is as defined in Equation 4-3. Equations 4-1 and 4-4 are the key results of IAST since both assume the formation of an ideal adsorbed phase at constant temperature and spreading pressure.

Equations 4-1 and 4-4 require that the single solute parameters, c°_i and q°_i, be evaluated at the same spreading pressure as the mixture. Therefore, in order to use the appropriate c°_i and q°_i for a given solute, the following condition must be satisfied:

$$\pi_T = \pi^{\circ}_i \qquad \text{for } i = 1 \text{ to } N. \qquad (4\text{-}5)$$

This expression simply equates the spreading pressure of the mixture, π_T, with the spreading pressure of each solute in a single solute system, π°_i. The values of π°_i are obtained from single solute isotherms as

$$\pi^{\bullet}{}_i = (RT/A) \int_0^{C^{\bullet}{}_i} (q^{\bullet}{}_i / C^{\bullet}{}_i)\ dC^{\bullet}{}_i$$

$$\text{for } i = 1 \text{ to } N \qquad (4\text{-}6)$$

where R is the ideal gas constant, T is the temperature of the adsorption process, and A is the area of the solution - solid interface. As pointed out by Radke and Prausnitz (1972), $\pi^{\bullet}{}_i$ is evaluated from data and, therefore, the single solute adsorption model used to describe the data does not need to be theoretical. However, the integration does require data down to $C^{\bullet}{}_i = 0$ implying that one needs single solute data from a surface loading of zero to a surface loading of $q^{\bullet}{}_i$ in order for the integration to accurately calculate $\pi^{\bullet}{}_i$. As shown by Kidnay and Myers (1966), the error in calculating $\pi^{\bullet}{}_i$ is reduced by transforming the integrating variable from $C^{\bullet}{}_i$ to $q^{\bullet}{}_i$:

$$\pi^{\bullet}{}_i = (RT/A) \int_0^{q^{\bullet}{}_i} [d(\ln C^{\bullet}{}_i) / d(\ln q^{\bullet}{}_i)]\ dq^{\bullet}{}_i$$

$$\text{for } i = 1 \text{ to } N \qquad (4\text{-}7)$$

Most IAST applications, particularly those reported by Crittenden and co-workers, are for solutes of known molecular weight such that molar concentrations are easily expressed. In the case of this work, the Freundlich

equation was used to describe the single solute behavior of the PCs on a TOC basis. The Freundlich expression is given by

$$q^*_{i,TOC} = K_{i,TOC} \cdot (C^*_{i,TOC})^{1/n_i}$$

$$\text{for } i = 1 \text{ to } N \qquad (4-8)$$

where $q^*_{i,TOC}$ and $C^*_{i,TOC}$ are the adsorbed and liquid phase TOC concentrations of solute i and $K_{i,TOC}$ and $1/n_i$ are the Freundlich parameters of solute i. $K_{i,TOC}$ represents the adsorption capacity of the adsorbent for solute i while $1/n_i$ represents the adsorption intensity of solute i.

Since Equation 4-8 is based on TOC concentrations (usually expressed in mg/l) further manipulation is required before the Freundlich isotherm can be incorporated into IAST, which was derived with molar concentrations. This manipulation has not been reported in the literature. The TOC concentrations are related to molar concentrations by

$$C^*_{i,TOC} = (C^*_i) \cdot (y_i) \cdot (MW_C)$$

$$\text{for } i = 1 \text{ to } N \qquad (4-9)$$

where y_i is the number of carbon atoms in a mole of solute i and MW_C is the atomic weight of carbon. Substituting Equation 4-9 into Equation 4-8 yields

$$q_i^* = K_{i,TOC} [(Y_i) \cdot (MW_C)]^{(1/n_i - 1)} [C_i^*]^{1/n_i}$$

$$\text{for } i = 1 \text{ to } N \qquad (4\text{-}10)$$

which becomes, upon linearization and solving for $\ln(C_i^*)$,

$$\ln C_i^* = n_i (\ln q_i^*) + n_i [\ln(Y_i \cdot MW_C / K_{i,TOC})]$$
$$- \ln(Y_i \cdot MW_C)$$

$$\text{for } i = 1 \text{ to } N \qquad (4\text{-}11)$$

The derivative of Equation 4-11 is

$$d(\ln C_i^*) / d(\ln q_i^*) = n_i$$

$$\text{for } i = 1 \text{ to } N \qquad (4\text{-}12)$$

and can be substituted into Equation 4-7 to yield, upon integration

$$\pi_i^* = (RT/A)(n_i)(q_i^*) \qquad \text{for } i = 1 \text{ to } N \qquad (4\text{-}13)$$

Substitution of Equation 4-13 into Equation 4-5 and the assumption that A applies to all solutes identically results in the expression

$$\pi_T A / RT = n_i \cdot q_i^*$$

$$\text{for } i = 1 \text{ to } N. \qquad (4\text{-}14)$$

58

IAST can be used to calculate the concentration of any component in a mixture by combining Equations 4-1, 4-2, 4-3, 4-4, 4-9, 4-10, and 4-14 in the order shown in Appendix A. As a result, the following function is obtained:

$$c_{i,TOC} = [(q_{i,TOC} / y_i) / \sum_{j=1}^{N}(q_{j,TOC} / y_j)]$$

$$\cdot [\sum_{j=1}^{N}(n_j \cdot q_{j,TOC} / y_j) / (n_i \cdot K_{i,TOC} / y_i)]^{n_i}$$

$$\text{for } i = 1 \text{ to } N \qquad (4\text{-}15)$$

Therefore, when the Freundlich isotherm is substituted into IAST, the resulting expression shows that the equilibrium TOC concentration of solute i in the liquid phase depends on the number of carbons per mole, the Freundlich parameters K and n, and the equilibrium TOC concentration in the adsorbed phase of each PC that is present in the mixture.

Each PC must also satisfy the mass balance given by

$$q_{i,TOC} = (c_{oi,TOC} - c_{i,TOC}) \cdot (V / M)$$

$$\text{for } i = 1 \text{ to } N \qquad (4\text{-}16)$$

where $c_{oi,TOC}$ is the concentration of solute i prior to adsorption, M is the mass of carbon added to the system, and V is the volume of the humic solution. Combining Equations 4-15 and 4-16 results in

$$c_{oi,TOC} - [q_{i,TOC} \cdot (M/V)]$$

$$- [(q_{i,TOC} / y_i) / \sum_{j=1}^{N}(q_{j,TOC} / y_j)]$$

$$\cdot [\sum_{j=1}^{N}(n_j \cdot q_{j,TOC} / y_j) / (n_i \cdot K_{i,TOC} / y_i)]^{n_i} = 0$$

$$\text{for } i = 1 \text{ to } N \qquad (4\text{-}17)$$

Thus, Equation 4-17 represents a set of N equations that must be satisfied for a given isotherm bottle. A nonlinear search routine would be performed, based on this equation, to find the values of $c_{oi,TOC}$, y_i, n_i, and $K_{i,TOC}$ for each PC. This routine would be similar to that given by Crittenden, _et al._ (1985), but now includes a search for the proper values of y_i, the variable introduced because of the use of TOC to describe PCs.

Several interesting notes can be made about Equation 4-17. Firstly, for the case where the system is modeled as a single PC (i.e., N = 1), Equation 4-17 reduces to the Freundlich equation as should be expected. Secondly, for systems modeled with two adsorbing PCs (i.e., N = 2), Equation 4-17 reduces, for PC 1, to

$$c_{o1,TOC} - [q_{1,TOC} \cdot (M/V)]$$

$$- (q_{1,TOC} / [q_{1,TOC} + (y_1 / y_2)(q_{2,TOC})])$$

$$\cdot ([q_{1,TOC} + (y_1 / y_2)(n_2 / n_1)(q_{2,TOC})] / K_{i,TOC})^{n_i}$$

$$= 0$$

$$\text{for } i = 1 \text{ to } N \qquad (4\text{-}18)$$

A similar equation exists for PC 2 and Equation 4-18 implies that the ratios $y_1:y_2$ and $n_1:n_2$ are important in determining the adsorption behavior of the mixture. Finally, if one assumes that each PC contains the same number of carbon atoms, then

$$y_1 = y_2 = \cdots = y_i = \cdots = y_N \qquad (4-19)$$

and Equation 4-17 reduces to

$$C_{oi,TOC} - [q_{i,TOC} \cdot (M/V)] - [q_{i,TOC} / \sum_{j=1}^{N} q_{j,TOC})]$$
$$\cdot \left[\sum_{j=1}^{N}(n_j \cdot q_{j,TOC}) / (n_i \cdot K_{i,TOC})\right]^{n_i} = 0$$

$$\text{for } i = 1 \text{ to } N \qquad (4-20)$$

This expression is identical to the objective function derived and used by Crittenden, et al. (1985), to describe the multicomponent adsorption of three synthetic mixtures and a contaminated groundwater on two activated carbons. Equation 4-20 was used in this work to describe the equilibrium adsorption behavior of the humic solutions noted in Chapter 3. Therefore, the simplifying assumption has been made that all PCs contain the same number of carbon atoms (y). In reality, humic mixtures have widely ranging y values, however, the question remains as to what level of detail can be included in modeling where supporting data are lacking. A sensitivity analysis was performed to determine

whether Equation 4-17, which includes y as a parameter, was better suited to modeling the adsorption equilibria of humic solutions. The results of this analysis are given below. From this point on, all concentrations will refer to TOC and, therefore, the TOC subscripts will be dropped for simplicity.

Fitting Isotherm Data

Equation 4-20 was used as the basis for a nonlinear routine that searched for the values of the free parameters (K_i, $1/n_i$, and C_{oi}) such that the differences between the isotherm data and the calculated isotherm were minimized. Each data point of the mixture isotherm was calculated from the mass balance equation

$$q_T = (C_{OT} - C_T) \cdot (V/M) \tag{4-21}$$

where q_T and C_T are the equilibrium TOC concentrations of the mixtures in the adsorbed and liquid phases, respectively, and C_{OT} is the initial TOC concentration of the bulk solution. As noted for Equation 4-17, the N expressions given by Equation 4-20 must all be satisfied for any given isotherm bottle. This set of equations may be solved with a Newton-Raphson approach as shown by Crittenden, et al.(1985), as long as the values of n_i, K_i, and C_{oi} are known for each solute. However, these

parameters were the unknowns in this study and, therefore, became free parameters in a search routine designed to minimize a squared, weighted difference expression between experimentally observed and theoretically calculated TOC concentrations in the mixture.

The following equation is the objective function to be minimized:

$$SSR = \sum_{i=1}^{m} [(C_{Ti,obs} - C_{Ti,calc}) / \sigma_{ci}]^2 \qquad (4-22)$$

where $C_{Ti,obs}$ and $C_{Ti,calc}$ are the observed and calculated TOC concentrations, respectively, in isotherm bottle i at equilibrium, σ_{ci} is the standard deviation of replicate measurements of $C_{Ti,obs}$, m is the total number of bottles (observations) used in the experiment, and SSR is the residual sum of squares. $C_{Ti,obs}$ is equivalent to the C_T variable of Equation 4-21 while the value of σ_{ci} should be calculated, not only from repeated measurements of $C_{Ti,obs}$, but also from repeated experiments at the same values of C_{OT}, M, and V. Since repeated experiments were not performed, all σ_{ci} values were set equal to the analytical error noted in Appendix B.

A method was employed to determine the maximum number of statistically valid PCs for each solution isotherm modeled. The procedure was begun by fitting a given isotherm with N = 1 (i.e., one adsorbing PC) and then calculating the corresponding value of SSR. The next two

63

steps fitted the same isotherm with $N = 2$ and $N = 3$, the SSRs of which were also calculated. After these fits were obtained, the residual root mean square error (RMSE) for each fit was calculated from

$$RMSE = [SSR / (m - p)]^{0.5} \qquad (4-23)$$

where p is the number of free parameters. For the model used in this study,

$$p = 3N - 1 \qquad (4-24)$$

One should note from Equation 4-23 that the RMSE can actually increase due to the addition of a PC and any additional PC that resulted in an increased RMSE was not used. In addition, any additional PC that did not yield a sufficient decrease in RMSE was also avoided. The determination of what constituted a sufficient decrease was somewhat arbitrary in nature and involved considerations of accuracy and computation time.

Equation 4-23 also indicates the possibility that increasing the number of observations can improve values of RMSE. Results from the 1986 data set had shown that none of the mixtures could be modeled with more than two adsorbing PCs and, therefore, the number of observations was increased for the 1987 data set. The 1987 data set provided, in general, smaller RMSEs although the use of three adsorbing PCs remained unjustifiable.

As shown by Weber, et al. (1983), humic mixtures may be comprised of a non-adsorbing fraction and, therefore, the model must be able to account for this fraction. Once the number of adsorbing PCs was determined, sensitivity analyses were performed to note the impact of the addition of a non-adsorbing PC on the isotherm fit. All of the fits exhibited a dependency of SSR on the concentration of the non-adsorbing PC (C_n) and, in all cases, some value of C_n provided a minimum in SSR. Thus, for any given mixture, the C_n that provided the smallest value of SSR was used in subsequent modeling. In addition, this value of C_n was checked with one, two, and three adsorbing PCs to ensure that the value of N determined above was still appropriate.

Example of the Procedure for Fitting Isotherms

An example is provided here to elucidate the approach used to fit isotherm data. The isotherm data set chosen for this example was obtained from the mixture in the 1987 data set that received an AOD of 5.48 mg O_3/mg TOC and biostablization. As noted above, the first step was to find the appropriate number of adsorbing PCs by using RMSE as the indicator. Table 4-1 shows the values of RMSE obtained by a fit to the data for each value of N and Figure 4-1 shows the description achieved for each case. As Figure 4-1 shows, the three models fit the data reasonably well but predict adsorption at lower solute concentrations where the data

65

TABLE 4-1

Root Mean Square Errors for Ozonated (AOD = 5.48) and Biostabilized Humics from the 1987 Data Set

Number of Adsorbing PCs (N)	RMSE
1	0.1249
2	0.0981
3	0.1561
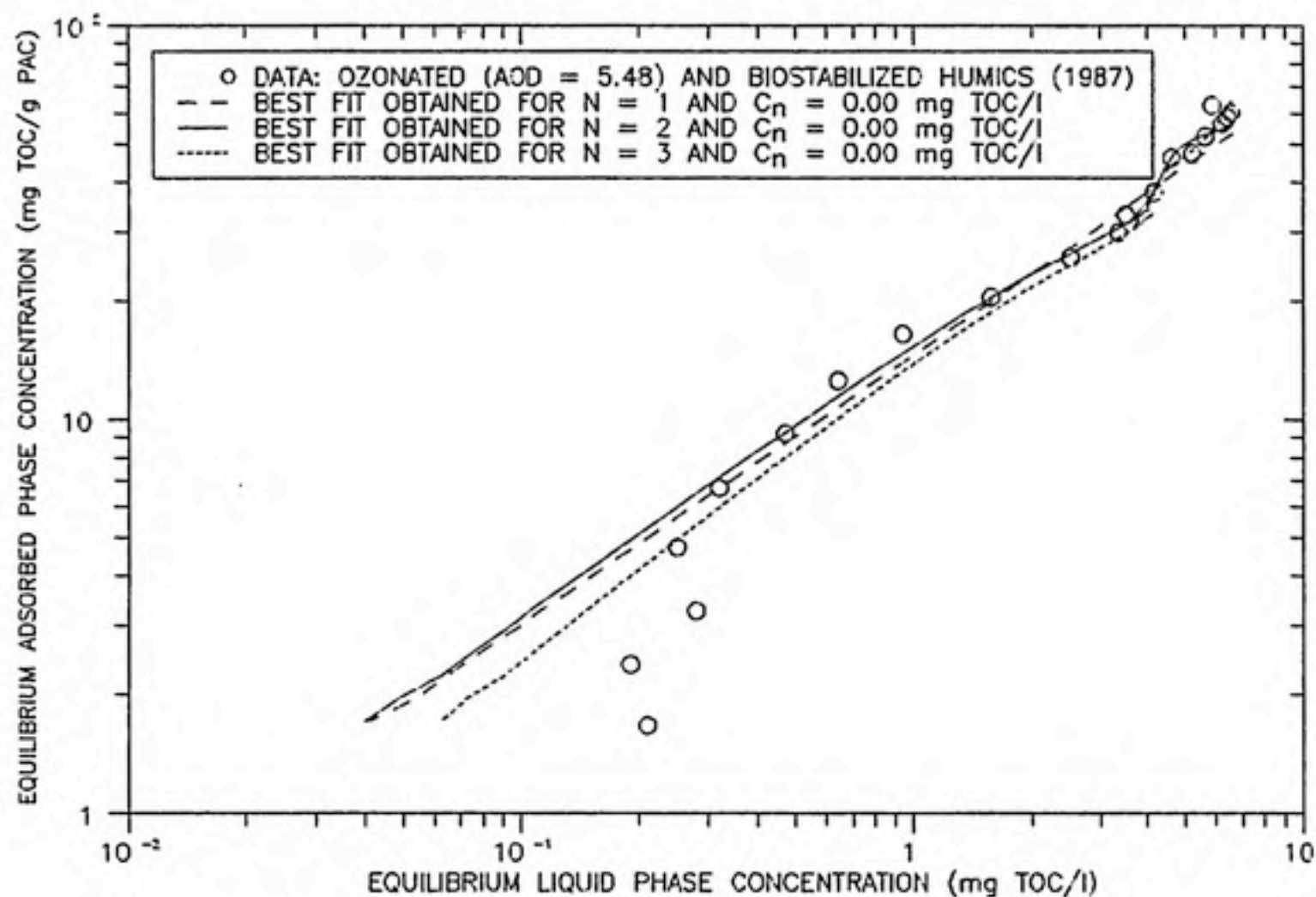
FIGURE 4-1: THE SENSITIVITY OF THE QUALITY OF FIT TO THE NUMBER OF ADSORBING PSEUDO-
COMPONENTS AT A NON-ADSORBING PSEUDO-COMPONENT CONCENTRATION OF 0.00 mg TOC/l
THE DATA REPRESENT THE ISOTHERM OF THE OZONATED (AOD = 5.48) AND BIOSTABILIZED
MIXTURE FROM THE 1987 DATA SET.

show that no further adsorption occurs. Table 4-1 shows that the RMSE was increased by the addition of the third PC and, therefore, the fit where $N = 2$ (i.e., two adsorbing PCs) is the best one in this case.

The isotherm data was then fit with the free parameters of two adsorbing PCs (C_{01}, C_{02}, K_1, K_2, $1/n_1$, $1/n_2$) and with varying values of C_n, a fixed parameter. The resulting dependence of SSR on C_n is shown in Figure 4-2 which indicates that the lowest value of SSR (i.e., the best fit) is obtained by setting C_n equal to 0.22 mg TOC/l. Figure 4-3 depicts the fit obtained by using a non-adsorbing PC in the model and compares it with the fit obtained without the non-adsorbing PC. As one can easily see, the model's description of the data is greatly enhanced when a non-adsorbing PC is included.

In order to determine that the number of adsorbing PCs was still appropriate, the data were fit with varying values of N at the value of C_n determined by the above procedure. For the isotherm data analyzed in this example, Figure 4-4 shows the resulting fits while Table 4-2 shows the resulting RMSEs. These results confirm that the isotherm data is best fit with $N = 2$ and $C_n = 0.22$ mg TOC/l. This method was employed for all isotherms and, in all cases but one, the maximum justifiable number of adsorbing PCs was two. Every mixture was also modeled with an appropriate value of C_n and the modeling results will be included for discussion in Chapter 5.
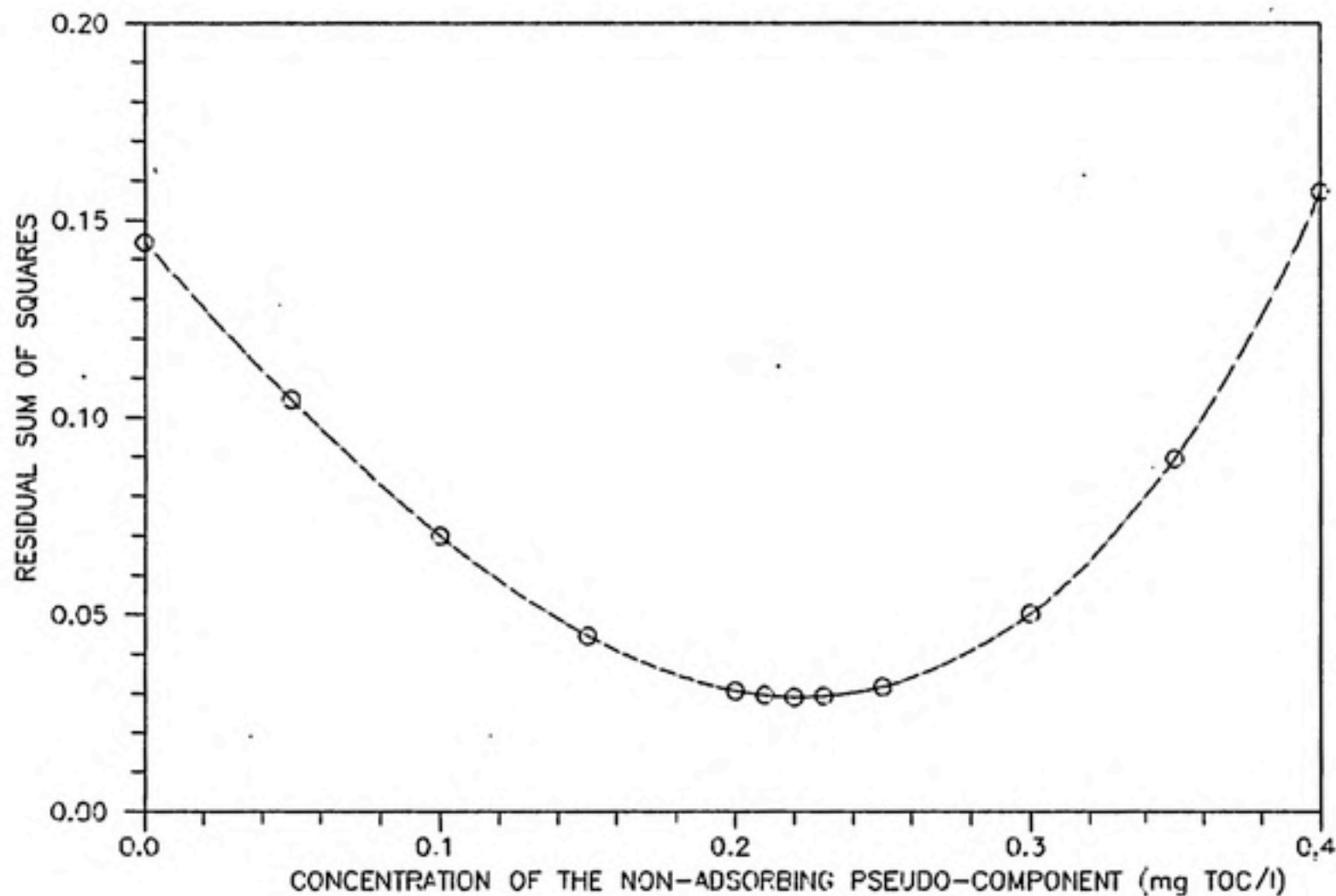
FIGURE 4-2: THE EFFECT OF THE NON-ADSORBING PSEUDO-COMPONENT CONCENTRATION ON THE QUALITY OF FIT TO ISOTHERM DATA. THE CURVE PRESENTED ABOVE WAS OBTAINED FROM A SENSITIVITY ANALYSIS ON THE ISOTHERM OF THE OZONATED (AOD = 5.48) AND BIOSTABILIZED MIXTURE FROM THE 1987 DATA SET
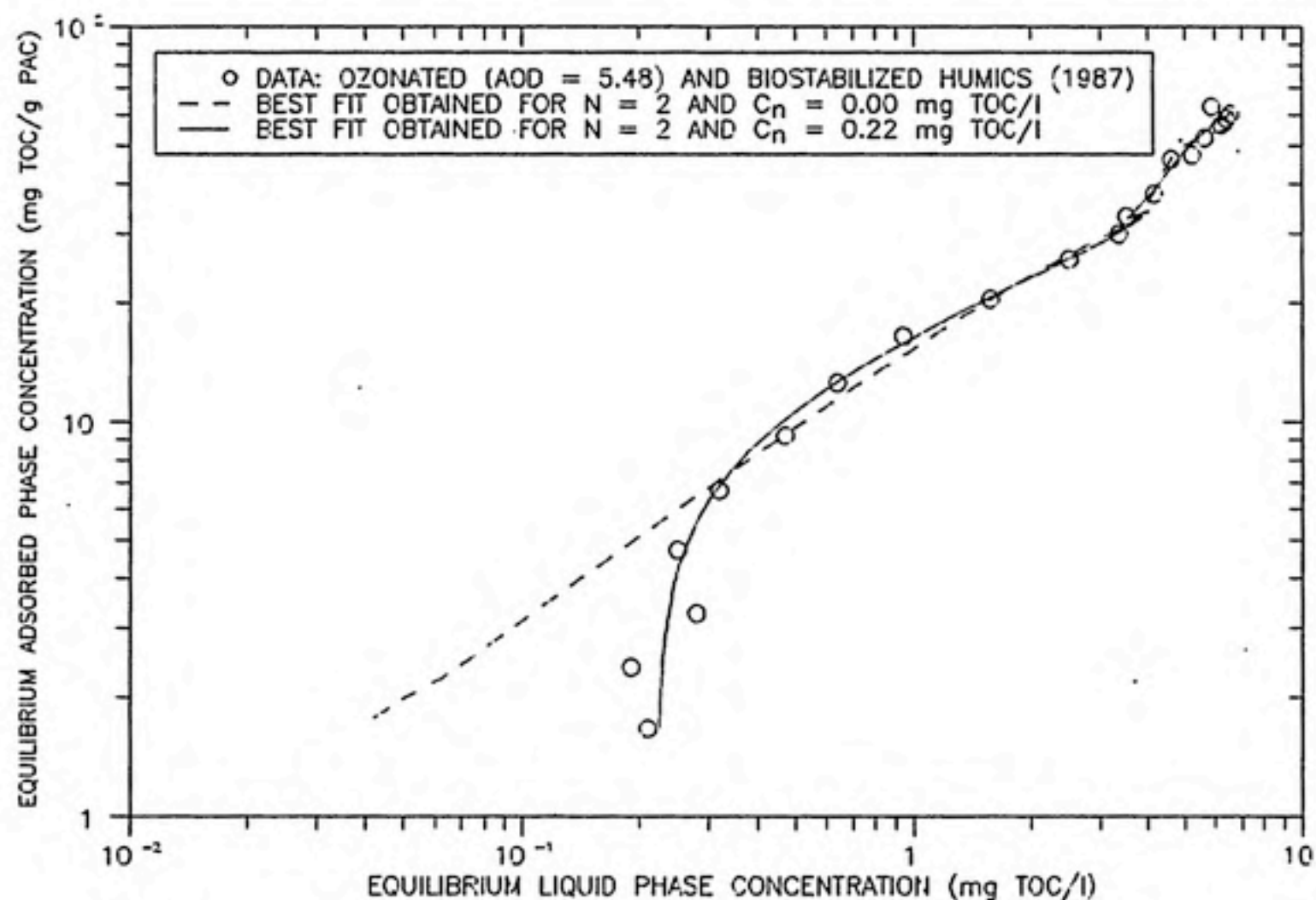
FIGURE 4–3: THE EFFECT OF ADDING A NON–ADSORBING PSEUDO–COMPONENT CONCENTRATION OF 0.22 mg TOC/l ON THE BEST FIT OF THE ISOTHERM FOR THE OZONATED (AOD = 5.48) AND BIOSTABILIZED MIXTURE FROM THE 1987 DATA SET. BOTH FITS WERE OBTAINED BY MODELING THE SYSTEM AS TWO ADSORBING PSEUDO–COMPONENTS.
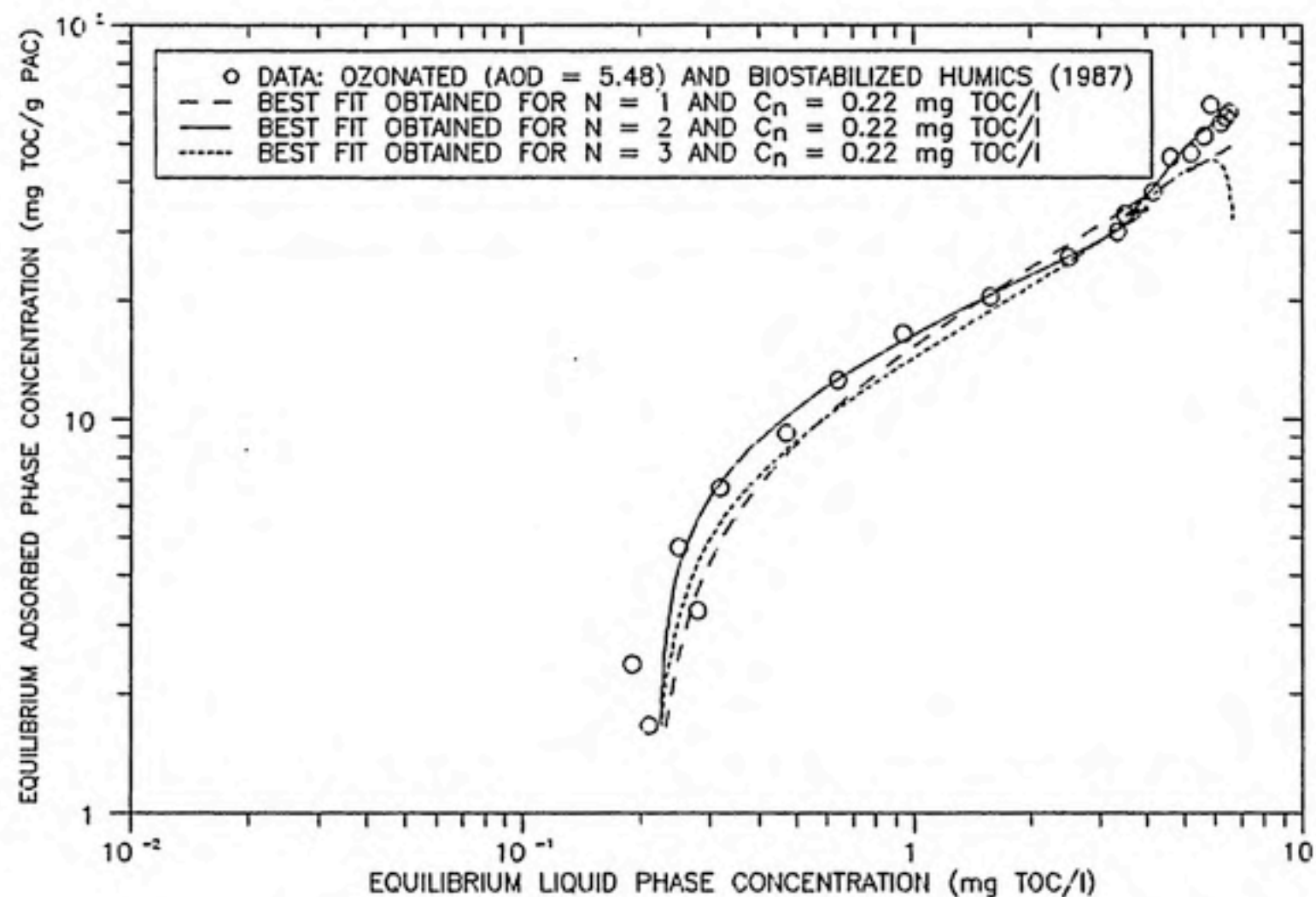
FIGURE 4-4: THE SENSITIVITY OF THE QUALITY OF FIT TO THE NUMBER OF ADSORBING PSEUDO-COMPONENTS AT A NON-ADSORBING PSEUDO-COMPONENT CONCENTRATION OF 0.22 mg TOC/l. THE DATA REPRESENT THE ISOTHERM OF THE OZONATED (AOD = 5.48) AND BIOSTABILIZED MIXTURE FROM THE 1987 DATA SET.

TABLE 4-2

Root Mean Square Errors for Ozonated (AOD = 5.48) and Biostabilized Humics from the 1987 Data Set when $C_{n,TOC} = 0.22$ mg TOC/l

Number of Adsorbing PCs (N)	RMSE
1	0.1217
2	0.0440
3	0.1595

Checking the Assumption of Equal Carbon Content

As noted earlier, Equation 4-19 expresses the assumption that each PC in a given mixture contains the same number of carbon atoms. A sensitivity analysis was performed to determine whether the quality of fit would dramatically improve with the addition of y_i variables to the IAST model. Since all of the mixtures in the 1987 data set were capable of being described by two adsorbing PCs, the two equations given by Equation 4-18 were used in the model with y_1 and y_2 as fixed parameters. In other words, the ratio y_1:y_2 was fixed for a given modeling run and the resulting value of SSR was recorded.

Table 4-3 lists the values of SSR obtained for each mixture at y_1:y_2 ratios of 100:1, 10:1, 5:1, 2:1, 1:1, 1:2, 1:5, 1:10, and 1:100. The value of SSR achieved for the 1:1 ratio was compared with each of the other SSR values and, as Table 4-3 shows, none of the ratios provided more than a 7% reduction in SSR when compared with the SSR obtained from the 1:1 ratio. Thus, the assumption that each PC contains the same number of carbon atoms appears to be appropriate enough for modeling humic substance adsorption.

Making Predictions with the IAST Model

The IAST model should be able to predict mixture isotherms at any concentration based on the results obtained

73

TABLE 4-3

Values Obtained for the Residual Sum of Squares (SSR) at Varying Ratios of $y_1:y_2$ for the 1987 Data Set

Humic Mixture	$y_1:y_2$								
	100:1	10:1	5:1	2:1	1:1	1:2	1:5	1:10	1:100
Pre-Filtered	----	6.36	6.44	8.81	6.83	7.58	7.11	7.75	13.1
Coagulated	5.09	4.06	2.97	2.46	2.46	27.1	3.00	25.1	4.99
Ozonated & Biostabilized									
AOD = 0.81 mg O_3/mg TOC	1.24	1.26	1.28	1.29	1.18	1.27	1.35	1.26	1.24
AOD = 2.43 mg O_3/mg TOC	0.99	0.74	0.76	0.78	0.65	0.73	0.72	0.74	24.6
AOD = 5.48 mg O_3/mg TOC	1.46	1.11	1.04	1.06	1.09	1.15	1.25	1.11	1.46

from the best fit of a single mixture isotherm. The prediction procedure is very straightforward since one can assume that any mixture, upon concentration or dilution, will not change in composition. In other words, the only best fit parameters that change upon dilution or concentration are the c_{oi} and c_n values and these change according to percent composition, a known variable. For example, solute i is known to be a certain fraction of the total mixture by finding $x_i = c_{oi} / c_{OT}$ for the isotherm that provided the fitted data. Then, for any change in c_{OT}, c_{oi} is appropriately adjusted by multiplying x_i by the new c_{OT}. Therefore, when one provides the K_i, $1/n_i$, and the properly adjusted c_{oi} values for each PC as input to the model, a prediction of the new mixture isotherm is achieved. This procedure is very important as it can be used to show how a certain treatment changes the adsorbability of a mixture. For example, a given treatment step may change a solution's compositon as well as its initial concentration. Therefore, if one can predict the isotherm of the new solution at the same initial concentration of the original solution, then one can determine how extensively the treatment changed the adsorbability of the original mixture through compositional changes.

The ability of IAST to predict changes in humic solution concentration was tested for the 1986 and 1987 data sets with their respective coagulated mixtures. In both cases, the original coagulated solution was diluted at a 1:2

ratio and IAST was used to predict the isotherm of the original solution from parameters obtained by the best fit of the isotherm of the diluted solution.

The results of these tests are shown in Figures 4-5 and 4-6. Both figures show that the IAST equilibrium model is capable of making reasonable predictions of the effect of initial concentration. However, the model tends to slightly overpredict the adsorbability of the original solution in the region where the weakly adsorbed components are being adsorbed (i.e., in the region of higher carbon doses and lower equilibrium TOC concentrations). After the 1986 data set was evaluated, the reason for this was thought to be due to the lack of enough data and the number of observations was increased for the 1987 data set. Since the same result was obtained in the 1987 data set, one may conclude that the adsorption of humic mixtures onto activated carbon tends to violate some of the assumptions made in developing the model. This deviation in the weakly adsorbing region was, for the purposes of this work, not considered large enough to warrant the use of a different modeling approach.

ADSORPTION KINETICS

Introduction

Prior to reaching the equilibrium state, all solutions must undergo some kinetic process that involves the transfer
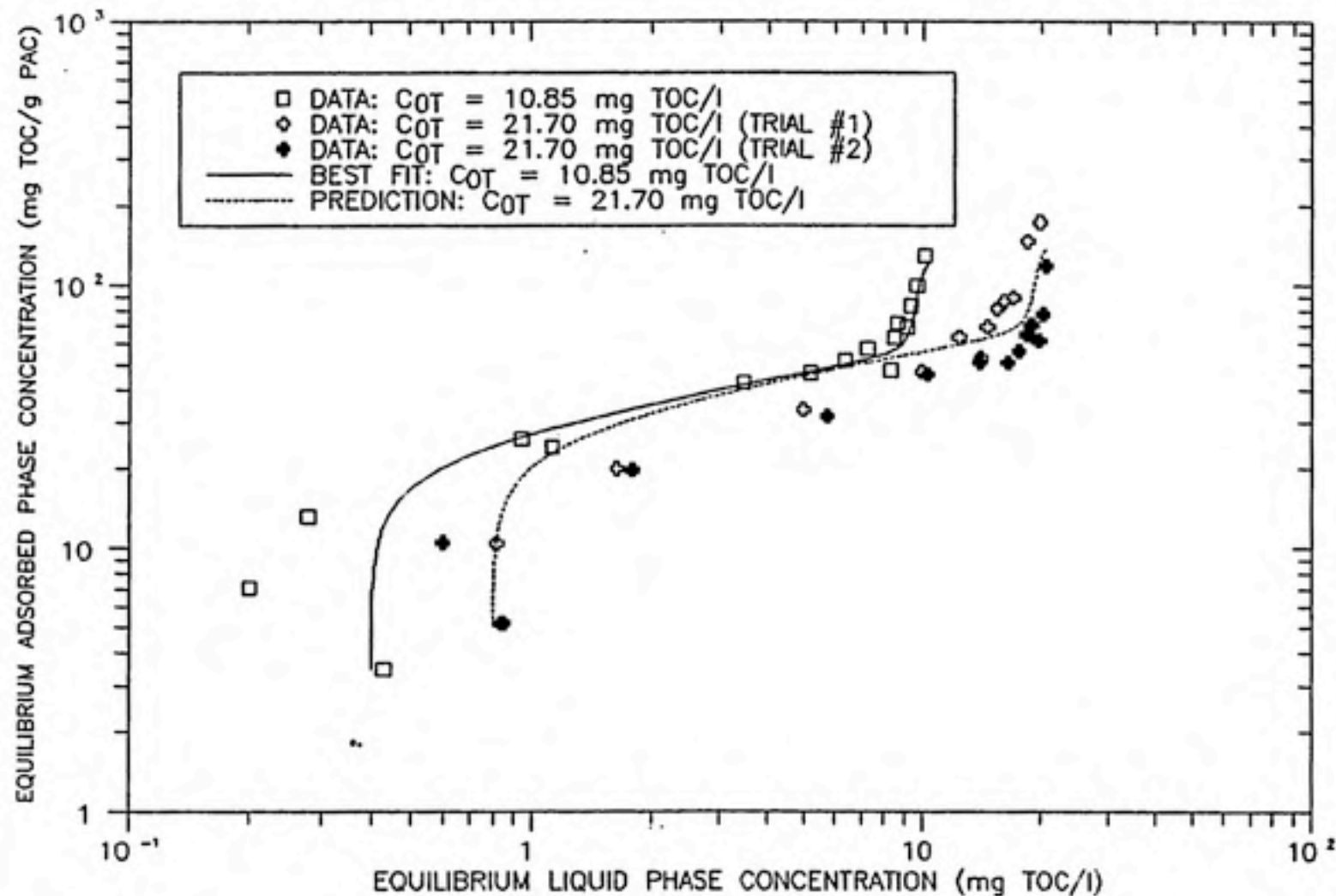
FIGURE 4–5: EFFECT OF INITIAL CONCENTRATION ON THE COAGULATED HUMIC ISOTHERM FROM THE 1986 DATA SET. THE DOTTED LINE SHOWS THE IAST PREDICTION OF THE MORE CONCENTRATED ISOTHERM BASED ON PARAMETERS OBTAINED FROM THE BEST FIT OF THE MORE DILUTE ISOTHERM.
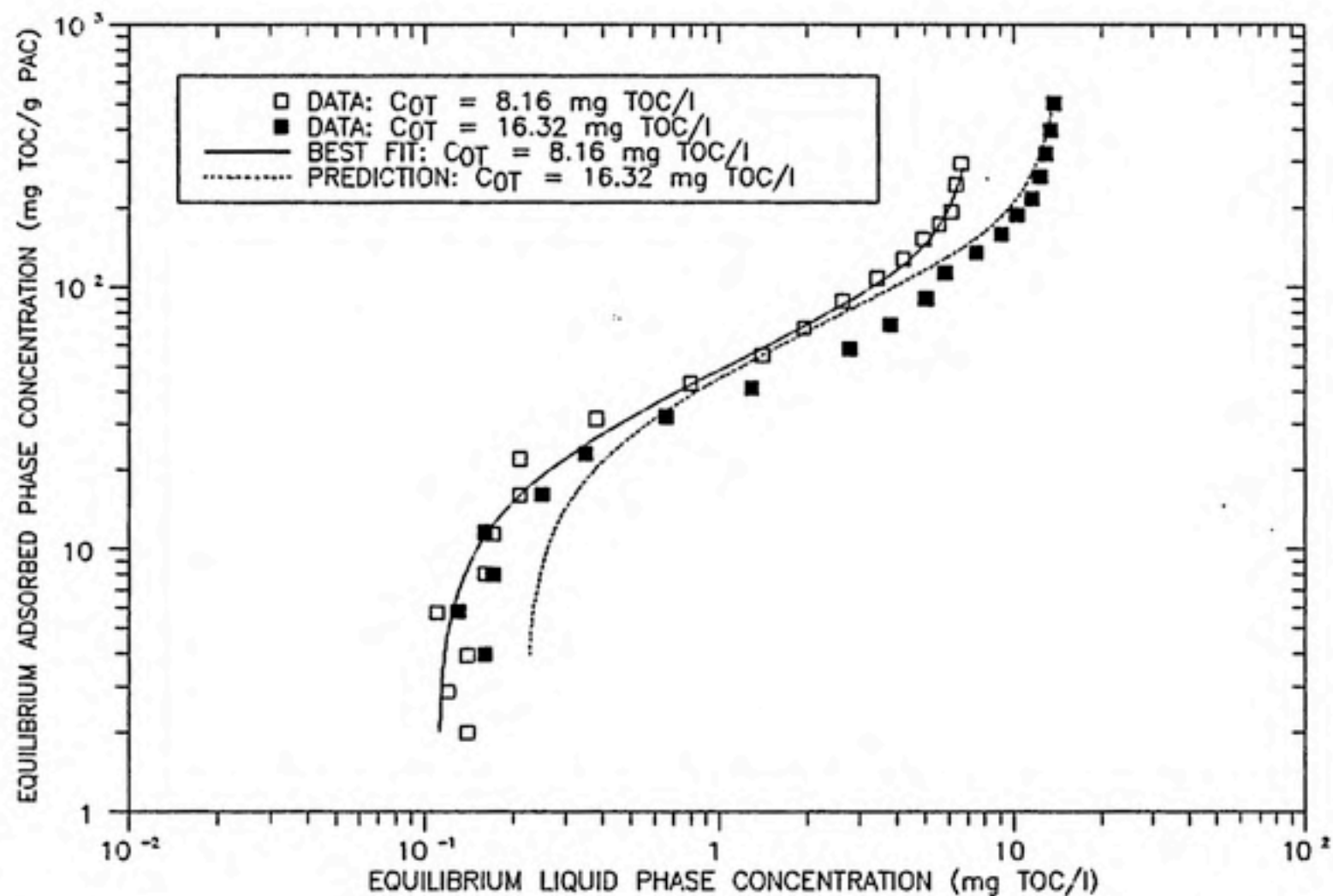
FIGURE 4-6: EFFECT OF INITIAL CONCENTRATION ON THE COAGULATED HUMIC ISOTHERM FROM THE 1987 DATA SET. THE DOTTED LINE SHOWS THE IAST PREDICTION OF THE MORE CONCENTRATED ISOTHERM BASED ON PARAMETERS OBTAINED FROM THE BEST FIT OF THE MORE DILUTE ISOTHERM.

of solute molecules from the bulk liquid phase to the adsorbed phase. The kinetics of adsorption onto activated carbon involves the consideration of many complex mechanisms and the purpose of this section is to describe the assumptions and modeling approaches used to determine mass transport properties.

External Mass Transport

Although there are many differences between batch and column adsorption processes, both have the characteristic that water is flowing past GAC particles in a relative sense. For batch systems, this flow is most likely to be turbulent in nature, thereby creating a well mixed bulk solution phase. For column systems, a well defined solute concentration that is independent of column radius can be assumed at any given axial distance in a column. Due to the relatively stationary aspect of the GAC particles, a thin film of solution is created around each GAC granule such that flow in the film is laminar in nature. As illustrated by Figure 4-7, the solute concentration near the GAC surface is lower than the solute concentration in the bulk liquid phase, thereby creating a driving force for solute transport to the particle. The diffusion of solute molecules across this laminar film is called "film diffusion" or "external mass transport", the latter term indicating that the solute transfer is being conducted outside of the GAC particle.
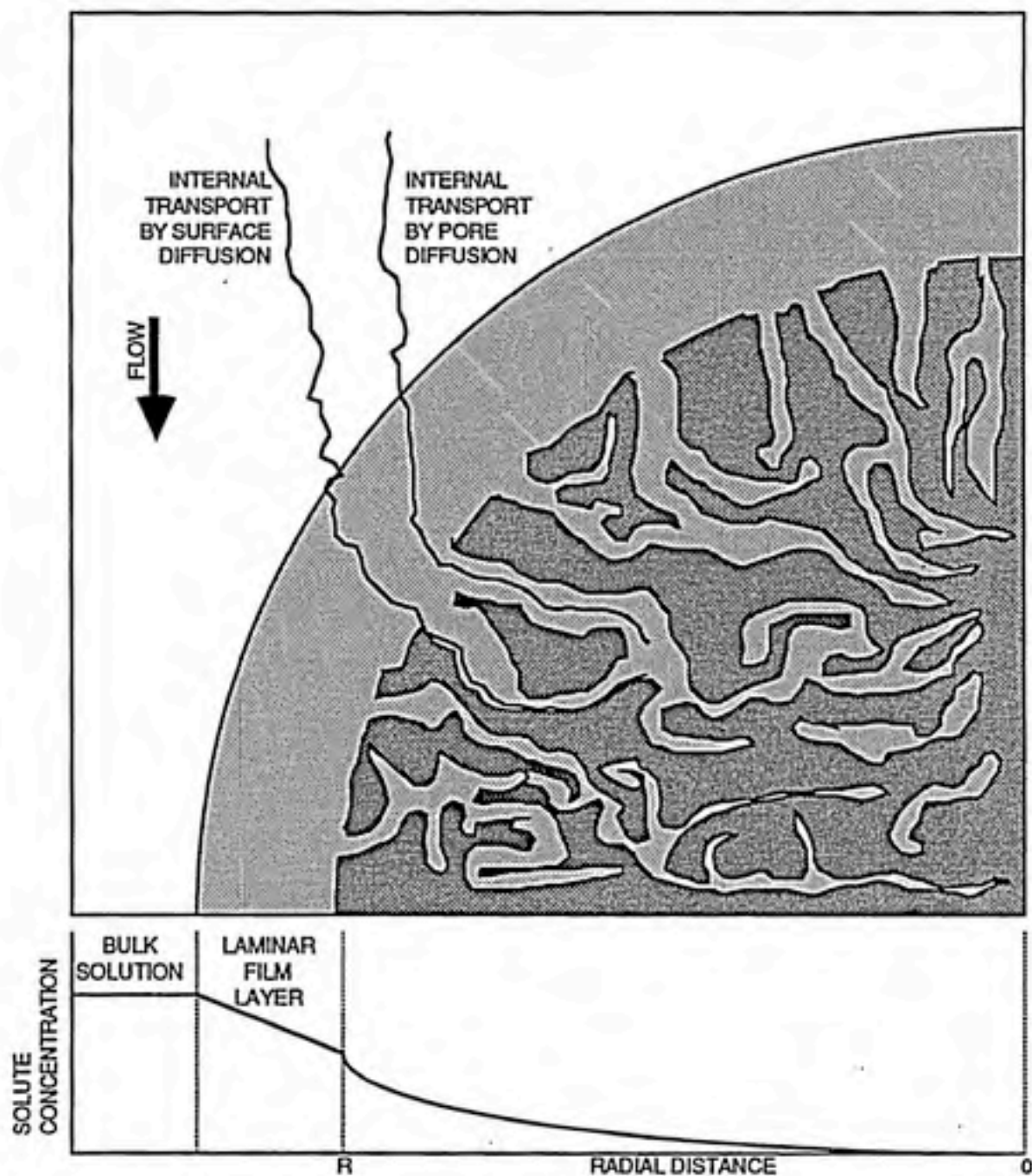
FIGURE 4-7: SCHEMATIC OF A GRANULAR ACTIVATED CARBON PARTICLE

Mass transfer rates in the laminar flow layer are generally considered to be linear as given by

$$N_T = K_L \cdot A \, (C_{tT} - C_{tS}) \tag{4-25}$$

where N_T is the mass flux of total organic carbon, A is the external surface area of the GAC particle, K_L is the external mass transfer coefficient, and C_{tT} and C_{tS} are the TOC concentrations of the bulk liquid phase and the GAC surface, respectively, at a given time t. As shown by Cornel, et al. (1986a), the following equation is derived when the assumptions of ideal plug flow and $dC_{tT} / dt = 0$ at small t are made:

$$C_{ET} / C_{OT} = \exp \left[-(M_C \cdot K_L \cdot a) / Q \right] \tag{4-26}$$

Equation 4-26 may be used on experimental data to determine the value of K_L. C_{ET} and C_{OT} were the experimentally determined effluent and influent TOC concentrations and M_C was the known mass of GAC placed in the column (see Chapter 3). The external specific surface area, a, was determined to be 7.27 m^2/kg by counting the number of granules (n) in a known mass of GAC (M), calculating the average particle diameter (d) from the sieve sizes used to screen the GAC, and substituting these quantities into

$$a = (\pi \cdot n \cdot d^2) / M \tag{4-27}$$

81

Equation 4-27 assumes that the GAC particles have a spherical shape. However, the dependence of mass transfer characteristics on particle shape can be accounted for by rewriting Equation 4-26 as

$$K_L = - [Q / (M_C \cdot a_{eff})]$$
$$\cdot \ln [C_{ET} / C_{OT}] \qquad (4-28)$$

where a_{eff} is the effective specific surface area given by

$$a_{eff} = S \cdot a \qquad (4-29)$$

S is the particle shape factor and approaches the value of 1 for spherical particles.

The value of S can be estimated by running an adsorbate with a known diffusivity through the column. For both the 1986 and 1987 data sets, paranitrophenol (PNP) was used to determine the particle shape of the GAC. The free liquid diffusivity of PNP was determined from the correlation of Wilke and Chang (1955) and the expected value of K_L was then determined from the Gnielinski correlation. This correlation, reviewed by Roberts, et al. (1985), is given by the following equation:

$$Sh = [2 + (Sh_{lam}^2 + Sh_{turb}^2)^{0.5}]$$
$$\cdot [1 + 1.5 \cdot (1 - \epsilon)] \qquad (4-30)$$

where ϵ is the porosity of the GAC bed. The Sherwood number (Sh) is a dimensionless quantity given by

$$Sh = K_L \cdot d / D_L \qquad (4\text{-}31)$$

where D_L is the free liquid diffusivity. The value of Sh_{lam} represents the contribution of mass transport in the laminar film and is given by

$$Sh_{lam} = 0.644 \cdot Re^{1/2} \cdot Sc^{1/3} \qquad (4\text{-}31)$$

while the value of Sh_{turb} represents the mass transport in the turbulent flow region and is given by

$$Sh_{turb} = [0.037 \cdot Re^{0.8} \cdot Sc]$$
$$/ [1 + 2.443 \cdot Re^{-0.1} \cdot (Sc^{2/3} - 1)] \qquad (4\text{-}32)$$

Equations 4-31 and 4-32 indicate that Sh is a function of the Reynolds number (Re) and the Schmidt number (Sc), each of which is given by the following two equations:

$$Re = u \cdot d / v \qquad (4\text{-}33)$$

$$Sc = v / D_L \qquad (4\text{-}34)$$

The value of u represents the interstitial velocity and the value of v represents the kinematic viscosity of water.

The value of K_L predicted by this correlation for PNP
was compared with the value of K_L calculated by Equation 426
from experimental results. Algebraic manipulations can show
that S is obtained from the ratio of the experimental K_L to
the predicted K_L and, for the 1986 and 1987 data sets, a
value of S = 1.54 was obtained for the GAC particles. Thus,
a value of 11.2 m^2/kg was used for a_{eff} in Equation 4-28.
The value of S obtained in this work compares favorably with
those reviewed by Roberts, et al. (1985).

The intent of examining external mass transport with
the mini-column technique was to use calculated K_L values to
obtain the "average" D_L values for any given humic mixture.
Any number of mass transfer correlations can be used for
this purpose. Roberts, et al. (1985), showed that the
Gnielinski correlation was best suited for the purposes of
the mini-column since they found it to be the only
correlation tested where the Reynold's number did not
influence the particle shape factor. In addition,
Crittenden, et al. (1987a), concluded that the Gnielinski
correlation was also the most accurate of four correlations
tested. Therefore, the values of D_L presented in Chapter 6
were determined from the Gnielinski correlation and
represent an overall free liquid diffusivity for the mixture
since attempts were not made to determine the D_L values of
the individual PCs.

The Pore-Surface Diffusion Model

Figure 4-7 also indicates the mechanisms by which internal mass transport takes place. For instance, a solute molecule can adsorb to the external surface of the GAC particle and diffuse through the adsorbed phase into the GAC pore structure. This phenomenon is known as "surface diffusion" since mass transport is along the surface of the GAC pores. In addition, a solute molecule can diffuse through the liquid phase of the pores before adsorbing to the internal surface. This process is known as "pore diffusion" and is considered to be related to the film diffusion process.

The competitive adsorption rate model, combining both internal diffusion mechanisms, is known as the pore-surface diffusion model (PSDM). This model, as described by Friedman (1984), assumes the following: (1) the pore and surface diffusion mechanisms are individually accounted for, (2) no solute-solute interactions occur in the adsorbed phase, (3) linear resistance to mass transfer exists at the external surface of the GAC, and (4) local equilibrium between the adsorbed and liquid phases can be described with the IAST multicomponent model. Thus, the PSDM requires the input of IAST parameters obtained for a given solution from an isotherm test and the free liquid diffusivity obtained from a mini-column rate test in addition to the data obtained from the batch rate test.

The process to be modeled is competitive adsorption onto GAC particles controlled by simultaneous pore and surface diffusion in a batch reactor. A TOC mass balance for each PC around the reactor gives:

$$[dc_{Bi} / dt] = - [3 \cdot M / (\epsilon_R \cdot V \cdot R^3)]$$

$$\cdot d\{ \int_0^R [q_{Pi} + (\epsilon_A \cdot c_{Pi} / rho)] \cdot r^2 \cdot dr\} / dt$$

$$\text{for } i = 1 \text{ to } N \qquad (4-35)$$

where ϵ_R is the fraction of reactor volume occupied by the bulk liquid phase, ϵ_A is the GAC porosity, rho is the apparent density of the GAC, M is the mass of GAC in the reactor, V is the total volume of the reactor (including GAC volume), and R is the mean radial distance from the center of a GAC particle to its external surface. In addition, c_{Bi} is the concentration of solute i in the bulk liquid phase and is a function of time only while c_{Pi} and q_{Pi}, the concentrations of solute i in the pore liquid phase and the adsorbed phase respectively, are functions of both time and radial distance. The following conditions are utilized at t = 0 in conjunction with Equation 4-35:

$$c_{Bi} = c_{Oi} \qquad \text{for } i = 1 \text{ to } N \qquad (4-36)$$

$$c_{Pi} = q_{Pi} = 0 \qquad \text{for } i = 1 \text{ to } N \qquad (4-37)$$

A mass balance about a radial element inside the GAC particle yields

$$(1 / r^2) \cdot d[r^2 \cdot D_{Si}(dq_{Pi} / dr) + r^2(D_{Pi} \cdot \epsilon_A / rho)$$
$$\cdot (dC_{Pi} / dr)] / dr = (dq_{Pi} / dt)$$
$$+ (\epsilon_A / rho) \cdot (dC_{Pi} / dt)$$
$$\text{for } i = 1 \text{ to } N \qquad (4\text{-}38)$$

where D_{Pi} is the pore diffusion coefficient and D_{Si} is the surface diffusion coefficient. Equation 4-38 is restricted by the following boundary conditions:

$$d\{\int_0^R [q_{Pi} + (\epsilon_A \cdot C_{Pi} / rho)] \cdot r^2 \cdot dr\} / dt$$

$$= (K_L \cdot R^2 / rho) \cdot [C_{Bi} - C_{Pi}]$$
$$\text{for } r = R \text{ and for } i = 1 \text{ to } N \qquad (4\text{-}39)$$

$$d[q_{Pi} + (\epsilon_A \cdot C_{Pi} / rho)] / dr = 0$$
$$\text{for } r = 0 \text{ and for } i = 1 \text{ to } N \qquad (4\text{-}40)$$

Equation 4-39 states that the mass flux of solute i through the laminar film at the external surface must be equal to the mass flux of solute i into the GAC particle. In addition, Equation 4-40 requires that the concentration gradient of solute i be equal to zero at the center of the GAC particle.

The above six equations are combined with the competitive equilibrium condition (Equation 4-20) to yield a set of 7N equations that are simultaneously solved by using orthogonal collocation. This method sets up a set of optimally placed points along the particle's radial axis (i.e., many points near $r = R$ where the concentration gradient is large and few points near $r = 0$ where the concentration gradient is small) and then solves the 7N simultaneous equations at each of these points after given time intervals. Each simulation was performed with a set of 14 collocation points after tests with 3, 4, 7, and 10 collocation points showed that 14 points gave only slightly different results than 10 points.

Determination of Internal Diffusion Parameters

As noted earlier, the modeling procedure involved the input of IAST equilibrium parameters and the external mass transfer coefficient. Since conditions in the batch system were different from those of the mini-column system, the values of K_F were also expected to be different. The values of K_F used for the batch rate tests were determined from D_L and the Gnielinski correlation (Equations 4-30 to 4-34) after Fettig (1986) determined the velocity through the impeller as approximately 100 m/hr. This velocity was not necessarily critical since the internal diffusion resistance was believed to be rate limiting and K_F, therefore, was not

expected to influence the results of internal diffusion modeling to a great degree. In addition to these inputs, the model required the input of GAC particle radius, apparent density, porosity, and dose.

As with the determination of D_L, the two internal diffusion coefficients were assumed to describe the kinetic behavior of each humic molecule in solution. Thus, the same D_P and D_S values were used for each PC in the competitive rate model. In this sense, they represent average values for a given humic mixture. The procedure involved the use of the PSDM to generate the total TOC concentration as a function of time for given values of D_P and D_S. These diffusion coefficients were then varied until the PSDM prediction gave a close match to the experimental data. This procedure was performed by fixing one of the diffusion parameters and systematicallly adjusting the other until the smallest residual sum of squares (i.e., the smallest difference between the predicted and observed TOC values) was achieved.

Unfortunately, the procedure did not involve the use of a regression technique, thereby implying that the smallest sum of squares does not necessarily indicate that the D_P and D_S combination achieved is the best one. For example, fixing D_P at one value and adjusting D_S until the best prediction is obtained does not necessarily provide a better combination of the diffusion coefficients than fixing D_P at a different value. In order to achieve unique combinations,

each mixture was examined with the homogeneous pore diffusion model (PDM) and the homogeneous surface diffusion model (SDM). These two models represent the opposite extremes of the PSDM since both assume only one transport mechanism. The PDM was determined by essentially setting D_S equal to zero (D_S was actually set to 1×10^{-20} cm^2/sec) and varying D_p until the smallest residual was reached. Similarly, the SDM was determined by essentially setting D_p equal to zero (D_p was also set to 1×10^{-20} cm^2/sec) and varying D_S.

Fettig and Sontheimer (1987) noted a procedure that allows for the determination of a unique combination of D_S and D_p for a given mixture. The procedure relies on additional information to characterize humic solutions: the adsorption isotherm (as measured by the bottle point method) for the solution remaining at the end of a given rate test. The PSDM can predict the concentration of each PC remaining at the end of a rate test, however, these predicted concentrations are dependent on the relative magnitudes of D_S and D_p. Therefore, the equilibrium behavior of the solution remaining at the end of a rate test is also dependent on the relative magnitudes of D_S and D_p since the equilibrium state is dependent on the initial concentrations of each PC. Combinations of D_S and D_p were used such that the predicted concentration of each PC at the end of a rate test was input into the IAST equilibrium model as an initial concentration to provide a prediction of the isotherm

describing the residual mixture. The combination that provided the best prediction of the new isotherm (i.e., the smallest sum of squares) was considered to be the best and the results provided by this technique are subsequently termed the heterogeneous diffusion model, HDM.

SUMMARY

The flow chart depicted by Figure 4-8 provides a good summary of how the data were collected and modeled. Equilibrium data were collected for each solution and described by the IAST multicomponent model such that each solution was divided into a set of three PCs (two adsorbing and one non-adsorbing). In addition, the average value of D_L was determined for each solution with the mini-column rate test and its accompanying model. These parameters were combined and input into a PSDM algorithm to simulate batch kinetic data and subsequently determine the PDM and SDM of each solution. In addition, the values of D_S and D_p were varied to find the best prediction of the equilibrium behavior of the mixture remaining at the end of a batch rate test. The resulting combination was considered the HDM of the humic mixture prior to the rate test.

TYPE OF DATA	METHOD OF ANALYSIS	PARAMETERS OBTAINED
BOTTLE POINT ISOTHERM DATA	IAST REGRESSION SEARCH FOR EQUILIBRIUM PARAMETERS	$K(i)$ $1/n(i)$ $C(0i, TOC)$ for $i = 1$ to N
BATCH RATE TEST DATA	PORE-SURFACE DIFFUSION MODEL	D(P) FROM PDM D(S) FROM SDM D(P) & D(S) FROM HDM
BOTTLE POINT ISOTHERM DATA FOR MIXTURE REMAINING AFTER BATCH RATE TEST	GNIELINSKI CORRELATION	ESTIMATED K(F) FOR BATCH RATE TEST
	GNIELINSKI CORRELATION	D(L)
MINI-COLUMN RATE TEST DATA	LOG-LINEAR REGRESSION	K(F)

FIGURE 4-8: FLOW CHART OF ANALYSIS

CHAPTER 5

EQUILIBRIUM RESULTS

EFFECT OF LONG TERM STORAGE

As noted in Chapter 3, the pre-filtered humic mixture was stored in a cool dark place for a period of 14 months between the 1986 and 1987 data sets. The differences noted in TOC between the two studies would tend to indicate changes in the mixture's adsorbability and, as shown in Figure 5-1, this was indeed the case. The pre-filtered solution in April of 1987 was adsorbed to a significantly greater extent than the original pre-filtered solution. Possible explanations for this result can be categorized in two ways, the first of which is "changes due to differences in experimental technique" and the second of which is "changes due to differences in solution composition."

There were two differences in experimental methodologies used for the two isotherms. First, a longer equilibration time (10 versus 7 days) was used for the isotherm of the 1986 data set than was used for the isotherm of the 1987 data set. This fact can not explain the observed result since a longer equilibration time would indicate better adsorbability for the pre-filtered solution of the 1986 data set (unless the rate of adsorption for the
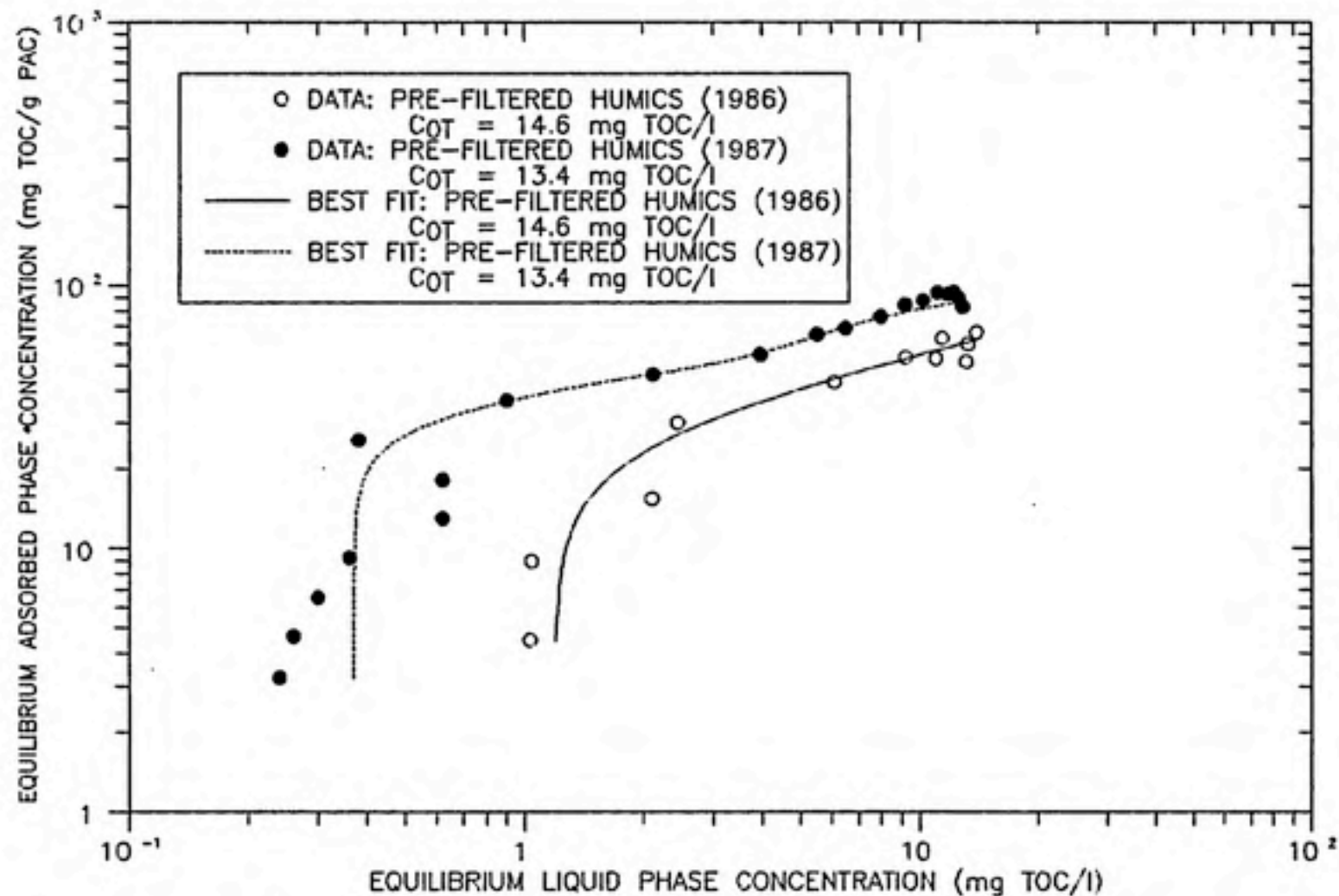
FIGURE 5-1: THE EFFECT OF AGING ON THE PRE-FILTERED HUMIC ISOTHERM. THE ISOTHERM OBTAINED FROM THE 1987 DATA SET (DOTTED LINE) WAS STARTED ON 4/13/87, SLIGHTLY OVER 14 MONTHS AFTER THE ISOTHERM OBTAINED FROM THE 1986 DATA SET (SOLID LINE). SEDIMENTATION WAS OBSERVED TO HAVE OCCURRED OVER THOSE 14 MONTHS.

solution from the 1987 data set was significantly faster than that of the solution from the 1986 data set). The second difference in technique was the use of 5 mg/l NaN_3 for biological inhibition in the 1987 data set, whereas none was used in the 1986 data set. Therefore, the 1987 pre-filtered mixture contained an additional 7.7×10^{-5} M Na^+ and could be adsorbed better as a result of the increased ionic strength. However, both solutions received the same amount of phosphate buffer to give $[Na^+] = 6.5 \times 10^{-3}$ M prior to adsorption and, as shown by Randtke and Jepsen (1982), the addition of such a relatively small concentration of Na^+ to the 1987 mixture would barely account for any increase in adsorptive capacity. Thus, neither difference in experimental methodology is thought to explain the differences between the adsorption isotherms presented in Figure 5-1.

Since the differences in methodology did not offer an explanation for the observed changes, the improved adsorbability is probably due to changes in solution composition over the 14 month storage period. Changes in the solution's chemical (i.e., concentrations of functional groups) and physical (i.e., the molecular weight distribution) nature may account for the observed increase. As noted in Chapter 3, some sedimentation was observed to have taken place when the pre-filtered solution was retrieved from storage in April of 1987. The mechanism for the observed sedimentation is unknown, however, the

possibility exists that the larger humic macromolecules were removed from solution. This would be consistent with observations by Lee, et al. (1981), and Summers (1986) that smaller molecular size fractions are better adsorbed due to the physical limitations of PAC pore sizes on larger molecular size fractions. An increase in adsorption capacity would also be observed due to an overall decrease in hydrophilicity of the humic mixture, a phenomenon that could be the result of biodegradation or the continued condensation of humic molecules. Condensation would produce higher molecular weight, less polar molecules and is a possible explanation for the greater removal of TOC by ozone in the solutions from the 1987 data set. Although the reason for the observed increase is unknown, Figure 5-1 clearly shows that the 1986 and 1987 data sets must be considered separately.

EFFECT OF ALUM COAGULATION

Figures 5-2 and 5-3 present the isotherm data obtained for the 1986 and 1987 data sets, respectively. In both cases, the isotherm data show improvement in adsorption capacity upon coagulation. However, the data do not indicate whether the improvement was due to compositional changes or to the difference in initial TOC concentration.

In order to find the appropriate explanation for the observed increase in adsorbability upon coagulation, all

FIGURE 5-2: THE EFFECT OF COAGULATION ON THE PRE-FILTERED HUMIC ISOTHERM FROM THE 1986 DATA SET. THE DOTTED LINE SHOWS THE IAST PREDICTION OF THE COAGULATED ISOTHERM AT THE SAME INITIAL CONCENTRATION AS THE PRE-FILTERED ISOTHERM. THE PREDICTION WAS BASED ON PARAMETERS OBTAINED FROM THE BEST FIT OF THE COAGULATED ISOTHERM.
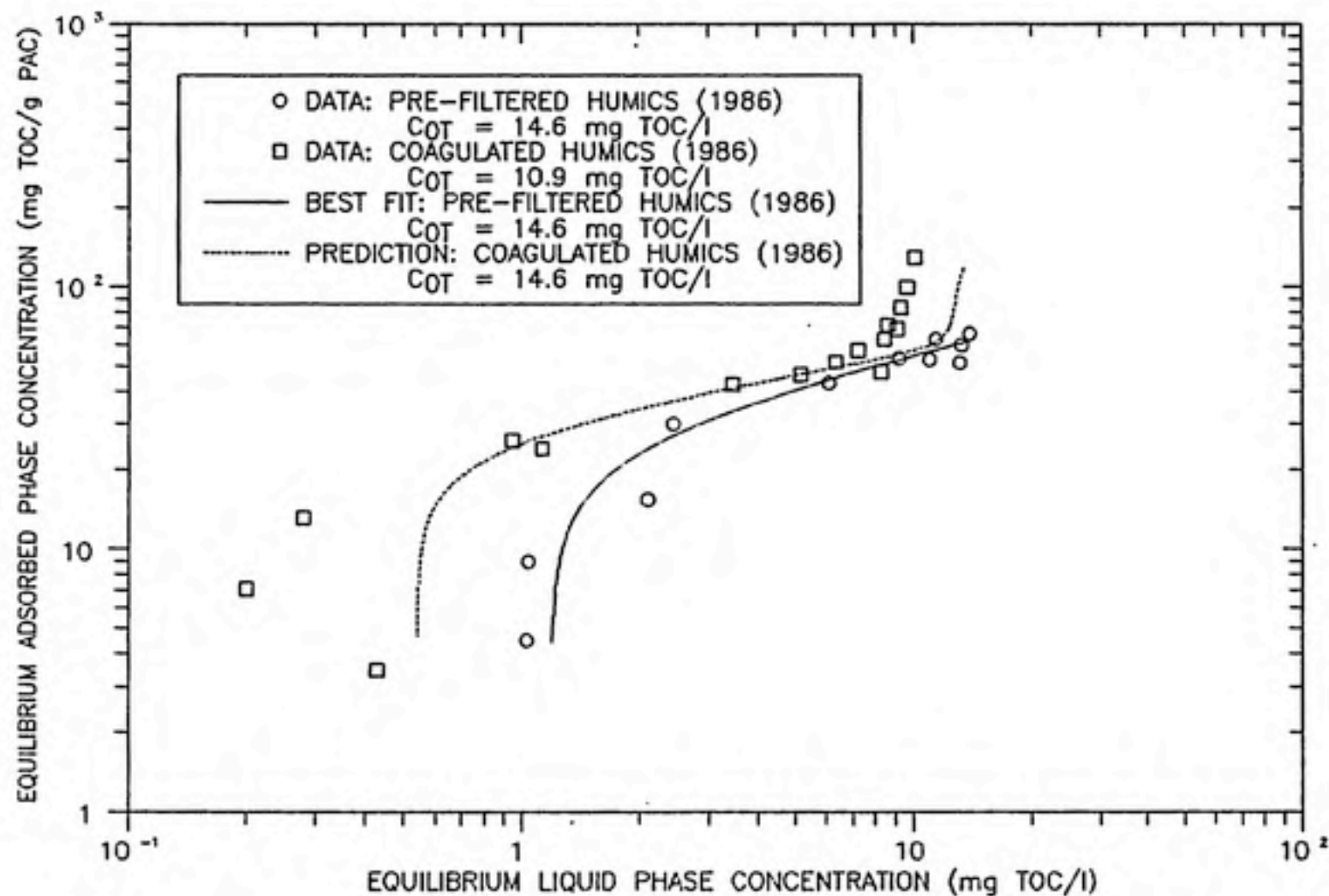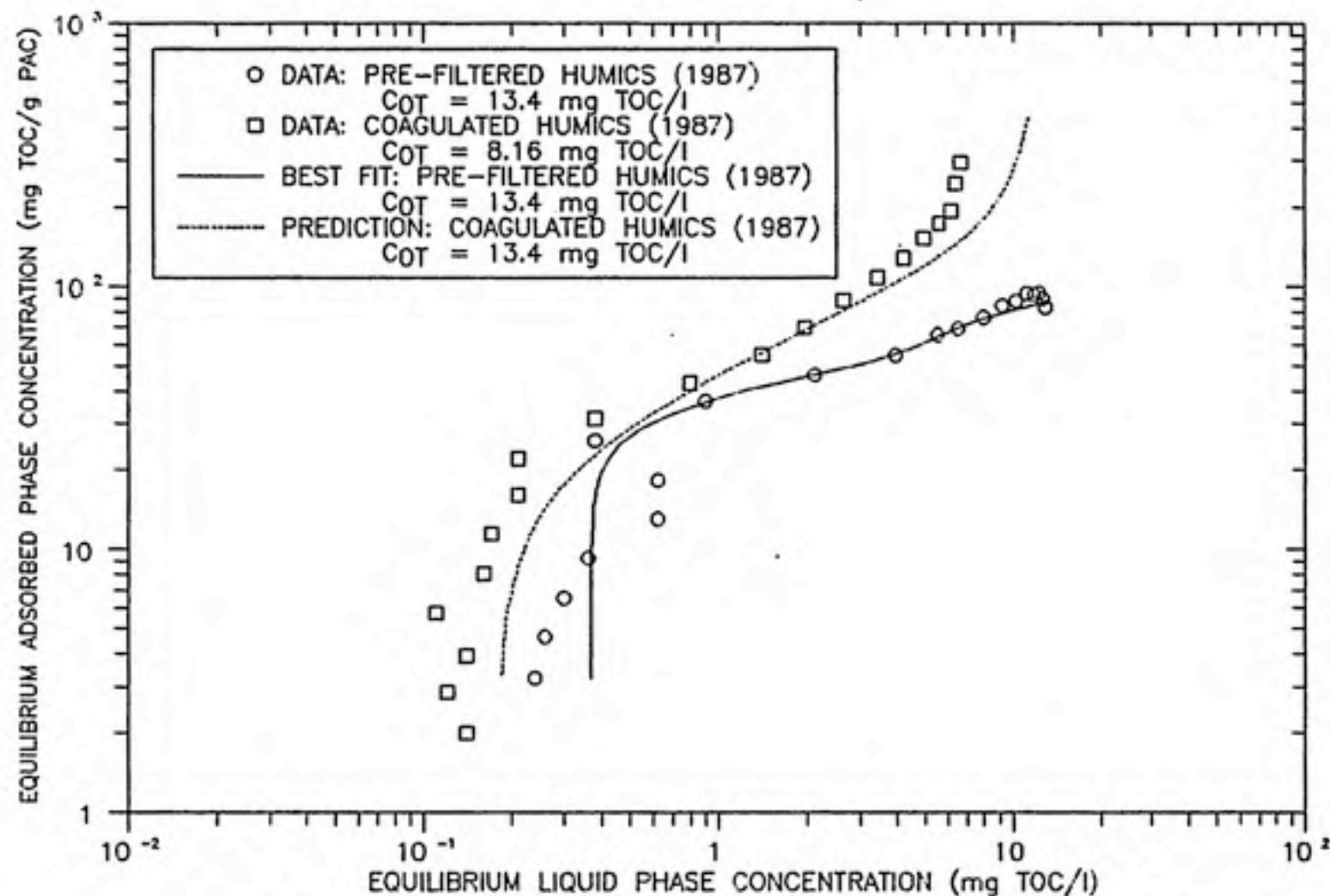
FIGURE 5-3: THE EFFECT OF COAGULATION ON THE PRE-FILTERED HUMIC ISOTHERM FROM THE 1987 DATA SET. THE DOTTED LINE SHOWS THE IAST PREDICTION OF THE COAGULATED ISOTHERM AT THE SAME INITIAL CONCENTRATION AS THE PRE-FILTERED ISOTHERM. THE PREDICTION WAS BASED ON PARAMETERS OBTAINED FROM THE BEST FIT OF THE COAGULATED ISOTHERM.

four isotherms were fit with the IAST model (according to the procedures noted earlier in Chapter 4) to determine the pseudo-component (PC) properties (K, $1/n$, C_0) of each solution. Once these properties were determined, the IAST model was used to predict the position of a coagulated humic isotherm if the coagulated solution was to have the same initial concentration as the pre-filtered solutions. The procedure used to perform these predictions was also described earlier in Chapter 4 and the ability of the IAST model to make such predictions was demonstrated in Figures 4-5 and 4-6.

The results of these predictions are plotted as dashed lines in Figures 5-2 and 5-3 and may be compared to the solid lines, which depict the best fits for the pre-filtered isotherms. This approach allows two mixtures to be compared for adsorbability without the interference of effects caused by differences in initial TOC concentration. The fact that the dashed and solid lines do not coincide proves that the changes induced in PC properties (i.e., K_i, $1/n_i$, and C_{0i}) by coagulation affect the shape of the adsorption isotherm, even when the total TOC of the two mixtures is made identical. Coagulation improves adsorbability by changing the composition of the uncoagulated solution and by decreasing the initial concentration of the uncoagulated solution.

Randtke and Jepsen (1981), after observing the same result, considered that the improvement was either due to

removal of weakly adsorbed species, changes in ionic strength as a result of added aluminum ions, or complexation between aluminum species and humic species creating species that are adsorbed better. The authors eventually concluded that the improvement was most likely a result of the complexation reactions. However, results from their own work, as well as from the work of Weber, et al. (1983), and Lee (1980), have shown that alum doses not resulting in coagulation tend to either decrease or produce no change in the adsorbability of humic solutions, thereby implying that the complexes may be less adsorbable.

Gel permeation chromatography (GPC) was used by Jodellah (1985) to examine the molecular weight distribution (MWD) of a commercial humic acid (CHA) before and after alum coagulation. The results show aggregation of humic molecules upon coagulation to shift the MWD to larger molecular sizes at 53% TOC removal and complete removal of the larger molecular sizes at 80% TOC removal. The author also notes that the alum dose resulting in 53% removal was not enough to induce precipitation. In addition, the author found decreased adsorption capacity for a CHA solution subjected to 50% TOC removal by alum coagulation. These results indicate that alum coagulation preferentially removes higher molecular weight materials as long as sedimentation takes place. Thus, the change in adsorption capacity is influenced by the ability of the alum coagulation process to change the solution's MWD.

In addition to changing the physical size characteristics of a humic solution, alum coagulation may also bring about change in the overall chemical characteristics as well. As noted in Chapter 3, the results of jar tests indicated a stoichiometric relationship between the humic carboxylic acid groups and the aluminum hydrolysis product. Therefore, the preferential removal of carboxylic humic macromolecules is conceivable. A study by van Breemen, et al. (1979), showed that iron coagulation of a fulvic acid to 60% TOC removal resulted in the removal of 96% of the carboxylic groups originally present. Since the carboxylic acid groups would tend to be hydrophilic, the solution remaining after alum coagulation could conceivably be more hydrophobic in nature than the original solution.

The extent to which such a change would improve adsorption is not known. However, the explanation of an overall decrease in molecular size is certainly adequate to explain the results observed in this work. In addition, coagulation appeared to improve adsorbability to a greater extent in the 1987 data set than in the 1986 data set. This result may be due to the higher TOC removal and, hence, higher removals of larger molecules in the coagulation stage from the 1987 data set although caution is advised in arriving at such a conclusion since the original solutions were not alike.

EFFECT OF OZONATION AND BIOSTABILIZATION

The isotherm data collected for the mixtures that were coagulated, ozonated, and biostabilized are presented in Figures 5-4 to 5-7 and, in each case, are compared with isotherm data for the mixtures that were coagulated only. As was done in comparing the adsorbability of humic mixtures before and after coagulation (see Figures 5-2 and 5-3), the IAST model was used to predict the effects of a change in initial concentration on the isotherm positions of the mixtures that were coagulated, ozonated, and biostabilized. This was accomplished by fitting each isotherm to obtain the Freundlich constants and initial concentration of each PC in a given coagulated, ozonated, and biostabilized mixture. The total TOC concentration of that mixture was increased to match that of the appropriate coagulated mixture and a new TOC isotherm was then predicted. These predictions are shown as dashed lines in Figures 5-4 to 5-7 and should be compared with the solid lines that represent the best fit isotherms for the coagulated mixtures.

The dashed line is below the solid line in each of the four figures, thereby showing that adsorbability was decreased by the combined treatments of ozonation and biostabilization. The fact that the dashed and solid lines represent the same initial TOC concentration implies that some of the decrease in adsorbability is due to compositional changes upon these treatments.

FIGURE 5-4: THE EFFECT OF OZONATION (AOD = 1.15) AND BIOSTABILIZATION ON THE COAGULATED HUMIC ISOTHERM FROM THE 1986 DATA SET. THE DOTTED LINE SHOWS THE IAST PREDICTION OF THE OZONATED AND BIOSTABILIZED ISOTHERM AT THE SAME INITIAL CONCENTRATION AS THE COAGULATED ISOTHERM.
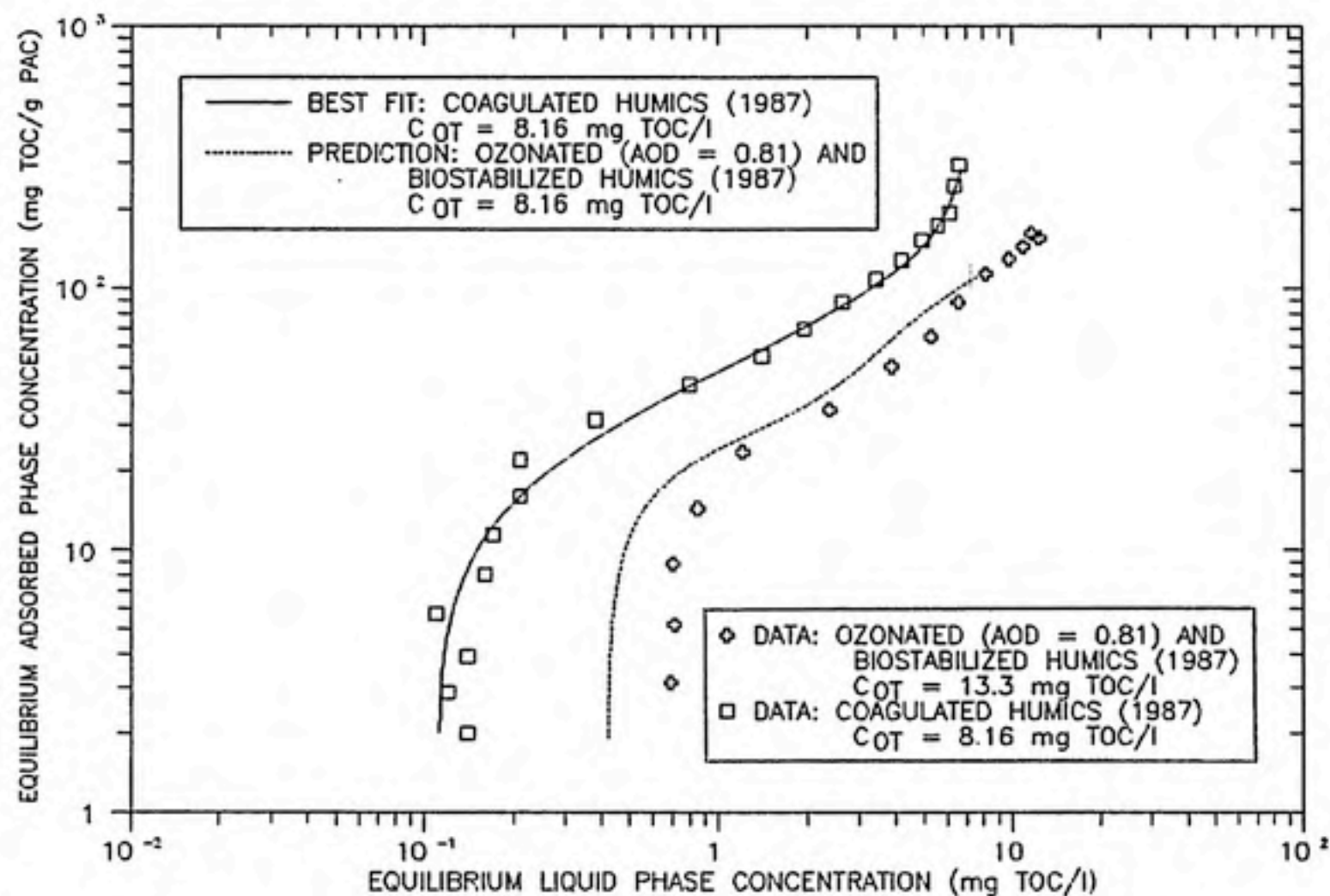
FIGURE 5-5: THE EFFECT OF OZONATION (AOD = 0.81) AND BIOSTABILIZATION ON THE COAGULATED HUMIC ISOTHERM FROM THE 1987 DATA SET. THE DOTTED LINE SHOWS THE IAST PREDICTION OF THE OZONATED AND BIOSTABILIZED ISOTHERM AT THE SAME INITIAL CONCENTRATION AS THE COAGULATED ISOTHERM.
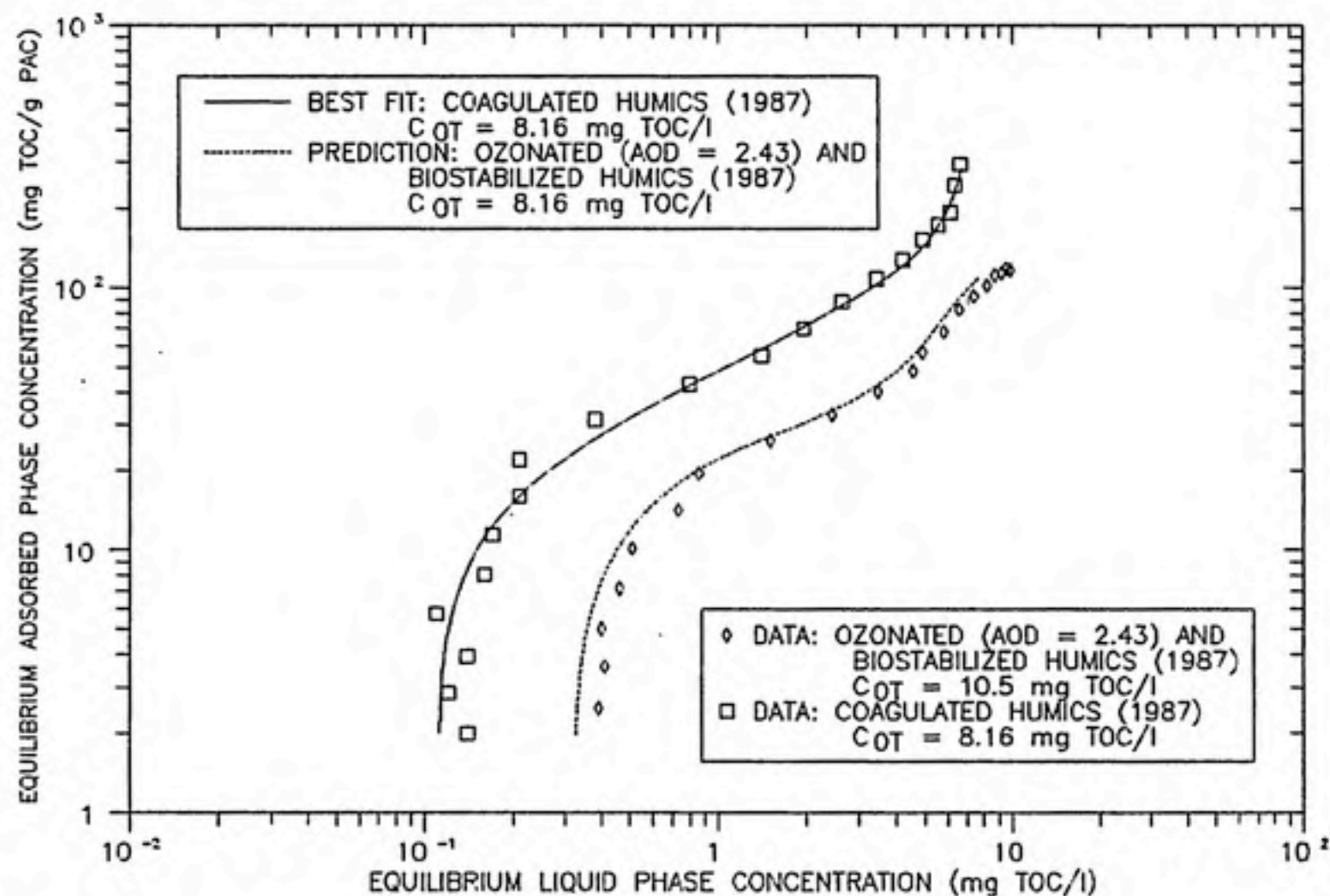
FIGURE 5-6: THE EFFECT OF OZONATION (AOD = 2.43) AND BIOSTABILIZATION ON THE COAGULATED HUMIC ISOTHERM FROM THE 1987 DATA SET. THE DOTTED LINE SHOWS THE IAST PREDICTION OF THE OZONATED AND BIOSTABILIZED ISOTHERM AT THE SAME INITIAL CONCENTRATION AS THE COAGULATED ISOTHERM.
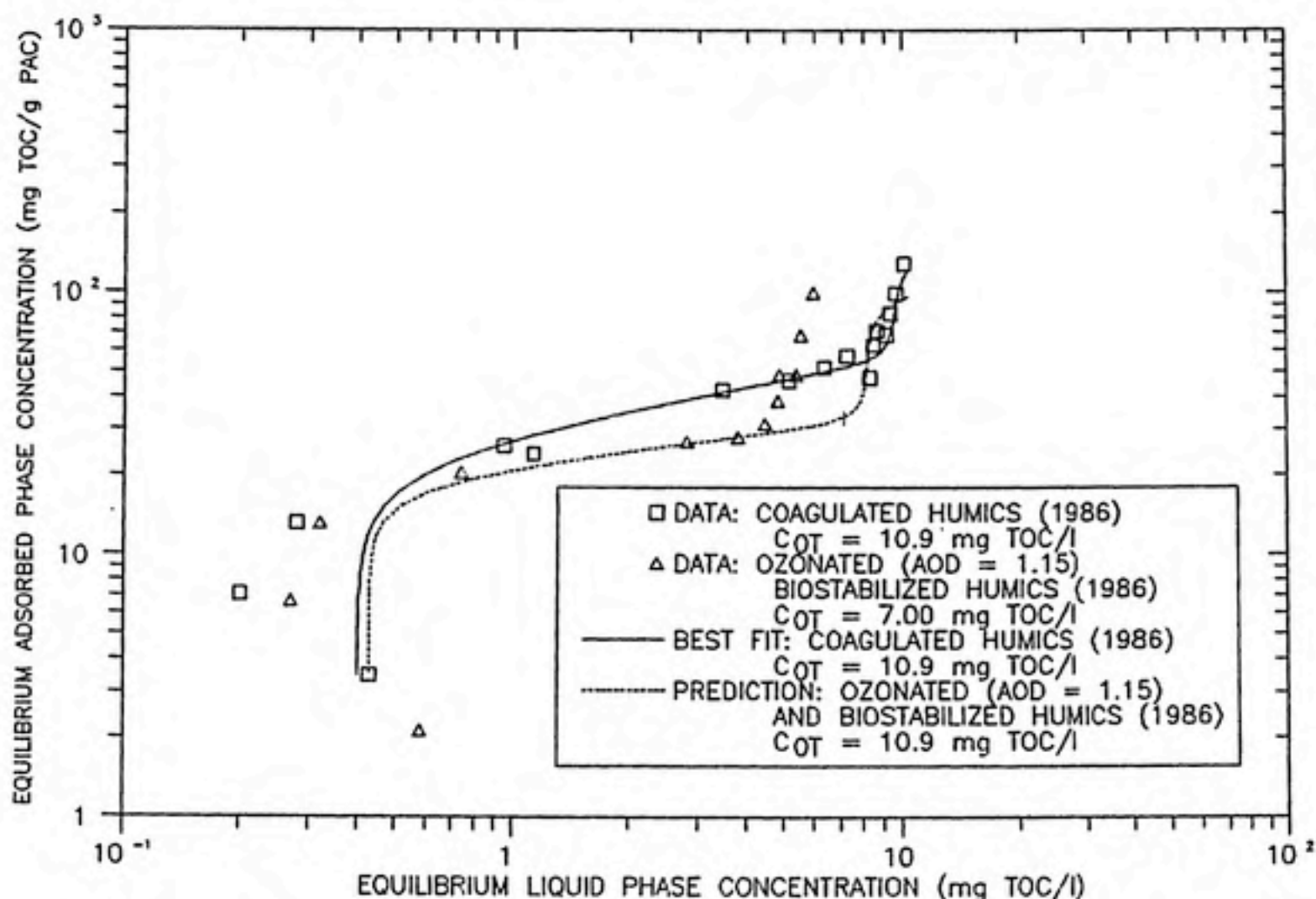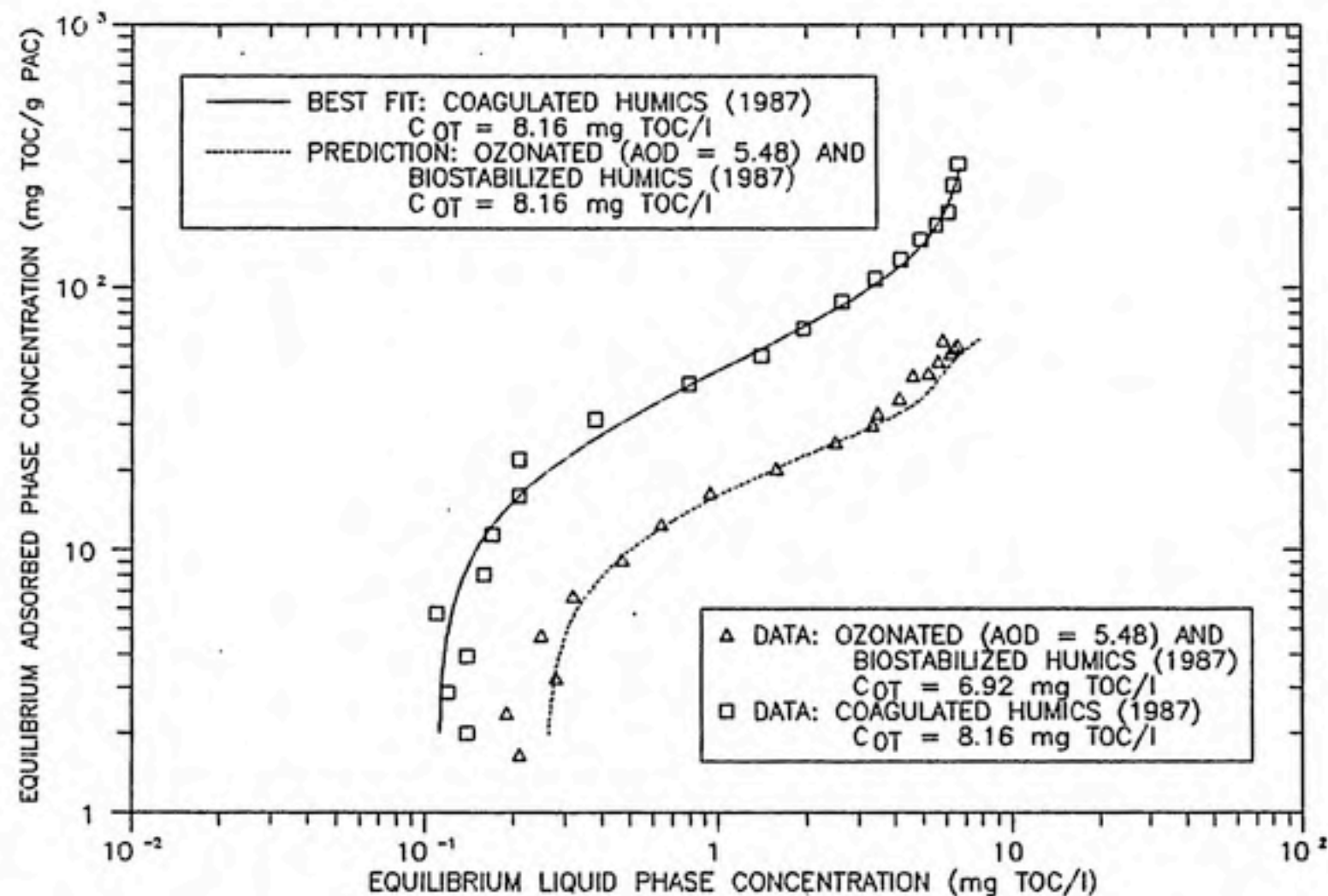
FIGURE 5—7: THE EFFECT OF OZONATION (AOD = 5.48) AND BIOSTABILIZATION ON THE COAGULATED HUMIC ISOTHERM FROM THE 1987 DATA SET. THE DOTTED LINE SHOWS THE IAST PREDICTION OF THE OZONATED AND BIOSTABILIZED ISOTHERM AT THE SAME INITIAL CONCENTRATION AS THE COAGULATED ISOTHERM.

The difference in adsorbability upon ozonation and biostabilization is least obvious in Figure 5-4 (which shows results from the 1986 data set), where similar adsorbabilities were noted in the regions dominated by strongly adsorbing species and non-adsorbing species. The region dominated by strongly adsorbing species is that part of the isotherm where observations were made from bottles having very small PAC doses such that only the strongly adsorbing species will be adsorbed. The region dominated by non-adsorbing species is that part of the isotherm where PAC doses are very large, thereby implying that all of the adsorbing species will find adsorption sites.

In order to note any dependence of adsorbability on apparent ozone dose (AOD), the predictions of the isotherms for the coagulated, ozonated, and biostabilized mixtures presented in Figures 5-5 to 5-7 were superimposed onto Figure 5-8 along with the best fit representation of the isotherm for the coagulated mixture. The results show a general decrease in adsorptive capacity with increased AOD, except in the region dominated by a non-adsorbing PC where an increase in AOD yields smaller fractions of the non-adsorbing PC.

The literature does not show entirely consistent results for the effect of ozonation on the adsorbability of humics. Sontheimer, et al. (1985) presented isotherms from Hubele (1984) that show a decrease in adsorbability upon ozonation and a subsequent increase in adsorbability, back
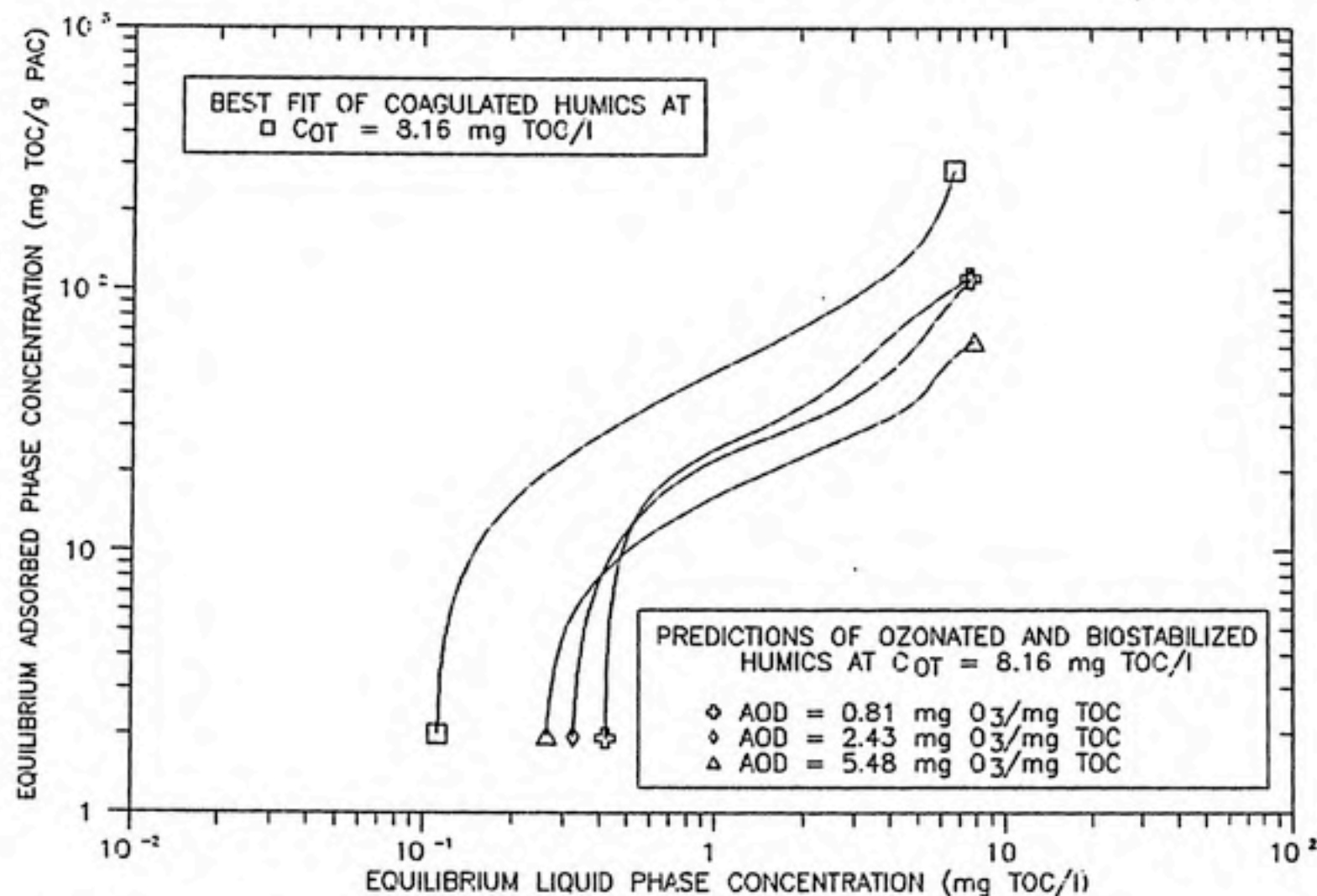
FIGURE 5-8: THE INFLUENCE OF AOD ON THE ISOTHERM OF COAGULATED HUMICS FROM THE 1987 DATA SET. THIS FIGURE SUPERIMPOSES THE PREDICTIONS OF EACH OZONATED AND BIOSTABILIZED HUMIC ISOTHERM AT THE SAME INITIAL CONCENTRATION AS THE COAGULATED HUMIC MIXTURE. DATA WERE NOT PRESENTED HERE FOR PURPOSES OF CLARITY.

to that of the original mixture, upon biostabilization. Different results were obtained by Benedek, et al. (1980), who showed a slight increase in adsorbability with an ozone dose of 0.44 mg O_3/mg TOC and a slight decrease in adsorbability with an ozone dose of 2.62 mg O_3/mg TOC. The authors concluded that ozonation did not change the isotherm of the original solution to a statistically significant extent. However, like Hubele, they found that these ozonated solutions yielded the same isotherm as the original solution after biostabilization. Chen, et al. (1987), noted decreased adsorbability at various pH values onto two activated carbons for a groundwater fulvic acid subjected to an ozone dose of 3.1 mg O_3/mg TOC. Glaze, et al. (1986), also presented isotherms that show a decrease in adsorption capacity for alum coagulated humics from Cross Lake, LA, upon receiving an ozone dose of 0.83 mg O_3/mg TOC. On the other hand, Kaastrup (1985) saw a significant increase in the adsorbability of Norwegian humic substances after ozonation at 1 mg O_3/mg TOC. Finally, Somiya, et al. (1986), presented a series of humic acid isotherms at a wide range of 10 different ozone doses and found fairly inconsistent changes in adsorbability.

There are several ways in which the results of this work and the results of others may be explained. First, being a very reactive oxidant, ozone would be expected to produce solutions comprised of a higher percentage of smaller molecules. Using ultrafiltration, Anderson, et al.

109

(1986), showed this to be the case and found that higher ozone doses produced larger fractions of smaller molecules. The same results were observed by Kaastrup (1985), Chen, et al. (1987), Flögstad and Ödegaard (1985), and Lienhard and Sontheimer (1979). Therefore, ozone would be expected to increase the adsorbability of those macromolecules that would otherwise be excluded due to pore size limitations.

Ozonation is also believed to increase the polarity of humic mixtures as evidenced by increased adsorption on polar adsorbents such as activated alumina (Chen, et al., 1987) and calcium carbonate (Lienhard and Sontheimer, 1979). A literature review by Bailey (1972) shows many reaction mechanisms between organics and ozone known at that time and indicates the production of many polar functional groups. Hoigné and Bader (1979) also indicate the formation of such functional groups upon ozonation. These results would lead to the decrease of humic substance adsorbability due to the resulting increase in hydrophilicity. Therefore, the extent of physical and chemical changes upon ozonation must be considered together in order to anticipate changes in adsorbability. Thus, one would expect waters having a high concentration of extremely large molecular materials (such as those studied by Kaastrup) to adsorb better after ozonation while other waters (such as those studied by Chen, et al.) would see decreased adsorbability.

Another indication of the change in solution composition upon ozonation is the increase in the

biodegradability of humic solutions as noted by Stephenson, et al. (1980), Yamada, et al. (1986), and Glaze, et al. (1981). The results of this work and those of Stephenson, et al., indicate that biological uptake of TOC increases with AOD, thereby implying that the extent of compositional changes upon ozonation is dependent on the AOD applied. In any case, the increased adsorbability observed upon biostabilization in Hubele's work, as well as in the work of Benedek, et al., may be due to the biological degradation of the highly polar molecules formed by ozonation. In regard to the results of this work, the isotherm observed after ozonation and biostabilization in the 1986 data set (Figure 5-4) was much closer to that of the coagulated mixture than the isotherms of the ozonated and biostabilized mixtures in the 1987 data set. As shown in Table 3-3, the percent removal of TOC after both ozonation and biodegradation in the 1986 data set was greater than that for a similar ozone dose in the 1987 data set. In addition, the decrease due to ozonation alone was much smaller for the solution in the 1986 data set than it was for those of the 1987 data set. These results indicate that more biodegradable components may have been created by the ozonation procedure of the 1986 data set. This latter observation may explain why the positions of the isotherms in the 1987 data set did not return all the way back to the position of the coagulated isotherm.

EFFECT OF TREATMENT ON IAST PARAMETERS

The values obtained for the Freundlich constants and initial concentrations of each PC from the best fit to each solution isotherm are presented in Table 5-1 to show how the various treatment steps affected them. The pre-filtered mixture from the 1986 data set was modeled with only one adsorbing PC while the pre-filtered mixture from the 1987 data set was modeled with two adsorbing PCs. However, just over 90% of each mixture's initial TOC was attributable to one adsorbing PC, a fairly homogeneous mixture in so far as adsorbability is concerned. The adsorbability of the major adsorbing PC in the 1987 data set, as measured by its Freundlich constants, was much stronger than that of the adsorbing PC in the 1986 data set. This suggests that the aging process increased the adsorbability of the pre-filtered solution.

The results from the 1986 data set clearly reveal improvement upon coagulation because the Freundlich constants for the two adsorbing PCs of the coagulated mixture change to reflect being more strongly adsorbing than the one adsorbing PC of the pre-filtered mixture; moreover, the percent composition of the non-adsorbing component decreased. The Freundlich constants obtained from the 1987 data set, however, do not show such a clear trend. Instead, the major PC of the coagulated mixture has a lower adsorbability than the major PC of the pre-filtered mixture.

TABLE 5-1

IAST Equilibrium Model Results

Humic Mixture	Pseudo-Component 1			Pseudo-Component 2			Non-Adsorbing Pseudo-Component
	K	1/n	%C_{OT}	K	1/n	%C_{OT}	%C_{OT}
1986 Data Set							
Pre-Filtered[a]	25	0.36	92	---	----	--	8
Coagulated	31	0.27	84	127	0.20	12	4
Ozonated & Biostabilized							
AOD = 1.15 mg O_3/mg TOC	23	0.17	71	87	0.14	25	4
1987 Data Set							
Pre-Filtered	51	0.21	91	14	0.05	7	2
Coagulated	41	0.47	79	454	0.98	20	1
Ozonated & Biostabilized							
AOD = 0.81 mg O_3/mg TOC	49	0.48	74	12	0.16	21	5
AOD = 2.43 mg O_3/mg TOC	48	0.54	63	14	0.14	33	4
AOD = 5.48 mg O_3/mg TOC	20	0.42	70	52	0.22	27	3

[a]A second pseudo-component was found to be statistically insignificant for the pre-filtered mixture from the 1986 data set.

Meanwhile, the minor PC of the coagulated mixture shows Freundlich constants that imply increased adsorbability and, moreover, its increase in percent composition implies a greater contribution to the overall adsorbability of the coagulated mixture than the minor PC of the pre-filtered mixture. Therefore, the Freundlich constants and initial concentrations of the PCs are not always easy to interpret. The combined treatment of ozonation and biostabilization also yields parameter changes that are difficult to interpret. Therefore, the graphical representations of the data and model predictions in presented in Figures 5-2 to 5-8 are preferable for studying the effects of any treatment process on adsorption.

THE NORMALIZED ADSORPTION ISOTHERM

The work of Summers (1986) has provided some insight into the polyelectrolytic nature of humic substance adsorption. The author points out that the effects of initial concentration (as shown in Figures 4-5 and 4-6 of this work) are the result of the heterodisperse nature of humic solutions. A heterodisperse solution would contain molecules having a wide range of sizes while a monodisperse solution would be comprised of molecules having the same sizes. Therefore, the concept of heterodispersity is entirely physical in nature. Polymer chemists have observed that the adsorption of a given polymer is dependent on the

114

ratio of adsorbent surface area to solution volume as a result of their heterodisperse nature (Fleer and Lyklema, 1983). In effect, the dependency of adsorption on this ratio can be accounted for by constructing a Freundlich isotherm plot for which the equilibrium liquid phase concentration is normalized by the PAC dose (Summers, 1986).

Figures 5-9 and 5-10 show the application of the nomalized adsorption isotherm to the results obtained during the 1987 data set. These figures indicate that the procedure does exceedingly well at eliminating the effects of initial concentration presented earlier in Figures 4-5 and 4-6 for the coagulated mixture isotherms. Summers shows similar results for a commercial humic acid at ten different initial concentrations ranging from 2.2 mg TOC/l to 141 mg TOC/l, a soil fulvic acid at five different initial concentrations ranging from 3.21 mg TOC/l to 17.4 mg TOC/l, an aquatic humic acid at three different initial concentrations ranging from 3.18 mg TOC/l to 9.62 mg TOC/l, and an aquatic fulvic acid at three different initial concentrations ranging from 2.90 mg TOC/l to 9.05 mg TOC/l.

The linearity observed by Summers, however, was restricted in this study to the region of the isotherm where normalized liquid phase concentrations exceeded 1 mg TOC/g PAC. Equilibrium concentrations below this value were indicative of the region where the influence of non-adsorbing species became significant. Summers did not
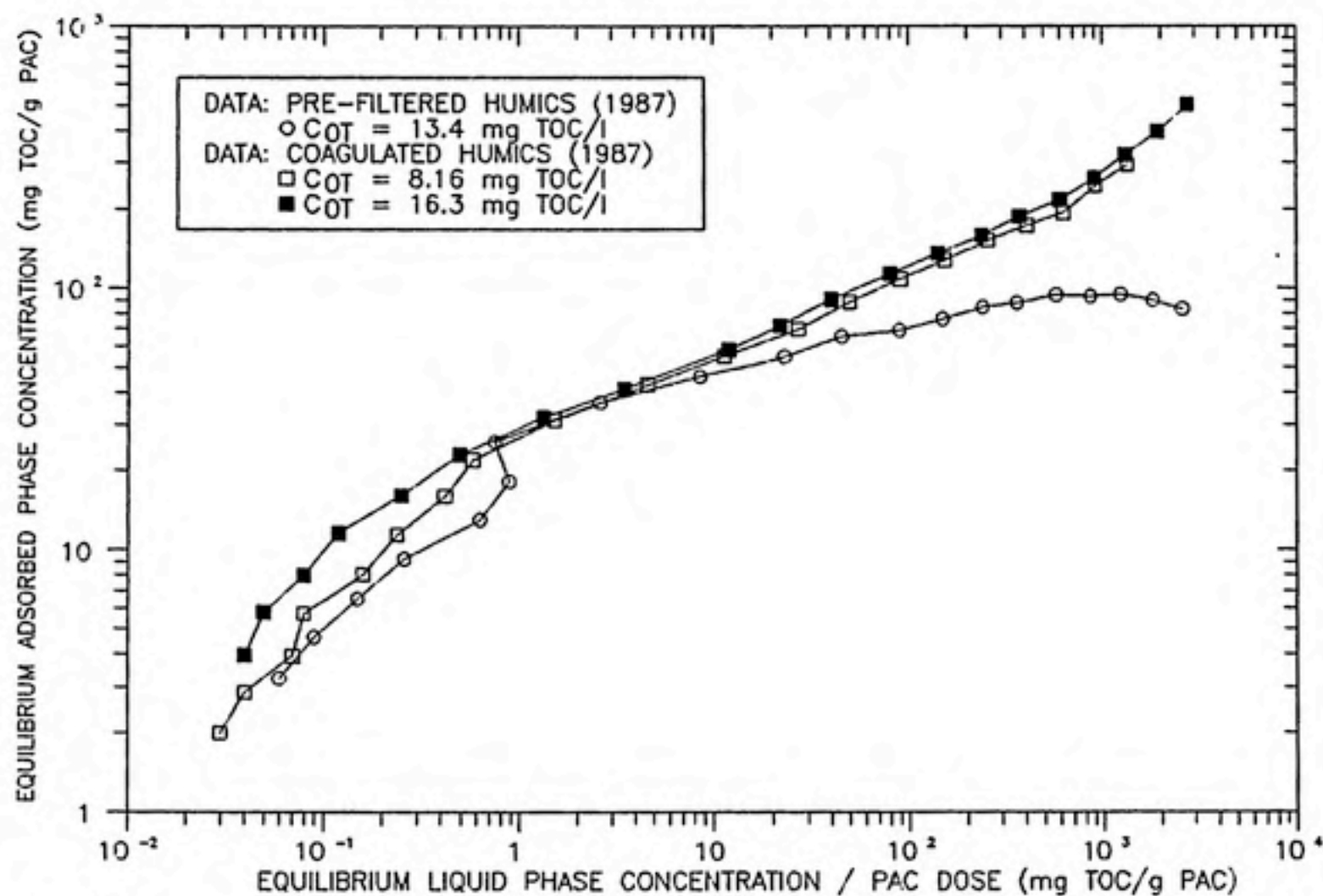
FIGURE 5-9: THE EFFECT OF COAGULATION ON THE PRE-FILTERED HUMIC ISOTHERM WHEN THE
EQUILIBRIUM LIQUID PHASE CONCENTRATION IS NORMALIZED BY THE PAC DOSE. ALL OF THE
ISOTHERMS PRESENTED HERE LOSE THEIR LINEARITY WHEN THE NON-ADSORBING PC BEGINS
TO DOMINATE AT LARGE PAC DOSES.
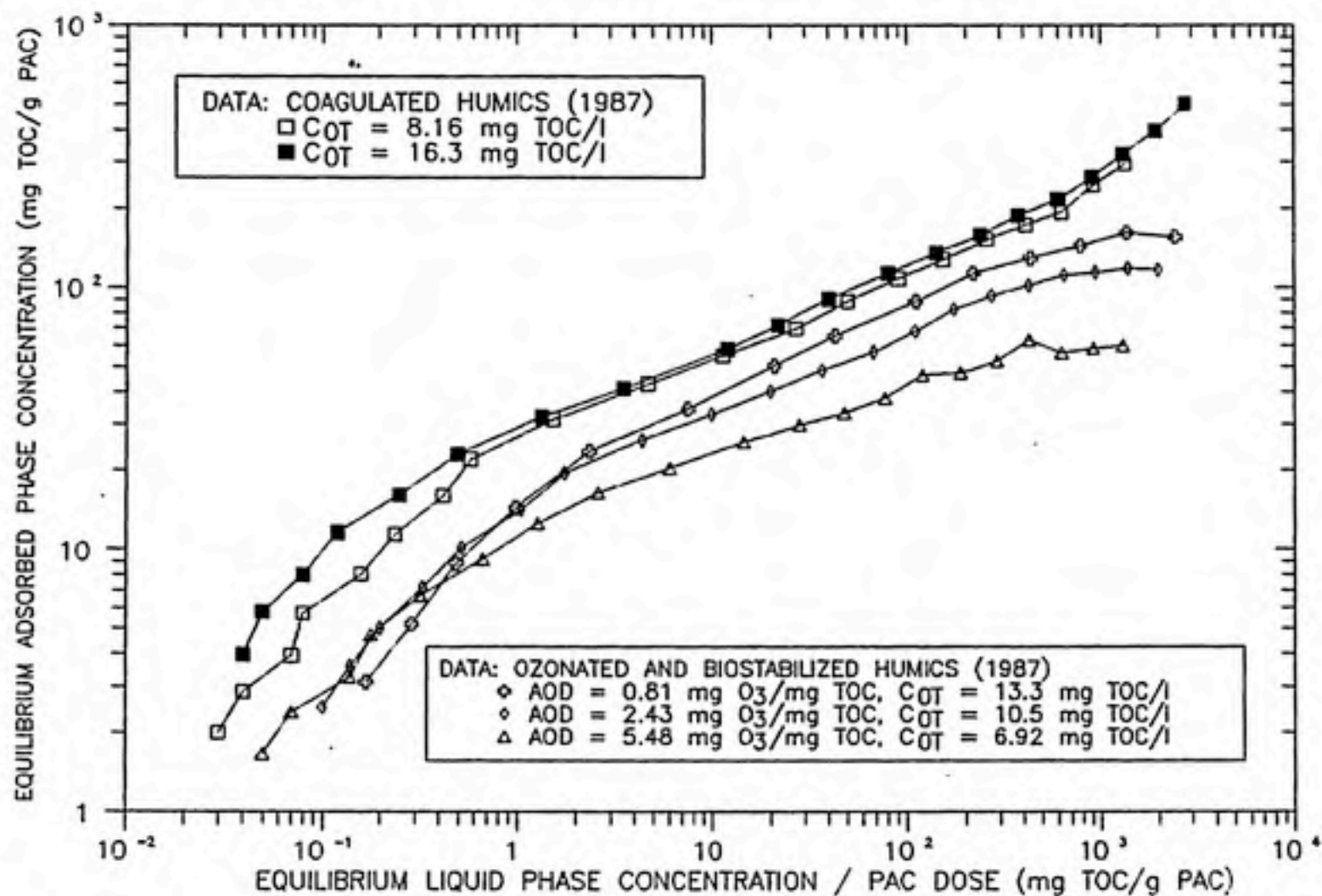
FIGURE 5-10: THE EFFECT OF OZONATION AND BIOSTABILIZTAION ON THE COAGULATED HUMIC ISOTHERM WHEN THE EQUILIBRIUM LIQUID PHASE CONCENTRATION IS NORMALIZED BY THE PAC DOSE. THIS FIGURE SHOWS THAT ADSORBABILITY DECREASES WITH OZONE DOSE AND THAT EACH ISOTHERM LOSES ITS LINEARITY WHEN THE NON-ADSORBING PC BEGINS TO DOMINATE.

acknowledge the existence of a non-adsorbing component in any of his mixtures.

Figures 5-9 and 5-10 provide a clear qualitative display of how various treatments affect the adsorbability of humic solutions through compositional changes. Coagulation is shown to increase adsorbabaility in most regions (Figure 5-9) while the additional treatment with ozonation and biostabilization is shown to decrease adsorbability, the extent of which depends on the AOD.

The effects of treatment on adsorbability can be quantified using the normalized adsorption isotherm:

$$q_T = K_T \cdot (C_T / D)^{1/n_T}$$

$$\text{for } (C_T/D) > 1 \text{ mg TOC/g PAC} \qquad (5-1)$$

where D is the PAC dose and is equilivalent to the ratio of mass of adsorbent added to volume of solution present. The deviation from linearity at $(C_T/D) < 1$ mg TOC/g PAC may be caused by non-adsorbing species and restricts the use of this approach. The resulting values of K_T and $1/n_T$ are posted in Table 5-2 and represent average properties of the mixture.

The K_T values presented in Table 5-2 indicate a decrease in adsorptive capacity for each treatment stage. However, this result is somewhat misleading because K_T is calculated only at the normalized concentration of 1 mg TOC/g PAC. In addition, Figure 5-9 shows that the overall

118

TABLE 5-2

Results from the Normalized Freundlich Equation

Humic Mixture[a]	K	1/n
Pre-Filtered	33	0.15
Coagulated	26	0.34
Ozonated & Biostabilized		
AOD = 0.81 mg O_3/mg TOC	21	0.29
AOD = 2.43 mg O_3/mg TOC	18	0.27
AOD = 5.48 mg O_3/mg TOC	13	0.23

[a]All mixtures in this table are from the 1987 data set.

adsorbability is improved upon coagulation. The Freundlich exponent, $1/n$, indicates an increase in adsorptive intensity upon coagulation and a subsequent decrease with increasing AOD. The effect of AOD on K_T and $1/n_T$ are graphically depicted in Figures 5-11 and 5-12, respectively. Although these results can only be interpreted as empirical, they show an approximate linear relationship with AOD above an AOD of 0.81 mg O_3/mg TOC.

FIGURE 5-11: THE EFFECT OF APPARENT OZONE DOSE ON THE VALUE OF THE NORMALIZED FREUNDLICH CONSTANT. THE DECREASE IN ADSORPTION CAPACITY AS GIVEN BY K APPEARS TO BE LINEAR WITH AOD AFTER THE AOD EXCEEDS 0.81 mg O_3/mg TOC.
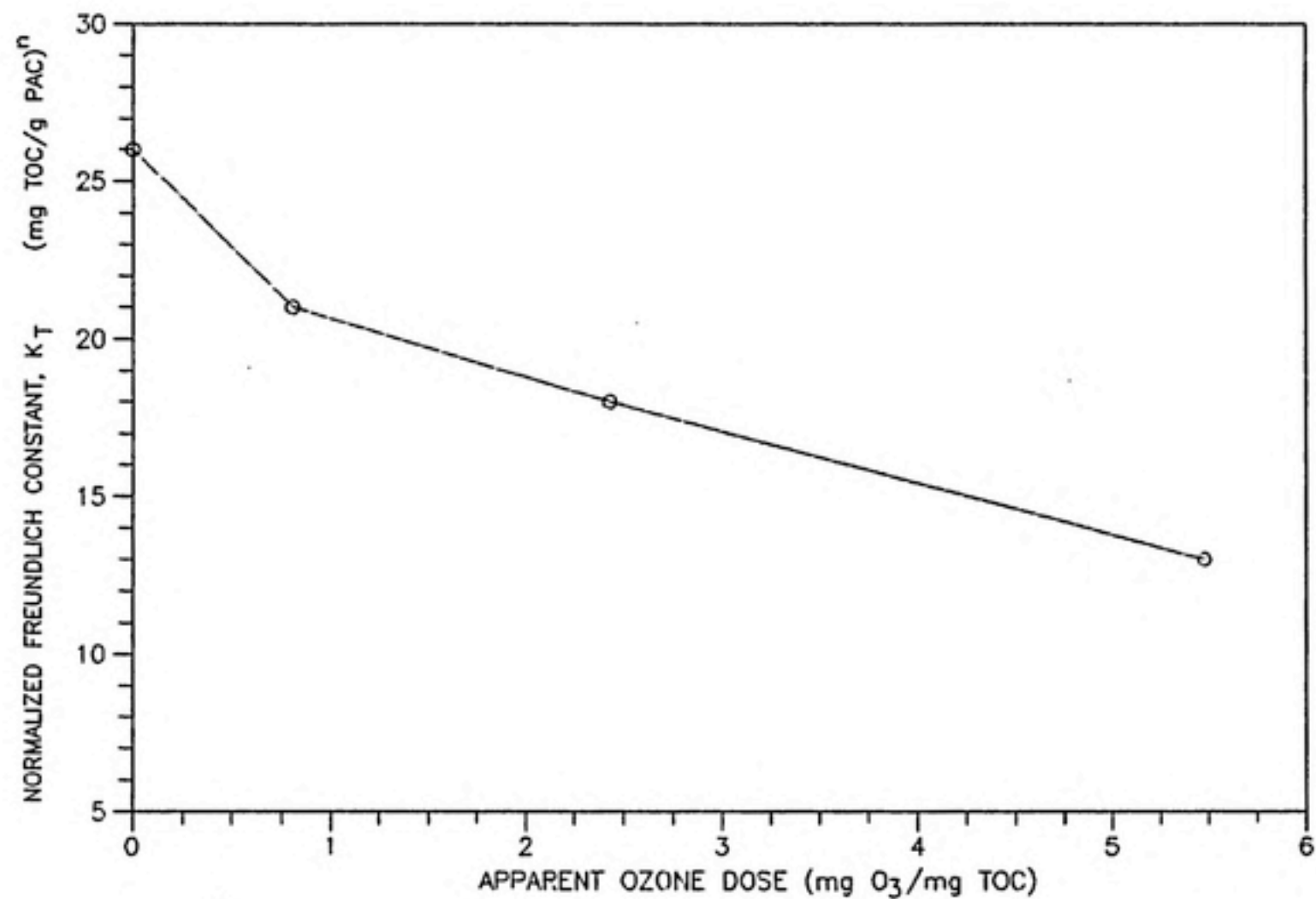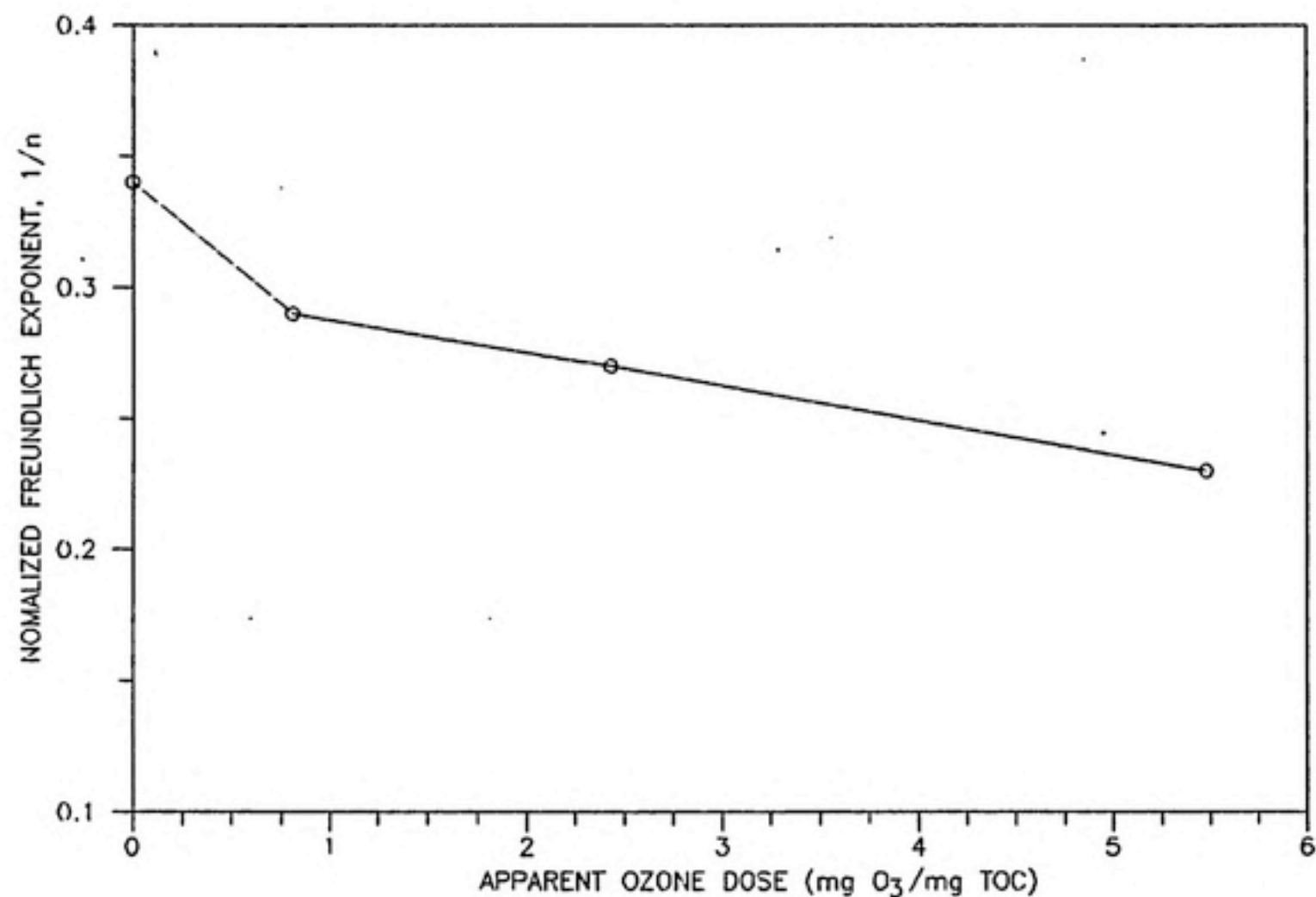
FIGURE 5—12: THE EFFECT OF APPARENT OZONE DOSE ON THE VALUE OF THE NORMALIZED FREUNDLICH EXPONENT. THE DECREASE IN ADSORPTION INTENSITY AS GIVEN BY $1/n$ APPEARS TO BE LINEAR WITH AOD WHEN THE AOD EXCEEDS 0.81 mg O_3/mg TOC.

CHAPTER 6

KINETIC RESULTS

EXTERNAL DIFFUSION

The mini-column technique used by Cornel, _et al._
(1986b), was used in this work to find the effects, if any,
of coagulation, ozonation, and biostabilization on the film
diffusion coefficients of aquatic humic materials. The
experimental procedures and modeling methods for this
technique were presented in Chapters 3 and 4, respectively.

Figure 6-1 shows a plot of results from a mini-column
test performed on the humic solution from the 1987 data set
that received coagulation, ozonation at an AOD of
2.43 mg O_3/mg TOC, and biostabilization. The values of C/C_O
presented in this figure were corrected by time dependent
dilution factors that were obtained by running a solute of
known C_O through the column (this is why a large value of
C/C_O appears for $t < \tau$). A constant value of C/C_O was
expected for the short time span of the test; however, there
was a general upward trend in C/C_O for this particular
mixture. As Cornel, _et al._ (1986a), point out, however,
such a result is to be expected from solutions that have
slow internal diffusion rates. That is, the experiment was
designed to make external diffusion the rate limiting step
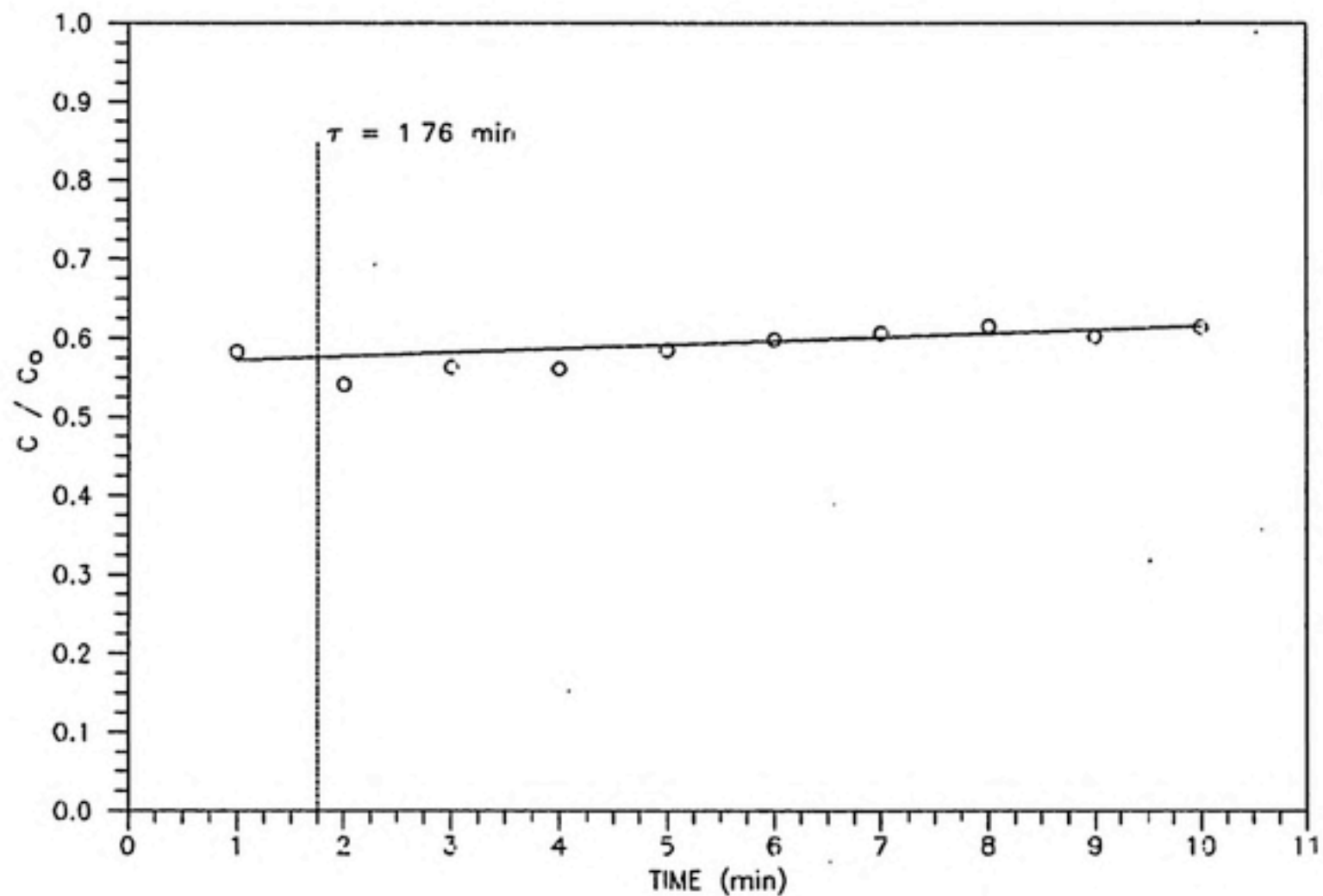
FIGURE 6-1: A TYPICAL PLOT OF THE RESULTS FROM A MINI-COLUMN RATE TEST. THE RESULTS SHOWN HERE WERE OBTAINED FOR THE SOLUTION FROM THE 1987 DATA SET THAT RECEIVED OZONATION AT AN AOD OF 2.43 mg O_3/mg TOC AND BIOSTABILIZATION.

but this may not have occurred if internal diffusion was too slow. Because of their large molecular weights, humic solutions will have very low internal diffusion coefficients and, therefore, the result observed in Figure 6-1 was not surprising. The question to be answered is which C/C_O value to use as input to Equation 4-28. The problem is solved by using the concentration ratio at $t = \tau$, the mean residence time of the reactor. The value of τ indicates the point of initial breakthrough in an ideal plug flow system. Linear regression was performed on the experimental data in the range of 5 min $\leq t \leq$ 10 min to find the intercept with $T = \tau$ and, therefore, the appropriate C/C_O ratio. This ratio was substituted into Equation 4-28 to obtain the value of K_L which was substituted into the Gnielinski correlation (Equations 4-30 to 4-34) to obtain the value of D_L.

The values of D_L obtained from both data sets are presented in Table 6-1 and several interesting comparisons can be made. Firstly, the value of D_L increased noticeably after the 14 month storage period and tends to indicate a general decrease in molecular size. This result is consistent with the observed sedimentation if larger humic molecules were preferentially removed but is not consistent if larger humic molecules were formed by condensation. Secondly, coagulation increased the value of D_L in both data sets, a result that was expected due to the expected decrease in overall molecular sizes. Finally, the ozonation and biostabilization treatments did not increase D_L as was

TABLE 6-1

Mini-Column Rate Test Results

Humic Mixture	D_L (x 10^6 cm^2/sec)
1986 Data Set	
Pre-Filtered	1.1
Coagulated	2.0
Ozonated & Biostabilized	
AOD = 1.15 mg O_3/mg TOC	2.0
1987 Data Set	
Pre-Filtered	1.9
Coagulated	2.6
Ozonated & Biostabilized	
AOD = 0.81 mg O_3/mg TOC	2.5
AOD = 2.43 mg O_3/mg TOC	3.0
AOD = 5.48 mg O_3/mg TOC	2.3

expected due to the production of smaller molecules. This result may imply that the smaller molecules were biologically removed.

The order of magnitude of D_L agrees with that obtained by Cornel, et al. (1986b), in similar mini-column experiments. The literature contains several studies that examine the effects of treatment on external mass transport. Unfortunately, none of these authors converted their K_F values to D_L values that could be subsequently compared with those of this work and with those of other experiments. Lee, et al. (1981), present film transfer coefficients, as determined from batch experiments, that show a general decrease in K_L upon coagulation of a peat fulvic acid. Later, Jodellah (1985) showed that K_L values (obtained from batch tests) of two commercial humic acids and one river water increased after coagulation. An increase in K_L could be accounted for if aggregated floc particles were removed by sedimentation while decreased values of K_L could result if these particles remained in suspension. Kaastrup (1985) showed an increase in K_L of humic mixtures from 2×10^{-4} cm/sec to 9×10^{-4} cm/sec at an AOD of 1 mg O_3/mg TOC. Cleavage of humic molecules is likely to explain a higher K_L, especially considering the fact that the molecular weight distribution before ozonation showed these humic substances to be very large.

The literature data and the results of this work do not give a clear picture of how treatment processes affect the

external mass transfer characteristics of humic solutions. In this work, coagulation increased external diffusion rates, probably because the large floc particles formed by coagulation were removed by sedimentation. A decreased rate of external diffusion could occur, however, if these particles were to remain stable. In addition, ozonation and biostabilization did not alter the external diffusion rate. Obviously, further work is required to examine the effects of various treatment processes on film diffusion rates.

INTERNAL DIFFUSION

The data obtained from the batch rate experiments are shown in Figures 6-2 and 6-3 for all of the solutions tested. Results from tests of the pre-filtered solution from the 1986 data set were not included because of an eleven month delay in running the test which, in light of the effects on adsorption properties noted with long term storage, would make data interpretation impossible. The other two solutions from this data set were tested immediately following their respective isotherm tests and, therefore, the results of these two tests are reported herein. The decrease in normalized TOC was plotted against the square root of time so that the data points at the start of the experiments were spread out and data points near the end of the experiments were condensed. TOC was normalized to show the approach to the final equilibrium position as

128

FIGURE 6-2: RESULTS OF BATCH RATE EXPERIMENTS FROM THE 1986 DATA SET INDICATING INCREASED RATES OF INTERNAL DIFFUSION UPON OZONATION AND BIOSTABILIZATION. THE SOLID LINES REPRESENT SIMULATIONS OF THE DATA OBTAINED FROM THE HETEROGENEOUS DIFFUSION MODEL (HDM).
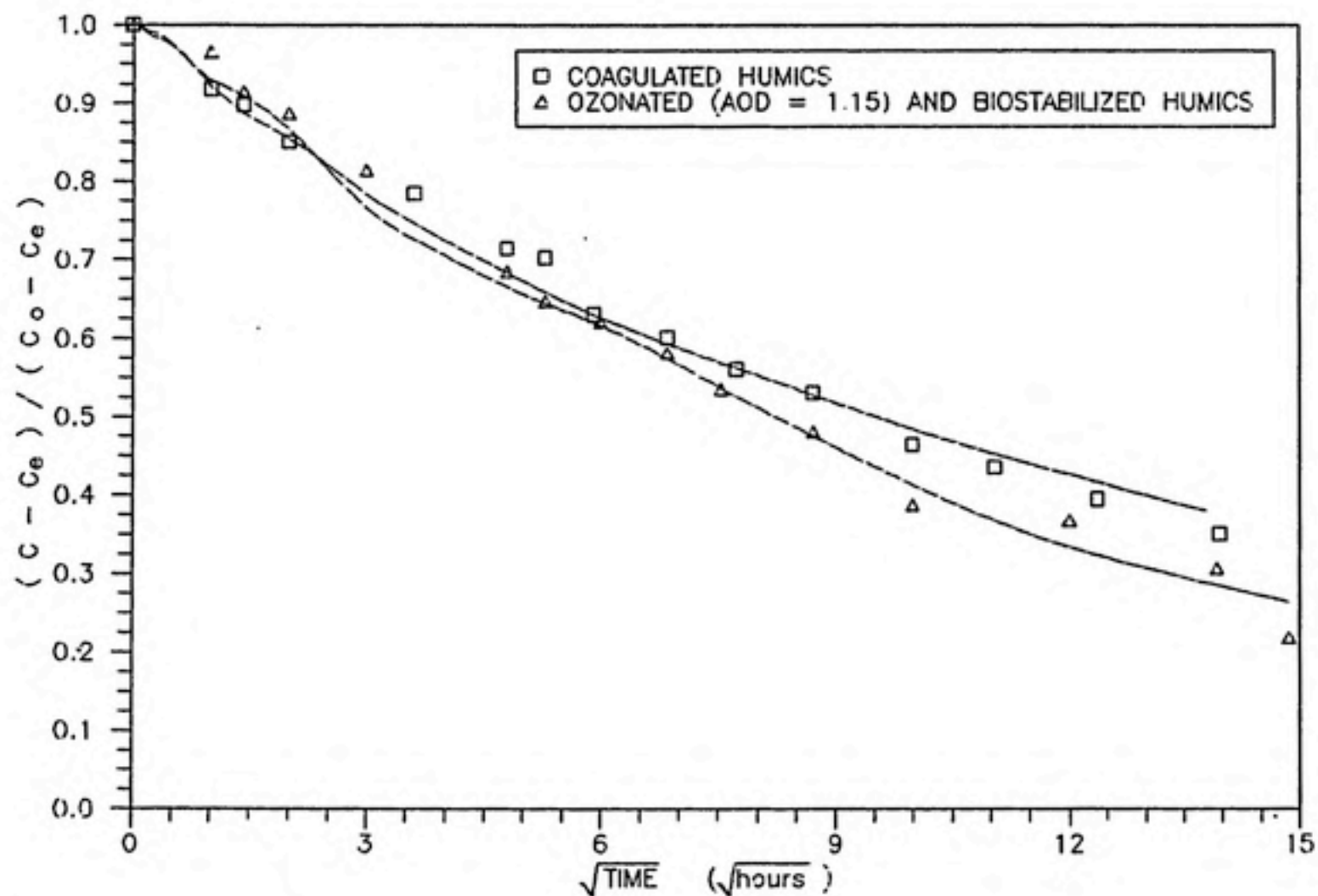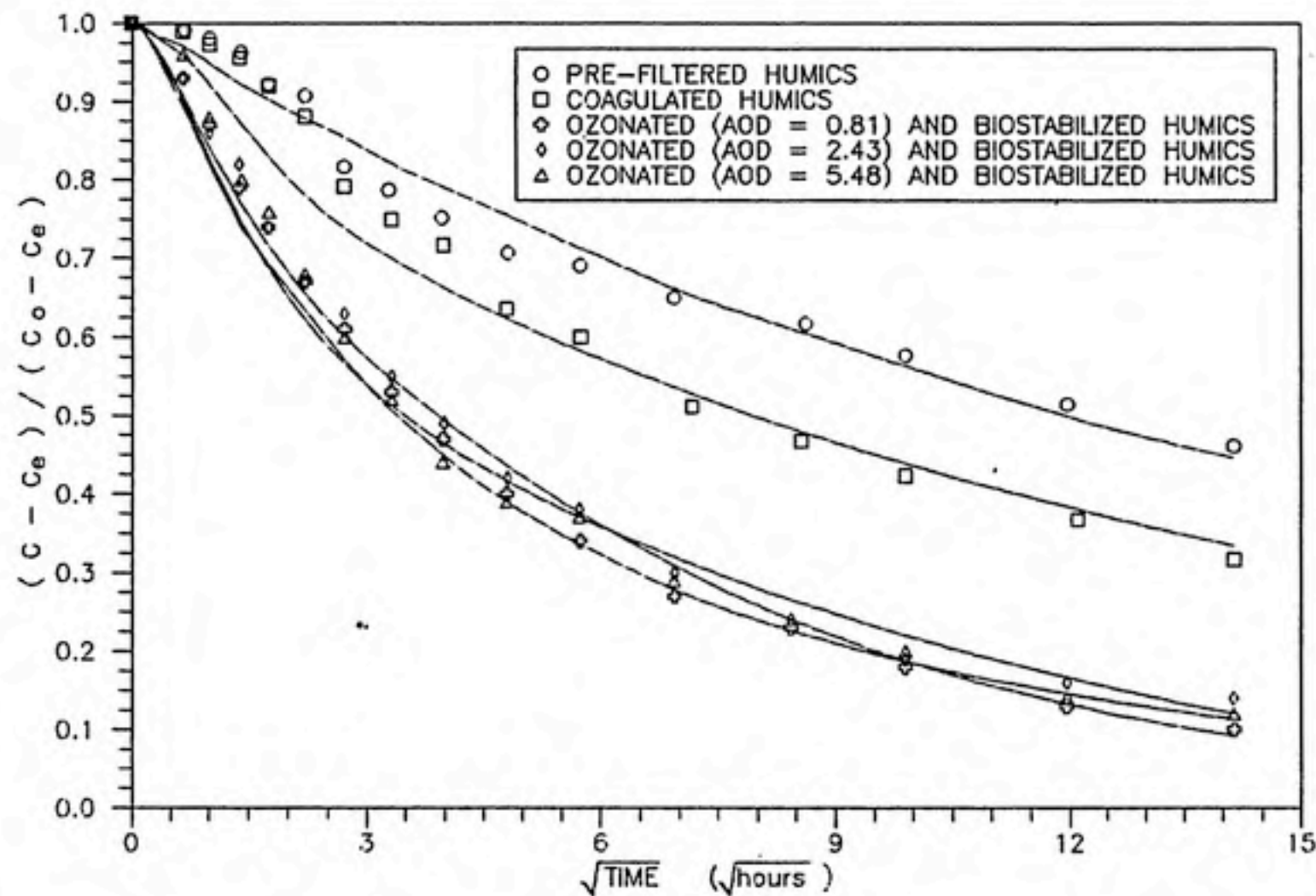
FIGURE 6-3: RESULTS OF BATCH RATE EXPERIMENTS FROM THE 1987 DATA SET INDICATING INCREASED RATES OF INTERNAL DIFFUSION UPON COAGULATION AND UPON THE ADDITIONAL TREATMENTS OF OZONATION AND BIOSTABILIZATION. THE SOLID LINES REPRESENT SIMULATIONS OF EACH DATA SET AS OBTAINED FROM THE HETEROGENEOUS DIFFUSION MODEL (HDM).

calculated by the IAST equilibrium model (i.e., the value of zero should be approached as the system approaches equilibrium). Having thus normalized for differences in equilibrium position for each of the mixtures, it is possible to compare the rate of approach for different sample treatments.

The results of Figure 6-3 show a significant increase in internal adsorption rates after coagulation and an additional significant increase after ozonation and biostabilization. Interestingly, the rate did not increase with the ozone dose.

Homogeneous Diffusion Model Results (PDM and SDM)

The pore diffusion model (PDM) and the surface diffusion model (SDM) yield the values of D_P and D_S, respectively, and these are shown in Table 6-2. In the 1987 data set, D_P was seen to increase to more than twice its original value upon coagulation while the value of D_S decreased. This contradictory result may actually be consistent with the observed increase in adsorbability upon coagulation since the surface diffusion mechanism must account for adsorption prior to diffusion. For instance, the coagulated mixture would have a much larger driving force for diffusion in the adsorbed phase than the pre-filtered mixture would. This must happen because the more strongly adsorbing mixture would put a higher concentration

131

TABLE 6-2

Homogeneous Diffusion Model Results

Humic Mixture	D_P (from PDM) ($\times 10^7$ cm^2/sec)	D_S (from SDM) ($\times 10^{11}$ cm^2/sec)
1986 Data Set		
Coagulated	4.0	6.8
Ozonated & Biostabilized		
AOD = 1.15 mg O$_3$/mg TOC	6.3	20.0
1987 Data Set		
Pre-Filtered	3.2	3.8
Coagulated	6.9	2.8
Ozonated & Biostabilized		
AOD = 0.81 mg O$_3$/mg TOC	13.0	13.0
AOD = 2.43 mg O$_3$/mg TOC	15.0	16.0
AOD = 5.48 mg O$_3$/mg TOC	13.0	18.0

of solute in the adsorbed phase at the external surface of the GAC particle than the more poorly adsorbing mixture. Thus, the concentration gradient is higher for the more strongly adsorbing mixture and, as a result, the mass flux in the adsorbed phase should also be higher. Because the value of D_S was obtained from mass flux data, this value must be related to the ratio of mass flux to concentration gradient. Therefore, even though Figure 6-3 shows an increased mass flux upon coagulation, the value of D_S could be smaller if the increased mass flux was not sufficient to overcome the increased concentration gradient.

Ozonation and biostabilization produced significant increases in D_p and D_S for both data sets. This result was not surprising as ozonation reduces overall molecular size. However, these values were quite similar for the various AODs examined in the 1987 data set. This may be an indication that molecules smaller than a certain size were biologically removed.

The order of magnitude in the SDM results is equivalent to those obtained in several studies which also examined the rate of humic diffusion with a surface diffusion model. Lee, et al. (1981), showed a slight increase in D_S after coagulation of a peat fulvic acid, while Jodellah (1985) found an increase in D_S for one commercial humic acid, a decrease in D_S for another, and no change for a river water upon coagulation. In addition, Kaastrup found no change in D_S with an AOD of 1 mg O_3/mg TOC. All of these authors

133

assumed that a single solute Freundlich isotherm could describe their data whereas two adsorbing PCs and a competitive adsorption approach were used in this work. Taken together, the results of all these rate studies are inconsistent and indicate that further work is required, just as was found for the external mass transfer studies.

Summers (1986) has produced the only report thus far that gives results of PDM analysis for humic solutions. Values of D_p for fractionated and unfractionated commercial humic acid are quite similar to those of this work. Not surprisingly, the smaller molecular size fractions were observed to have higher values of D_p which also agrees with this work wherein each treatment stage was expected to reduce the overall size of humic solutions.

The Heterogeneous Diffusion Model (HDM)

The HDM approach, as detailed in Chapter 4, is more involved than either the PDM or SDM approaches and should be understood before proceeding with this section. As noted in that chapter, the results from the IAST equilibrium model and the HDM kinetic model should predict the equilibrium behavior of a humic solution remaining at the end of a batch rate test. In order to apply this technique, collection of TOC isotherm data was necessary for each humic solution that remained after a batch rate test. Figures 6-4 through 6-10 present the isotherm data collected for each solution before
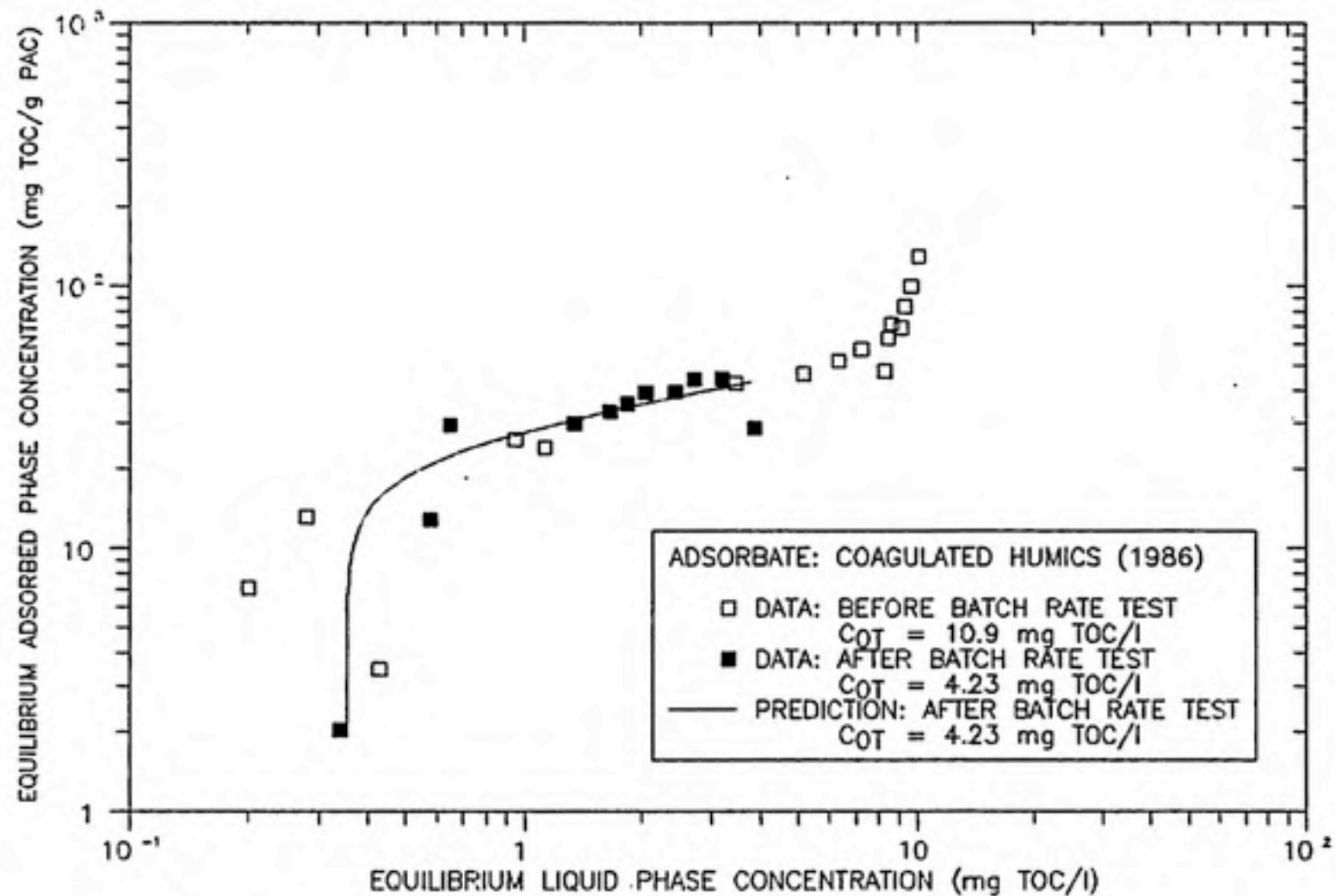
FIGURE 6—4: PREDICTION OF THE ISOTHERM FOR COAGULATED HUMICS REMAINING AFTER A 1986 BATCH RATE TEST. THE PREDICTION WAS MADE BY USING FREUNDLICH PARAMETERS OBTAINED FROM THE ORIGINAL MIXTURE (OPEN SQUARES) AND BY USING PERCENT CONCENTRATIONS FOR THE RESIDUAL MIXTURE AS PREDICTED BY THE HETEROGENEOUS DIFFUSION MODEL (HDM).

FIGURE 6–5: PREDICTION OF THE ISOTHERM FOR OZONATED (AOD = 1.15) AND BIOSTABILIZED HUMICS REMAINING AFTER A 1986 BATCH RATE TEST. THE PREDICTION WAS MADE BY USING FREUNDLICH PARAMETERS OBTAINED FOR THE ORIGINAL MIXTURE (OPEN TRIANGLES) AND FROM PERCENT CONCENTRATIONS OF THE RESIDUAL MIXTURE AS PREDICTED BY THE HDM.
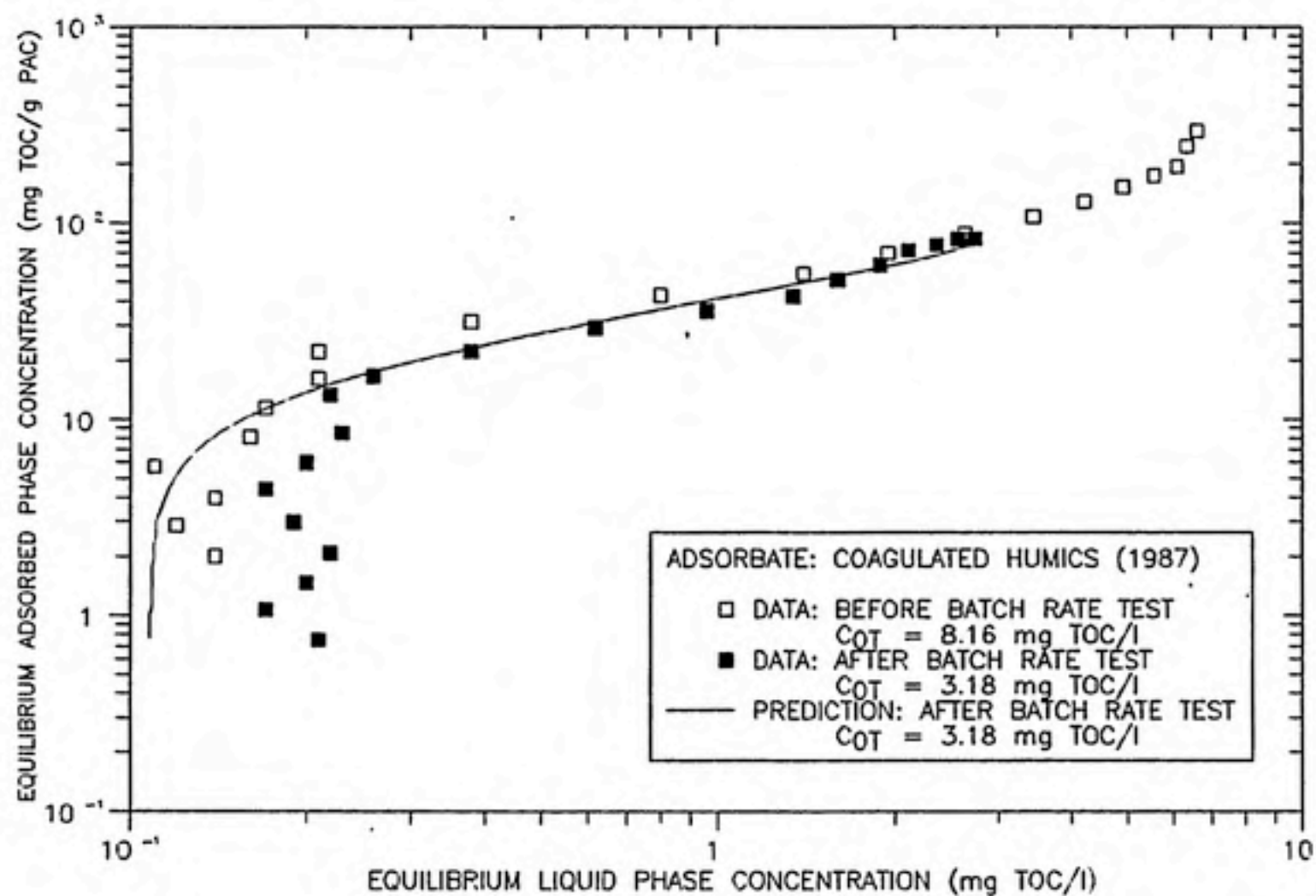
FIGURE 6-7: PREDICTION OF THE ISOTHERM FOR COAGULATED HUMICS REMAINING AFTER A 1987 BATCH RATE TEST. THE PREDICTION WAS MADE BY USING FREUNDLICH PARAMETERS OBTAINED FROM THE ORIGINAL MIXTURE (OPEN SQUARES) AND BY USING PERCENT CONCENTRATIONS FOR THE RESIDUAL MIXTURE AS PREDICTED BY THE HETEROGENEOUS DIFFUSION MODEL (HDM).
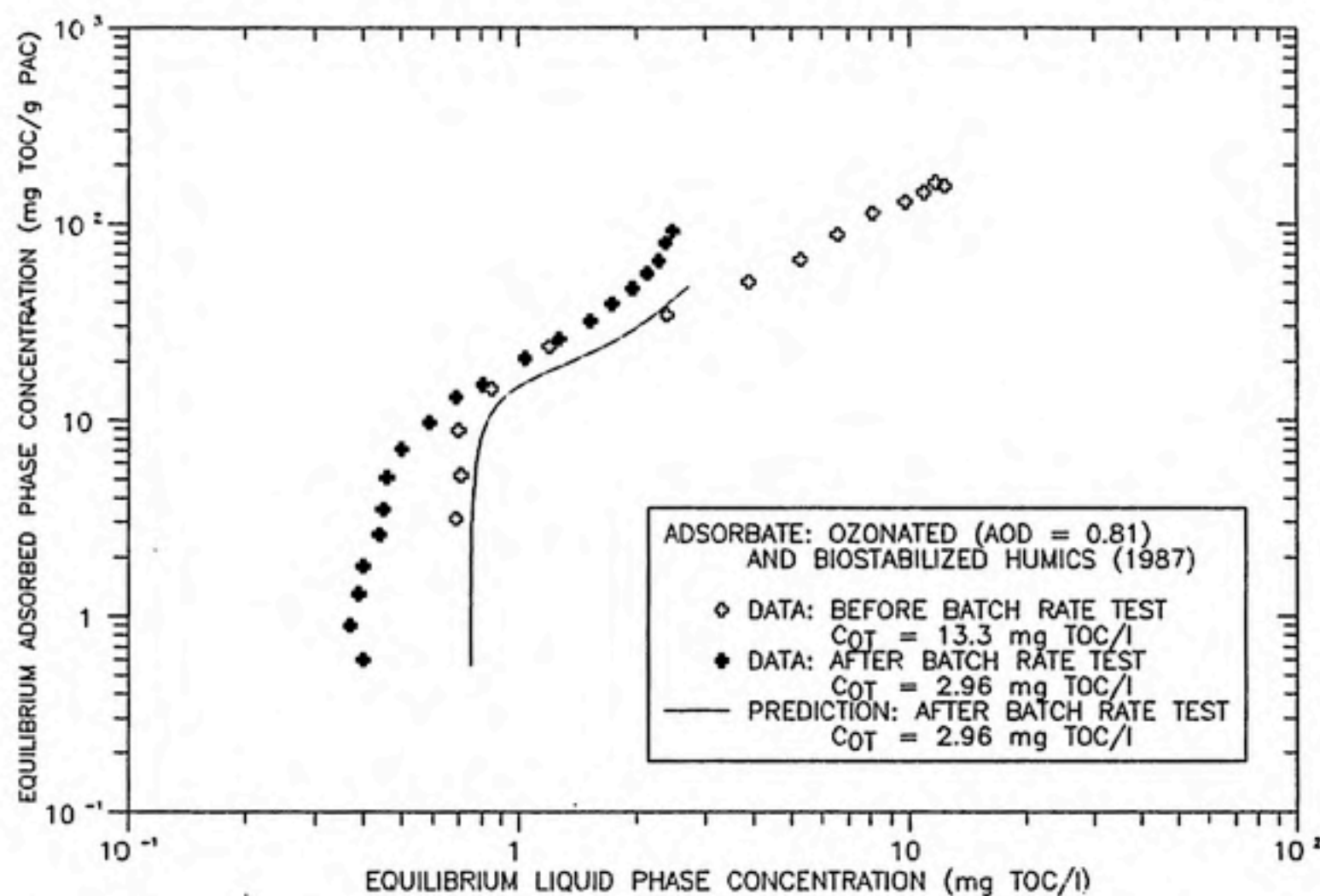
FIGURE 6—8: PREDICTION OF THE ISOTHERM FOR OZONATED (AOD = 0.81) AND BIOSTABILIZED HUMICS REMAINING AFTER A 1987 BATCH RATE TEST. THE PREDICTION WAS MADE BY USING FREUNDLICH PARAMETERS OBTAINED FOR THE ORIGINAL MIXTURE (OPEN CROSSES) AND FROM PERCENT CONCENTRATIONS OF THE RESIDUAL MIXTURE AS PREDICTED BY THE HDM.
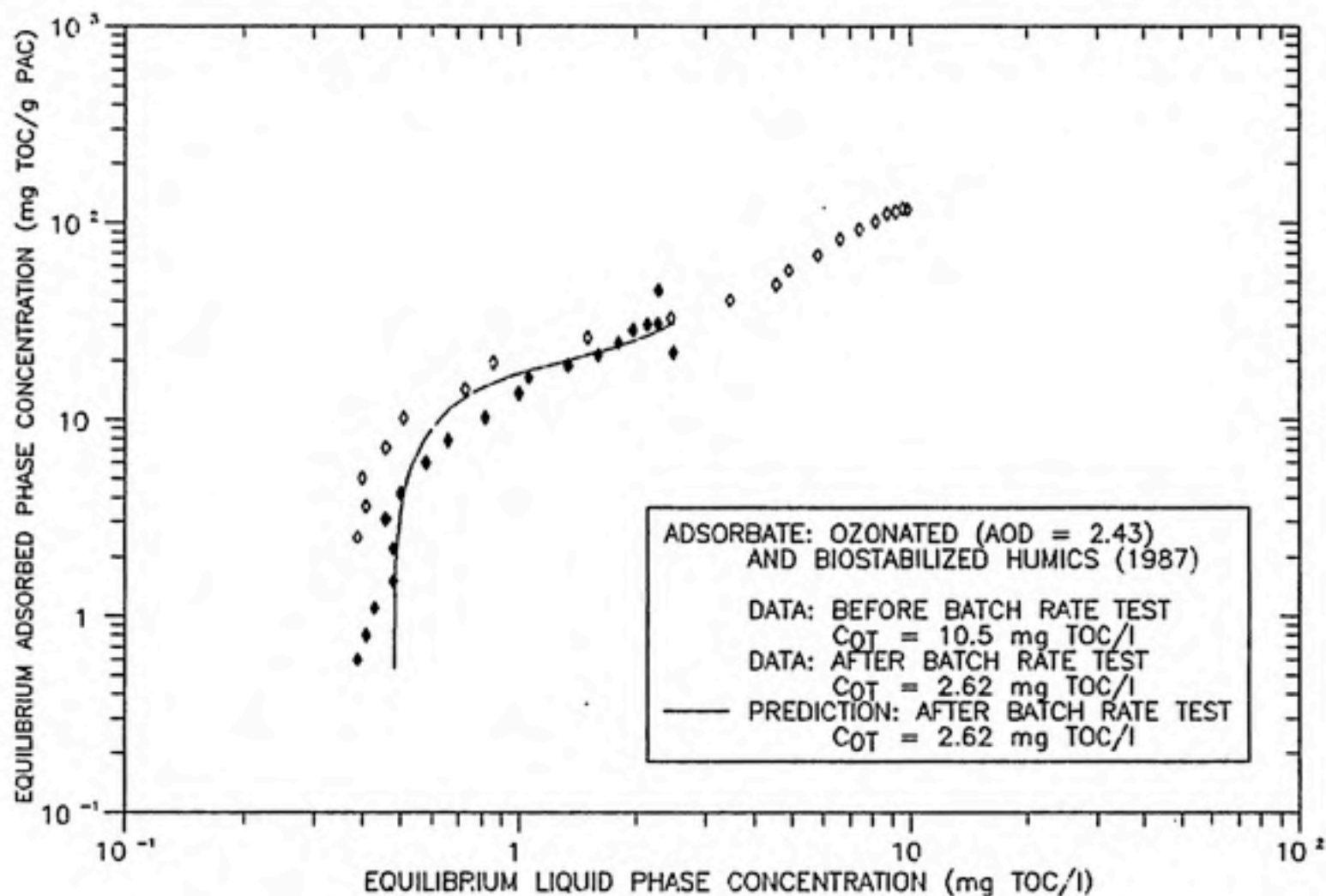
FIGURE 6-9: PREDICTION OF THE ISOTHERM FOR OZONATED (AOD = 2.43) AND BIOSTABILIZED HUMICS REMAINING AFTER A 1987 BATCH RATE TEST. THE PREDICTION WAS MADE BY USING FREUNDLICH PARAMETERS OBTAINED FOR THE ORIGINAL MIXTURE (OPEN DIAMONDS) AND FROM PERCENT CONCENTRATIONS OF THE RESIDUAL MIXTURE AS PREDICTED BY THE HDM.
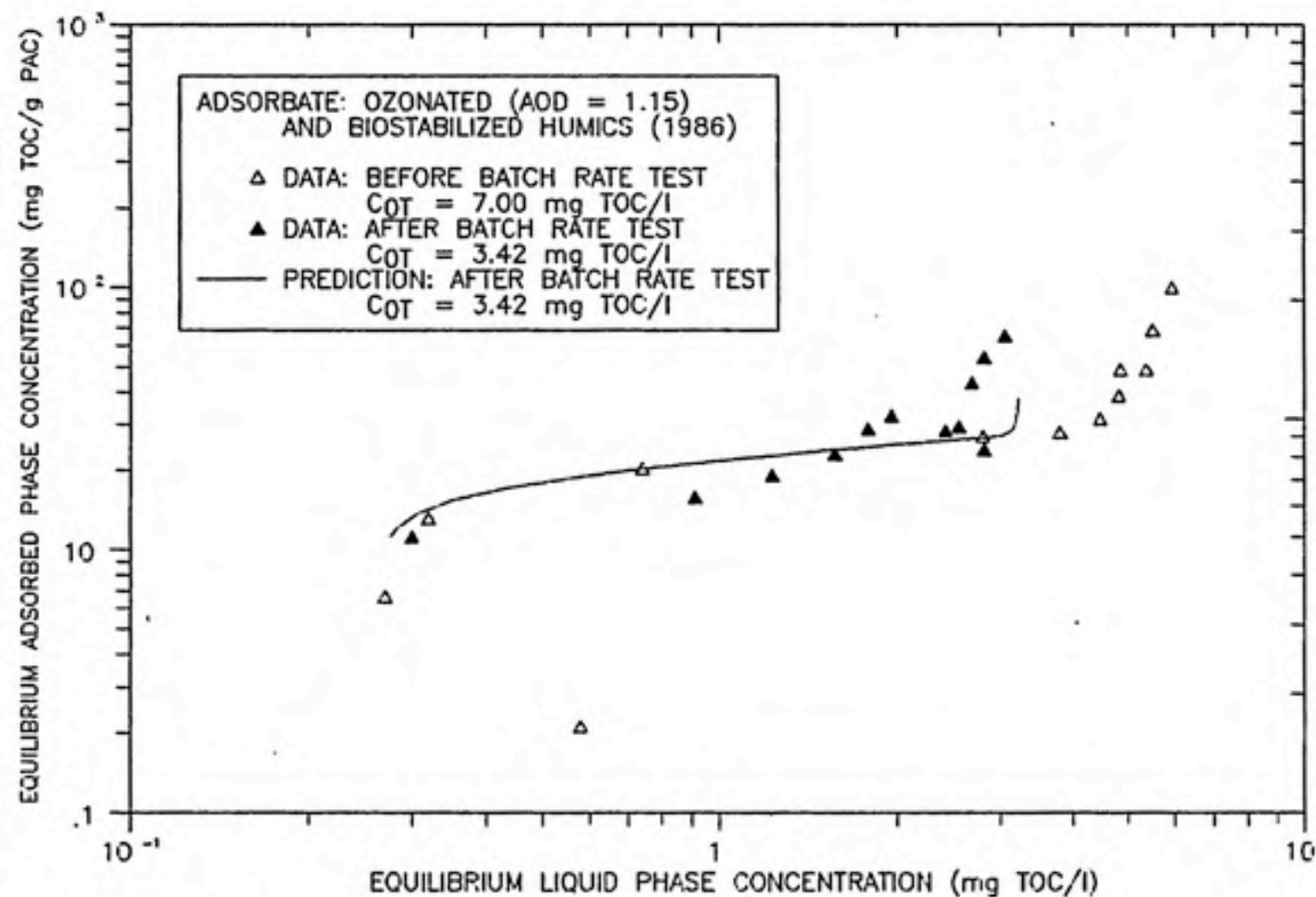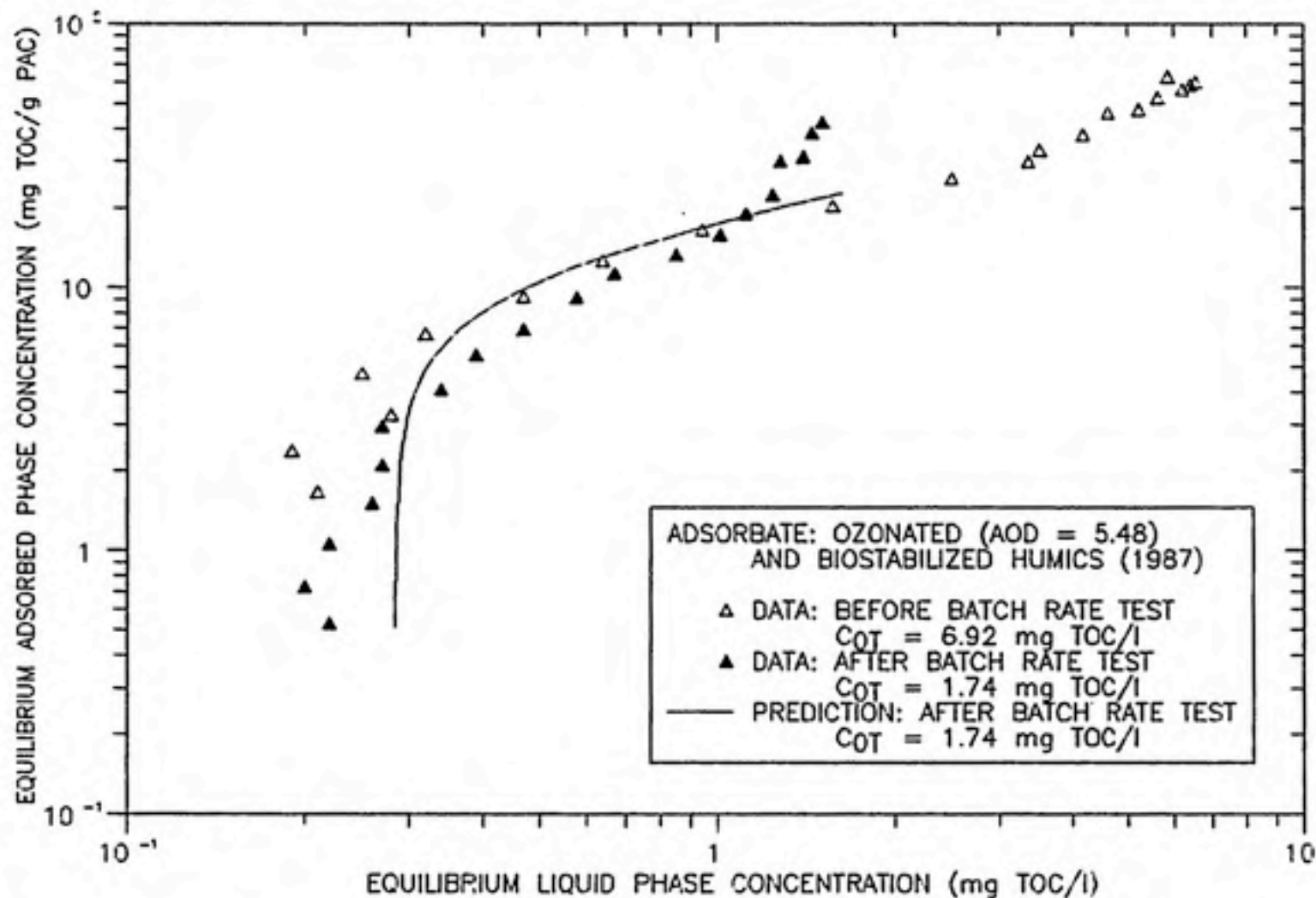
FIGURE 6-10: PREDICTION OF THE ISOTHERM FOR OZONATED (AOD = 5.48) AND BIOSTABILIZED HUMICS REMAINING AFTER A 1987 BATCH RATE TEST. THE PREDICTION WAS MADE BY USING FREUNDLICH PARAMETERS OBTAINED FOR THE ORIGINAL MIXTURE (OPEN TRIANGLES) AND FROM PERCENT CONCENTRATIONS OF THE RESIDUAL MIXTURE AS PREDICTED BY THE HDM.

and after batch rate testing in addition to the predictions obtained from the HDM and IAST models. Table 6-3 shows the HDM predictions for the PC composition of each solution at the end of a rate test and compares them with the PC compositions determined by the IAST model prior to a rate test. The results show the preferential removal of the more strongly adsorbed PC in each case, as should be expected.

The values of D_P and D_S that made the predictions shown in Figures 6-4 to 6-10 are posted in Table 6-4. A comparison was made between the D_S and D_P values obtained by the HDM and the D_S and D_P values obtained by the homogeneous models in order to examine the mechanism for diffusion as set forth by this technique. In several cases, the HDM reproduced the results of the PDM and, in one case, the HDM reproduced the results of the SDM. Therefore, the modeling procedures indicated a pore diffusion mechanism for both solutions from the 1986 data set, the pre-filtered solution from the 1987 data set, and the ozonated (AOD = 0.81 mg O_3/mg TOC) and biostabilized solution from the 1987 data set. A surface diffusion mechanism was indicated by the HDM for the ozonated (AOD = 2.43 mg O_3/mg TOC) and biostabilized solution from the 1987 data set while a combination of the two mechanisms was proposed for the remaining solutions.

TABLE 6-3

Compositions of Humic Mixtures Before and After Batch Rate Testing

Humic Mixture	Pseudo-Component 1		Pseudo-Component 2		Non-Adsorbing Pseudo-Component	
	Before Batch Rate Test	After Batch Rate Test	Before Batch Rate Test	After Batch Rate Test	Before Batch Rate Test	After Batch Rate Test
1986 Data Set						
Coagulated	84	92	12	0	4	8
Ozonated & Biostabilized						
AOD = 1.15 mg O_3/mg TOC	71	87	25	5	4	8
1987 Data Set						
Pre-Filtered	91	87	7	8	2	5
Coagulated	79	92	20	4	1	4
Ozonated & Biostabilized						
AOD = 0.81 mg O_3/mg TOC	74	45	21	29	5	26
AOD = 2.43 mg O_3/mg TOC	63	39	33	43	4	18
AOD = 5.48 mg O_3/mg TOC	70	84	27	0	3	16

TABLE 6-4

Heterogeneous Diffusion Model Results

Humic Mixture	D_P (x 10^7 cm^2/sec)	D_S (x 10^{11} cm^2/sec)
1986 Data Set		
Coagulated	4.0	0.22
Ozonated & Biostabilized		
AOD = 1.15 mg O$_3$/mg TOC	6.3	0.00
1987 Data Set		
Pre-Filtered	3.2	0.10
Coagulated	4.3	0.65
Ozonated & Biostabilized		
AOD = 0.81 mg O$_3$/mg TOC	13.0	0.02
AOD = 2.43 mg O$_3$/mg TOC	0.00	16.0
AOD = 5.48 mg O$_3$/mg TOC	4.1	13.0

Comparing the Results of the PDM, SDM, and HDM

Figures 6-11 and 6-12 provide evidence that caution should be advised when interpreting model predictions for mass transfer mechanisms. Figure 6-11 shows the best simulations obtained for the batch rate data of the coagulated solution from the 1987 data set by each of the three modeling approaches. A comparison of Tables 6-2 and 6-4 shows that each approach yielded a different set of diffusion coefficients for this mixture, however, Figure 6-11 indicates that all three modeling approaches describe the rate data quite adequately.

As noted earlier, the HDM was obtained from the combination of D_P and D_S that provided the best prediction of the residual mixture isotherm. Therefore, each of the models was tested for its ability to predict this isotherm and the results of the tests are depicted in Figure 6-12. Figure 6-12 clearly shows that all three diffusion models provide very good predictions of the isotherm for the coagulated mixture remaining after a batch rate test. Thus, comparing the HDM results with the PDM and SDM results was not an adequate method for determining the mode of internal mass transport. In addition, these figures show that rate data can be sufficiently described by either one of the diffusion models. Summers (1986) arrived at the same conclusion when comparing the PDM and the SDM for descriptions of humic rate data.
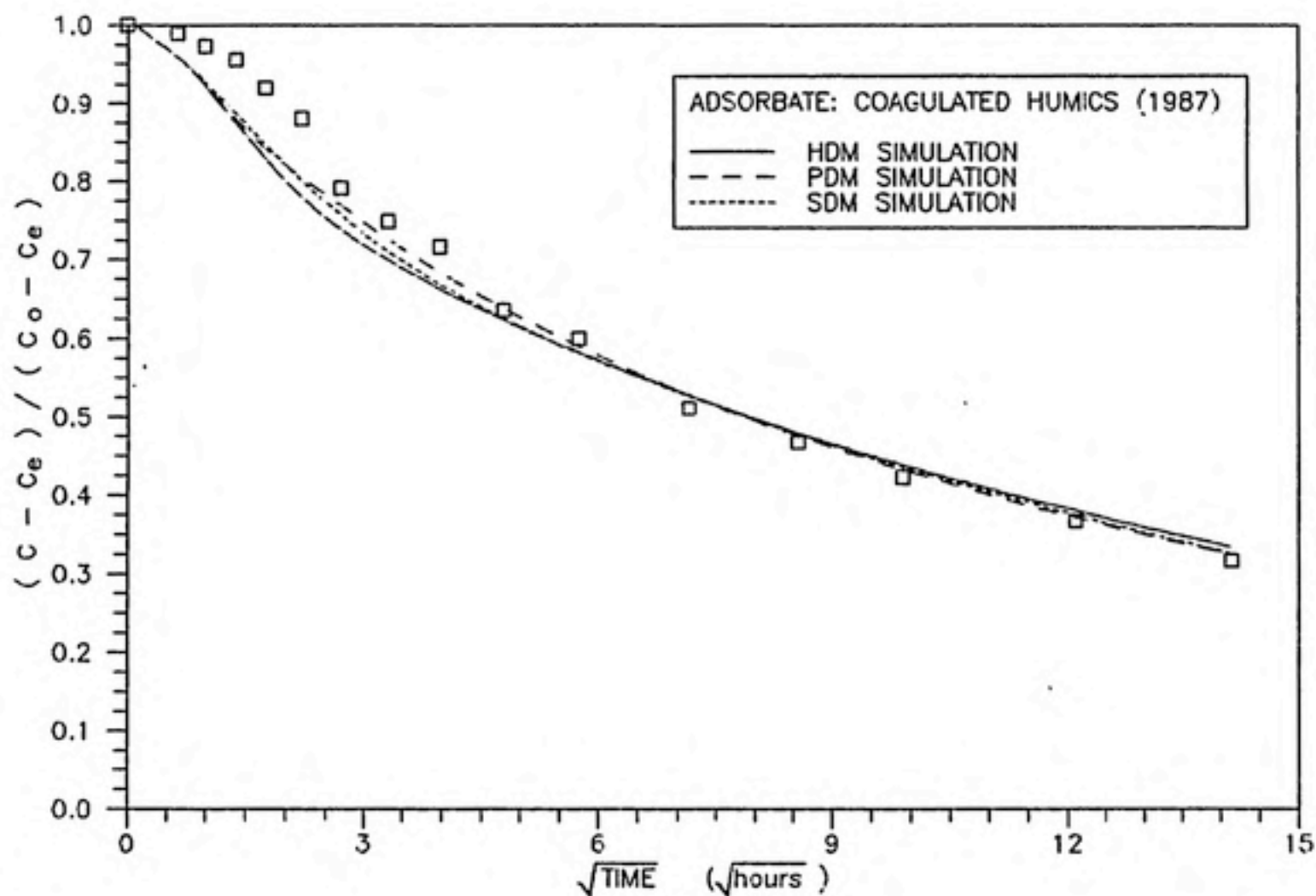
FIGURE 6-11: A COMPARISON OF EACH DIFFUSION MODEL'S ABILITY TO DESCRIBE THE BATCH RATE TEST DATA OBTAINED FOR THE COAGULATED HUMICS OF THE 1987 DATA SET. THE COAGULATED MIXTURE WAS CHOSEN SINCE EACH MODEL YIELDED A DIFFERENT SET OF DIFFUSION PARAMETERS.
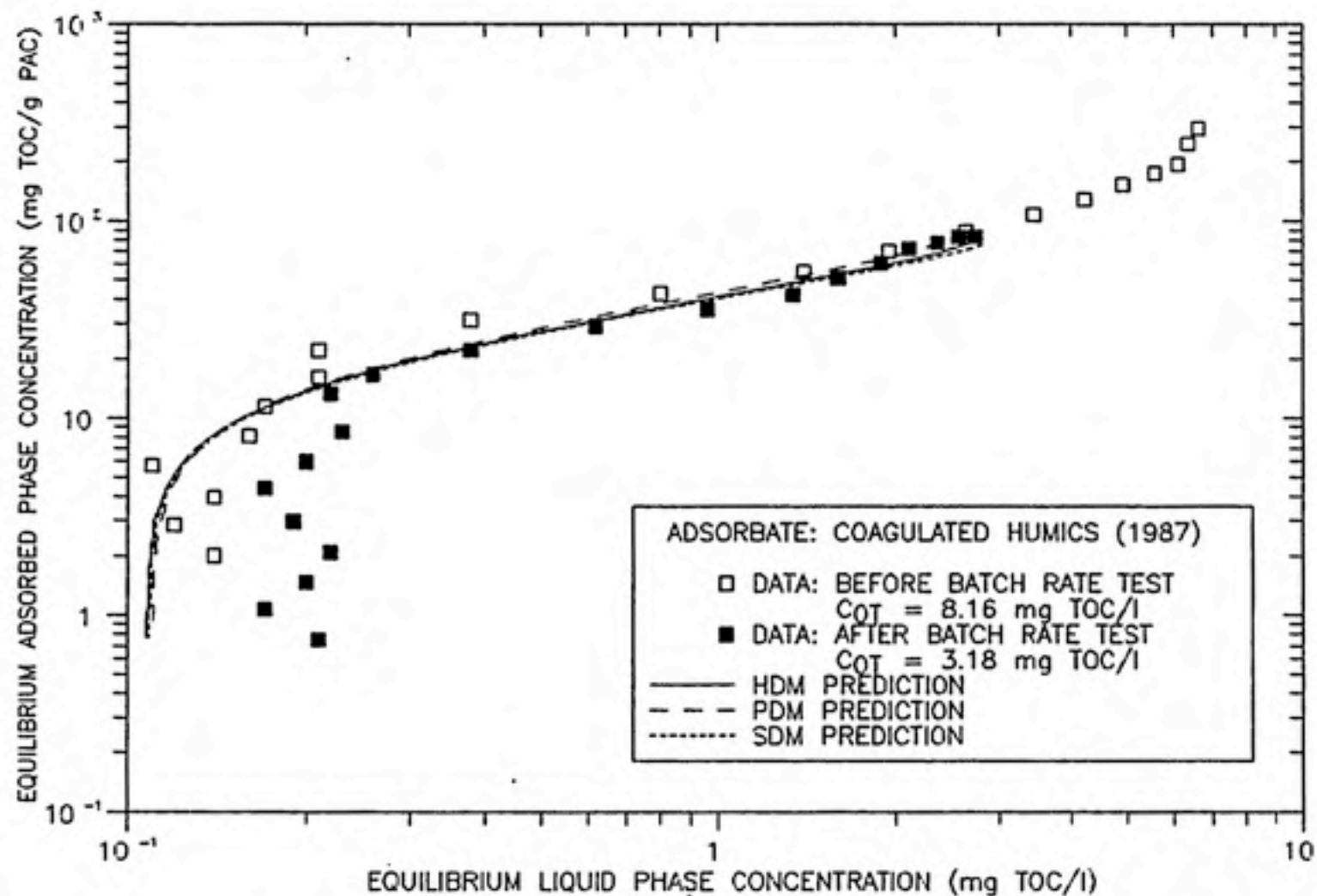
FIGURE 6-12: A COMPARISON OF EACH DIFFUSION MODEL'S ABILITY TO PREDICT THE ISOTHERM OF THE COAGULATED HUMIC SUBSTANCES REMAINING AFTER A 1987 BATCH RATE TEST. THE COAGULATED MIXTURE WAS CHOSEN SINCE EACH MODEL PRODUCED A DIFFERENT SET OF DIFFUSION PARAMETERS.

Summers also points out, in regard to polyelectrolyte adsorption theory, that the early stages of internal diffusion are probably dominated by a pore diffusion mechanism since multisite attachment of humic macromolecules to the carbon surface would provide a large obstacle to transport in the adsorbed phase. Once the available sites were filled, further diffusion would only be able to occur upon rearrangement of adsorbed humic molecules, thereby implying that a slow surface diffusion mechanism would dominate the latter stages of internal diffusion. In addition, the physical exclusion of humic macromolecules from interior portions of the activated carbon particle may imply that a two domain diffusion model would be better suited to humic substance adsorption.

CHAPTER 7

CONCLUSIONS AND RECOMMENDATIONS

CONCLUSIONS

The effects of alum coagulation and the subsequent treatments of ozonation and biodegradation on the equilibrium adsorption behavior of aquatic humic materials were studied through the use of a multicomponent adsorption model - the ideal adsorbed solution theory (IAST). Meanwhile the effects of these treatment processes on the kinetic adsorption behavior of aquatic humic materials were assessed through the use of a pore-surface diffusion model (PSDM) that incorporated the IAST equilibrium conditions.

The IAST model seems appropriate for interpreting laboratory adsorption data to examine the effects of coagulation, ozonation, and biostabilization. The modeling approach consisted of the description of complex humic solutions as a set of two or three pseudo-components (PCs), each of which represented a group of species having similar adsorbabilities. A simplification was made that each of the adsorbing PCs contained the same number of carbon atoms. Such an assumption is extremely tenuous for complex humic mixtures having a large variety of molecular sizes; however, results showed the assumption to be adequate for the

purposes of this work. IAST was also sufficiently capable of predicting the effects of changing the initial concentration of two coagulated humic solutions. This result allowed the analysis of treatment effects without the interference of initial concentration effects.

The significant results from treatment analysis indicated increased adsorbability after coagulation, decreased adsorbability after the combined treatments of ozonation and biostabilization, and increased adsorbability with long term storage. Coagulation was thought to improve humic substance adsorbability by preferentially removing large humic molecules that were physically constrained from adsorbing into the microporous structure of activated carbon. Decreased adsorbability upon ozonation and biostabilization was considered to be a result of the more polar and, therefore, more hydrophilic nature of the humic mixture after these treatments. The adsorbability of the humic material used in this study was also observed to decrease with increasing ozone dose, probably due to the production of a higher concentration of highly polar and non-biodegradable components. The increased adsorbability observed after long term storage was believed to be a result of natural aging mechanisms (such as molecular condensation) that altered the composition of the solution to increased hydrophobicity.

The normalized adsorption isotherm presented in Chapter 5 provides a much easier method for describing the

equilibrium adsorption behavior of complex heterogeneous mixtures such as humic solutions. The results observed through the use of this isotherm showed the same effects of coagulation, ozonation, and biodegradation as the IAST modeling did. In addition, this isotherm showed that the decreases in the Freundlich parameters K and 1/n were linear above an apparent ozone dose of 0.81 mg O_3/mg TOC. However, this isotherm may be limited in its usefulness since it may not be able to describe competitive adsorption phenomena between humic substances and trace organic pollutants. This approach needs to be extended in some manner to include a description of a non-adsorbing pseudo-component and the applicability of this isotherm in kinetic modeling needs to be assessed (i.e., the adsorbent dose at an infinitesimally small location can not be determined when an assumption about local equilibrium needs to be made).

Kinetic testing showed increases in the free liquid diffusion coefficient (D_L) upon coagulation but no significant changes in D_L were found after ozonation and biostabilization. Internal mass transport was found to increase after coagulation as well as after ozonation and biostabilization. Ozone dose was not observed to be a factor in either external or internal diffusion characteristics. Each treatment process was expected to increase external and internal mass transfer rates because of their ability to reduce the average molecular size of a given humic solution.

151

The heterogeneous diffusion model (HDM), in combination with the IAST equilibrium model, was found to provide excellent predictions of the equilibrium behavior of a humic solution remaining at the end of a batch rate test. Comparisons between the results of the HDM and the homogeneous diffusion models (i.e., the pore diffusion model and the surface diffusion model) allowed the assessment of a transport mechanism for a given solution. However, all three kinetic models were shown to provide equal levels of accuracy in describing rate behavior and predicting the equilibrium behavior of the solution remaining after a rate test. Therefore, the actual transport mechanism could not be assessed by using the HDM approach.

While the modeling approaches used in this work are not new, they have not been previously used to examine the changes created in humic substance adsorption by various treatment processes. The modeling procedure used to describe both equilibrium and kinetics (Figure 4-8) requires the collection of three different types of experimental data - a bottle point isotherm, a mini-column initial sorption rate, and a batch sorption rate - and the application of several fairly sophisticated computer software packages. A good understanding of the underlying theories is essential for interpretation of these results. After some experience with the use of these techniques, the flow chart presented in Figure 4-8 can be completed in a time span of three weeks for an individual mixture. The amount of time expended on a

study such as this is also influenced by the amount of available equipment (i.e., a study of a large number of mixtures with little equipment may become prohibitively time consuming) and by the upkeep of laboratory analyzers.

The ultimate goal, of course, is to apply such modeling to the design of GAC adsorbers for water treatment so that the breakthrough of humic substances and competing trace organic pollutants can be better predicted. The approach taken in this research can be valuable if changes in TOC adsorbability upon coagulation, ozonation, and biodegradation are predictable. The results thus far do not suggest a simple way to predict such changes. Thus, the complexity of the overall modeling approach will prevent its application to practical design work until more experience can suggest some empirical way to adjust adsorption parameters with pre-treatment. Another important potential of such modeling is the improved ability to describe competitive adsorption between humic materials and trace organic pollutants. If the consideration of humic mixtures as several pseudo-components improves the description of this competition, then there will be greater justification for the use of this modeling approach in practice.

RECOMMENDATIONS

The applicability of the IAST model to humic substance adsorption needs to be examined more thoroughly. One

possible manner in which such an examination might be carried out is to separate various humic solutions into several molecular size fractions. The equilibrium adsorption behavior of each fraction could be described with a single solute model such as the Freundlich equation. Each fraction, therefore, would be treated as a PC and the Freundlich parameters of each fraction could be used to predict the overall adsorption of the entire solution. This approach would also allow the assignment of diffusion coefficients that represent individual components rather than an entire mixture.

In addition, the IAST model needs to be examined for its ability to describe and predict the competitive interactions between humic molecules and trace organic pollutants. For the IAST model to be used in any practical application requires the accurate prediction of these interactions because high performance is needed to justify the use of such a complex approach. If IAST is found to be inappropriate, then further work is needed to find simpler approaches to describing competitive adsorption phenomena.

Further work is also required for the examination of the treatment processes used in this work and their effect on humic substance adsorption. The effects of coagualtion need to be tested further to elucidate those coagulation conditions (such as alum dose) that best improve humic substance adsorbability. Similar work needs to be performed for the ozonation process. In addition, future kinetic

studies need to report values of D_L rather than K_L in order to make valid comparisons between different experiments.

ALGEBRAIC MANIPULATIONS USED TO DERIVE THE IAST MODEL

As noted in Chapter 4, the equilibrium liquid phase
concentration of a given solute i ($C_{i,TOC}$) can be described
as a function of the equilibrium adsorbed phase
concentrations for all components present in the mixture of
interest. In order to achieve this description, several
algebraic manipulations are required to combine Equations
4-1, 4-2, 4-3, 4-4, 4-9, 4-10, and 4-14. These manipulations
are presented below and, for the sake of convenience, the
equations just noted are also presented as follows:

$$1/q_T = \sum_{i=1}^{N} (z_i / q_i^*) \tag{4-1}$$

$$q_T = \sum_{i=1}^{N} (q_i) \tag{4-2}$$

$$z_i = q_i/q_T \qquad\qquad \text{for } i = 1 \text{ to } N \tag{4-3}$$

$$c_i = z_i \cdot c_i^* \qquad\qquad \text{for } i = 1 \text{ to } N \tag{4-4}$$

$$C_{i,TOC}^* = (C_i^*) \cdot (y_i) \cdot (MW_C)$$
$$\qquad\qquad\qquad \text{for } i = 1 \text{ to } N \tag{4-9}$$

156

$$q^*_i = K_{i,TOC} \cdot ((Y_i) \cdot (MW_C))^{(1/n_i - 1)} \cdot (C^*_i)^{1/n_i}$$

$$\text{for } i = 1 \text{ to } N \qquad (4\text{-}10)$$

$$n_1 \cdot q^*_1 = n_k \cdot q^*_k \qquad \text{for } k = 2 \text{ to } N \qquad (4\text{-}14)$$

Now that the appropriate equations have been listed, the manipulation begins by substituting Equation 4-14 into Equation 4-1 to give

$$1/q_T = (n_1 \cdot z_1)/(n_i \cdot q^*_i) = (n_k \cdot z_k)/(n_i \cdot q^*_i)$$

$$\text{for } i = 1 \text{ to } N \text{ and } k = 2 \text{ to } N \qquad (A\text{-}1)$$

By substituting Equation 4-3 into Equation A-1, the following is obtained upon rearrangement:

$$n_i \cdot q^*_i = \sum_{j=1}^{N} (n_j \cdot q_j) \qquad \text{for } i = 1 \text{ to } N \qquad (A\text{-}2)$$

The value of q^*_i is given by the Freundlich equation and, therefore, Equation 4-10 is used in Equation A-2 to yield, upon rearrangement,

$$C^*_i = \{1 / (Y_i \cdot MW_C)\}$$

$$\cdot \{\sum_{j=1}^{N} (n_j \cdot q_j) / [(n_i \cdot K_{i,TOC}) / (Y_i \cdot MW_C)]\}^{n_i}$$

$$\text{for } i = 1 \text{ to } N \qquad (A\text{-}3)$$

157

By substitution of Equation 4-4 into the above equation, one obtains

$$c_i = (z_i / (y_i \cdot MW_C))$$

$$\cdot \{\sum_{j=1}^{N}(n_j \cdot q_j) / [(n_i \cdot K_{i,TOC}) / (y_i \cdot MW_C)]\}^{n_i}$$

$$\text{for } i = 1 \text{ to } N \qquad (A-4)$$

The mole fraction of solute i in the adsorbed phase is removed by substitution of Equation 4-3 to yield

$$c_i = (q_i / (q_T \cdot y_i \cdot MW_C))$$

$$\cdot \{\sum_{j=1}^{N}(n_j \cdot q_j) / [(n_i \cdot K_{i,TOC}) / (y_i \cdot MW_C)]\}^{n_i}$$

$$\text{for } i = 1 \text{ to } N \qquad (A-5)$$

Equation 4-2 is then used to replace q_T in the above expression to give

$$c_i = (q_i / (y_i \cdot MW_C \cdot \sum_{j=1}^{N}q_j))$$

$$\cdot \{\sum_{j=1}^{N}(n_j \cdot q_j) / [(n_i \cdot K_{i,TOC}) / (y_i \cdot MW_C)]\}^{n_i}$$

$$\text{for } i = 1 \text{ to } N \qquad (A-6)$$

Finally, by converting each molar concentration to a TOC concentration (see Equation 4-9), the desired result is obtained:

$$c_{i,TOC} = ((q_{i,TOC} / y_i) / \sum_{j=1}^{N}(q_{j,TOC} / y_j))$$

$$\cdot \left\{ \sum_{j=1}^{N}(n_j \cdot q_{j,TOC} / y_j) / (n_i \cdot K_{i,TOC} / y_i) \right\}^{n_i}$$

for $i = 1$ to N \hspace{2cm} (A-7)

One should note that Equations A-7 and 4-15 are identical and, therefore, the algebraic manipulations are complete.

APPENDIX B

ERROR ANALYSIS OF ISOTHERM DATA

Adsorbed phase concentrations were calculated from the mass balance expression given by Equation 4-21, which is shown here for the sake of convenience:

$$q_{T,TOC} = (C_{0T,TOC} - C_{T,TOC}) \cdot (V/M) \qquad (4\text{-}21)$$

Obviously, $q_{T,TOC}$ depends on several variables that are obtained by methods subject to human and analytical errors. Therefore, the value of $q_{T,TOC}$ is also subject to the errors made in measuring these variables. The standard error of $q_{T,TOC}$ may be found from the following equation:

$$\sigma_q^2 = \{(dq/dC_{0T,TOC})^2 \cdot \sigma_{C0}^2\} + \{(dq/dC_{T,TOC})^2 \cdot \sigma_C^2\}$$
$$+ \{(dq/dV)^2 \cdot \sigma_V^2\} + \{(dq/dM)^2 \cdot \sigma_M^2\} \qquad (B\text{-}1)$$

Equation B-1 shows that confidence in the calculated value of $q_{T,TOC}$ depends on the accuracy of measuring $C_{0T,TOC}$, $C_{T,TOC}$, V, and M.

Expressions can be obtained for the partial derivatives noted in Equation B-1 from Equation 4-21 and are as follows:

$$(dq/dC_{0T,TOC}) = V/M \qquad (B\text{-}2)$$

160

$$(dq/dc_{T,TOC}) = - (V/M) \tag{B-3}$$

$$(dq/dV) = (c_{0T,TOC} - c_{T,TOC}) / M \tag{B-4}$$

$$(dq/dM) = - (c_{0T,TOC} - c_{T,TOC}) \cdot (V/M^2) \tag{B-5}$$

By combining Equations B-1 to B-5, one obtains the following expression for the error propagated by the calculation of $q_{T,TOC}$:

$$
\begin{aligned}
\sigma_q^2 = &(V/M)^2 \cdot (\sigma_{c0}^2 + \sigma_c^2) \\
&+ \left((c_{0T,TOC} - c_{T,TOC}) / M\right)^2 \cdot \sigma_V^2 \\
&+ \left((c_{0T,TOC} - c_{T,TOC}) \cdot (V/M^2)\right)^2 \cdot \sigma_M^2
\end{aligned} \tag{B-6}
$$

Analysis of Equation B-6 shows that the error propagated into the calculation of $q_{T,TOC}$ also depends on the magnitude of the variables. The magnitude of σ_q increases as V/M increases, as $(c_{0T,TOC} - c_{T,TOC})$ increases, and as M decreases. Thus, the value of σ_q may be expected to be large at either end of an isotherm plot and an example plot is shown in Figure B-1, complete with error bars showing the ranges of σ_q and σ_c. This figure shows the isotherm obtained for the 1987 mixture that received an AOD of 2.43 mg O_3/mg TOC and indicates that the value of σ_q depends strongly on the value of M. This dependence is not surprising since the value of M covers a range of four orders of magnitude while the value of $(c_{0T,TOC} - c_{T,TOC})$

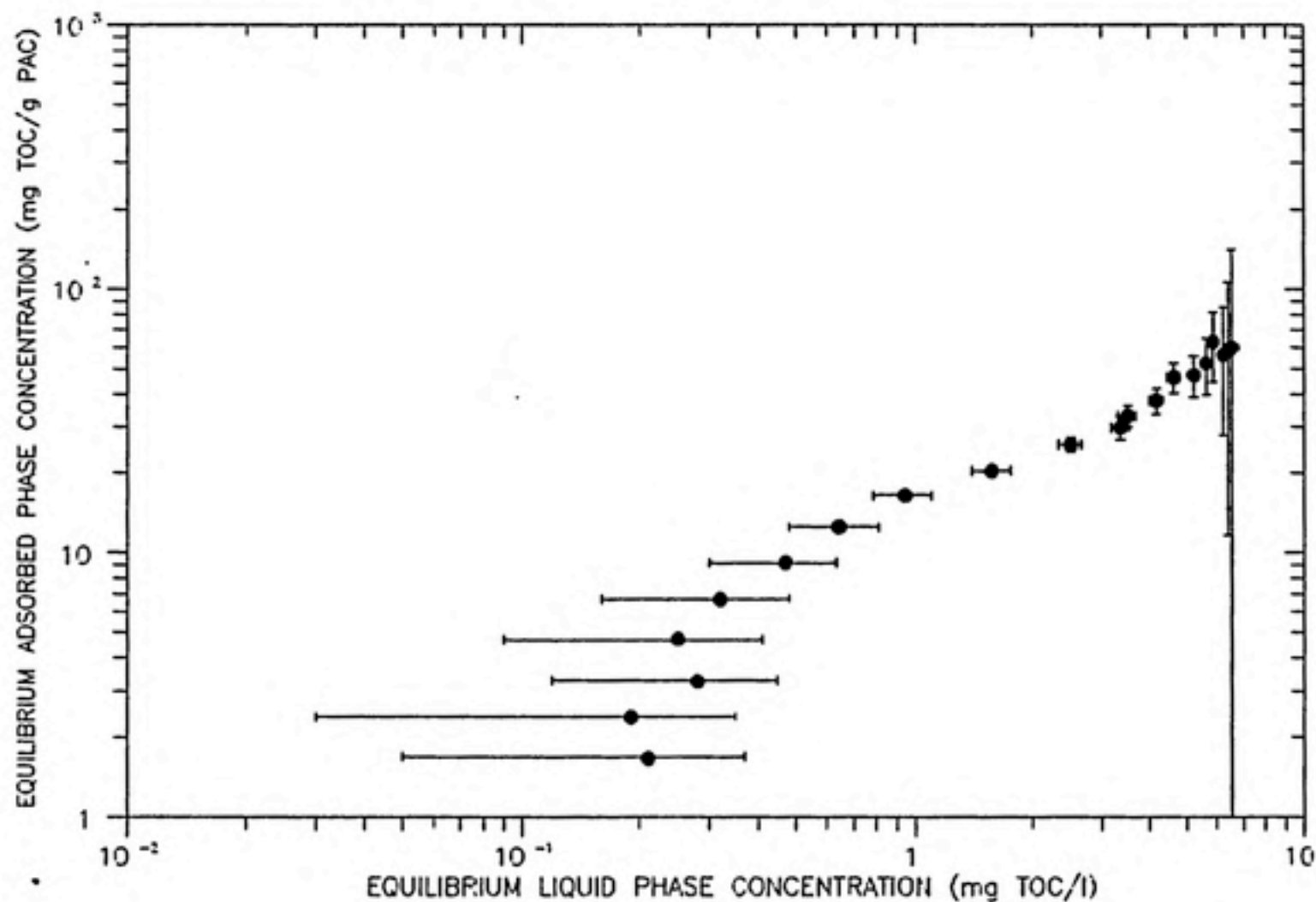FIGURE B-1: ERROR ANALYSIS FOR THE 1987 SAMPLE THAT RECEIVED AN AOD OF 2.43 mg O₃/mg TOC AND BIOSTABILIZATION. THE ERROR BARS REPRESENT A CONFIDENCE INTERVAL ABOUT A GIVEN DATA POINT BASED ON ANALYTICAL ERROR CONSIDERATIONS ONLY.

remains relatively constant. In addition, this dependence implies that very small carbon doses (M/V < 100 mg PAC/l) should be performed in larger bottles to reduce the value of σ_q at those doses.

In order to calculate the value of σ_q, values are required for σ_{C0}, σ_C, σ_V, and σ_M. Each isotherm bottle was filled with 100 ml of solution from a 100 ml pipet that was specified to have a maximum error of $\sigma_V = 0.10$ ml. In addition, weighing the PAC was considered to be associated with a maximum error of $\sigma_M = 1.00$ mg. Finally, the values of σ_{C0} and σ_C were computed from the following expression:

$$\sigma_C^2 = \sigma_S^2 + \sigma_L^2 + \sigma_R^2 \qquad\qquad (B-7)$$

where σ_S is the standard error of several TOC measurements on a given sample, σ_L is the error associated with the assumption of a linear standard curve, and σ_R is the error associated with the ability of the TOC analyzer to replicate the results from day to day operation. One should note that σ_L and σ_R were obtained from manufacturer's specifications and that σ_R differs from σ_S in that σ_S only accounts for error between samples measured on the same calibration curve while σ_R attempts to account for the error associated with the ability to repeat the calibration conditions from day to day. The values of σ_C given by Equation B-7 are equivalent to the values of σ_{Ci} noted in Equation 4-22 and are also plotted on Figure B-1.

REFERENCES

Anderson, L.J., J.D. Johnson, and R.F. Christman, 1986.
"Extent of Ozone's Reaction with Isolated Fulvic Acid,"
Environ. Sci. Technol., 20(7), 739-742.

Atkins, P.W., 1982. Physical Chemistry, W.H. Freeman and
Co., San Francisco, CA.

Babcock, D.B., and P.C. Singer, 1979. "Chlorination and
Coagulation of Humic and Fulvic Acids," J. Am. Water
Works Assoc., 71(3), 149-152.

Bailey, P.S., 1972. "Organic Groupings Reactive Toward
Ozone: Mechanisms in Aqueous Media," in Ozone in Water
and Wastewater Treatment, F.L. Evans, ed., Ann Arbor
Science Publishers, Inc., pp. 29-59.

Benedek, A., J.J. Bancsi, M. Malaiyandi, and E.A. Lancaster,
1979. "The Effect of Ozone on the Biological
Degradation and Activated Carbon Adsorption of Natural
and Synthetic Organics in Water. Part II: Adsorption,"
Ozone Sci. and Eng., 1(4), pp. 347-356.

Cantor, K.P., R. Hoover, P. Hartge, T.J. Mason, D.T.
Silverman, and L.I. Levin, 1985. "Drinking Water Source
and Risk of Bladder Cancer: A Case-Control Study," in
Water Chlorination: Chemistry, Environmental Impact,
and Health Effects, vol. 5, pp. 145-152.

Carter, C.W., and I.H. Suffet, 1982. "Binding of DDT to
Dissolved Humic Materials," Environ. Sci. Technol.,
16(11), pp. 735-740.

Chen, A.S.C., V.L. Snoeyink, and F. Fiessinger, 1987.
"Activated Alumina Adsorption of Dissolved Organic
Compounds before and after Ozonation," Environ. Sci.
Technol., 21(1), pp. 83-90.

Christman, R.F. and G. Ghassemi, 1966. "Chemical Nature of
Organic Color in Water," J. Am. Water Works Assoc.,
58(6), pp. 723-741.

Code of Federal Regulations, Title 40: Protection of
Environment. Part 141: National Primary Drinking Water
Regulations, 1987a.

Code of Federal Regulations, Title 40: Protection of
    Environment. Part 142: National Interim Primary
    Drinking Water Regulations Implementation, 1987b.

Cook, M.B., and D.W. Schnare, 1986. "Amended SDWA Marks New
    Era in the Water Industry," J. Am. Water Works Assoc.,
    78(8), pp. 66-69.

Cornel, P., H. Sontheimer, R.S. Summers, and P.V. Roberts,
    1986a. "Sorption of Dissolved Organics from Aqueous
    Solution by Polystyrene Resins. II: External and
    Internal Mass Transfer," Chem. Eng. Sci., 41(7), pp.
    1801-1810.

Cornel, P.K., R.S. Summers, and P.V. Roberts, 1986b.
    "Diffusion of Humic Acid in Dilute Aqueous Solution,"
    J. Colloid Interface Sci., 110(1), 149-164.

Cragle, D.L., C.M. Shy, R.J. Struba, and E.J. Siff, 1985. "A
    Case-Control Study of Colon Cancer and Water
    Chlorination in North Carolina," in Water Chlorination:
    Chemistry, Environmental Impact, and Health Effects,
    vol. 5, pp. 153-159.

Crittenden, J.C., D.W. Hand, H. Arora, and B.W. Lykins,
    1987a. "Design Considerations for GAC Treatment of
    Organic Chemicals," J. Am. Water Works Assoc., 79(1),
    pp. 74-82.

Crittenden, J.C., P. Luft, and D.W. Hand, 1987b. "Prediction
    of Fixed-Bed Adsorber Removal of Organics in Unknown
    Mixtures," J. Env. Eng., 113(3), pp. 486-498.

Crittenden, J.C., P. Luft, and D.W. Hand, 1985. "Prediction
    of Multicomponent Adsorption Equilibria in Background
    Mixtures of Unknown Composition," Water Res., 19(12),
    pp. 1537-1548.

Crittenden, J.C., and W.J. Weber, 1978. "Predictive Model
    for Design of Fixed-Bed Adsorbers: Parameter Estimation
    and Model Development," J. Env. Eng., vol. 104, pp.
    185-197.

DeWaters, J.E., 1987. "Biological Activity on Granular
    Activated Carbon in the Presence of Ozonated Naturally
    Occurring Humic Substances," Master's Thesis, Univ. of
    North Carolina, Chapel Hill, NC.

DiGiano, F.A., G. Baldauf, B. Frick, and H. Sontheimer,
    1978. "A Simplified Competitive Equilibrium Adsorption
    Model," Chem. Eng. Sci., vol. 33, pp. 1667-1673.

Dragunov, S., 1961. in Soil Organic Matter, M.M. Kononova,
    ed., Pergamon Press, p. 65.

Edzwald, J.K., W.C. Becker, and K.L. Wattier, 1985. "Surrogate Parameters for Monitoring Organic Matter and THM Precursors," J. Amer. Water Works Assoc., 77(4), 122-132.

Fettig, J., 1986. Personal Communication.

Fettig, J., and H. Sontheimer, 1987. "Kinetics of Adsorption on Activated Carbon. III: Natural Organic Material," J. Env. Eng., 113(4), pp. 795-810.

Fleer, G.J., and J. Lyklema, 1983. "Adsorption of Polymers," in Adsorption from Solution at the Solid/Liquid Interface, G.D. Parfitt and C.H. Rochester, eds., pp. 153-220.

Fleischacker, S.J., and S.J. Randtke, 1983. "Formation of Organic Chlorine in Public Water Supplies," J. Am. Water Works Assoc., 75(3), p. 132.

Flogstad, H., and H. Odegaard, 1985. "Treatment of Humic Waters by Ozone," Ozone Sci. and Eng., 7(2), pp. 121-136.

Frick, B.R., and H. Sontheimer, 1983. "Adsorption Equilibria in Multisolute Mixtures of Known and Unknown Composition," in Treatment of Water by Granular Activated Carbon, M.J. McGuire and I.H. Suffet, eds., Amer. Chem. Soc., Washington, D.C., pp. 247-268.

Friedman, G., 1984. "Mathematical Modeling of Multicomponent Adsorption in Batch and Fixed-Bed Reactors," Master's Thesis, Michigan Technological Univ., Houghton, MI.

Ghosh, K., and M. Schnitzer, 1980. "Macromolecular Structures of Humic Substances," Soil Science, 129(5), pp. 266-276.

Glaze, W.H., C.C. Lin, J.C. Crittenden, and R. Cotton, 1986. "Adsorption and Microbiological Mechanisms for Removal of Natural Organics in Granular Activated Carbon Columns," Ozone Sci. and Eng., vol. 8, pp. 299-319.

Glaze, W.H., J.L. Wallace, D. Wilcox, K.R. Johansson, K.L. Dickson, B. Scalf, R. Noack, and A.W. Busch, 1981. "Effects of Ozone on GAC Removal of THM Precursors: A Pilot Study," in Wasser Berlin '81, proceedings of the 5th Int. Ozone Assoc. World Congress, pp. 486-497.

Hoigne, J., and H. Bader, 1979. "Ozonation of Water: Selectivity and Rate of Oxidation of Solutes," Ozone Sci. and Eng., 1(1), pp. 73-85.

Hubele, C., 1984. "Adsorption und biologischer Abbau von Huminstoffen in Activkohlefiltern," Dissertation, Univ. Karlsruhe, Karlsruhe, Fed. Rep. of Germany (in German).

Jodellah, A.M.M., 1985. "Removal of Humic Substances and THM Precursors by Activated Carbon: Effects of Heterogeneity, Chemical Pretreatment, and System Characteristics," Ph.D. Dissertation, Univ. of Michigan, Ann Arbor, MI.

Johnson, D.E., and S.J. Randtke, 1983. "Removing Nonvolatile Organic Chlorine and its Precursors by Coagulation and Softening," J. Am. Water Works Assoc., 75(5), pp. 249-253.

Kaastrup, E., 1985. "Activated Carbon Adsorption of Humic Substances and the Influence of Preozonation on Such," Dr. Ing. Dissertation, Univ. of Trondheim, Norwegian Inst. of Technol., Trondheim, Norway.

Kidnay, A.J., and A.L. Myers, 1966. "A Simplified Method for the Prediction of Multicomponent Adsorption Equilibria from Single Gas Isotherms," AIChE J., 12(5), pp. 981-986.

Lee, M.C., 1980. "Humic Substances Removal by Activated Carbon," Ph.D. Dissertation, Univ. of Illinois, Champaign-Urbana, IL.

Lee, M.C., J.C. Crittenden, V.L. Snoeyink, and M. Ari, 1983. "Design of Carbon Beds to Remove Humic Substances," J. Env. Eng., 109(3), pp. 631-645.

Lee, M.C., V.L. Snoeyink, and J.C. Crittenden, 1981. "Activated Carbon Adsorption of Humic Substances," J. Am. Water Works Assoc., 73(8), pp. 440-446.

Liao, W., R.F. Christman, J.D. Johnson, and D.S. Millington, 1982. "Structural Characterization of Aquatic Organic Material," Environ. Sci. Technol., 16(7), 403-410.

Lienhard, H., and H. Sontheimer, 1979. "Influence of Process Conditions on the Effect of Ozone Treatment of Organic Substances in the Water," Ozone Sci. and Eng., 1(4), pp. 61-72.

Maloney, S.W., I.H. Suffet, K. Bancroft, and H.M. Neukrug, 1985. "Ozone-GAC Following Conventional U.S. Drinking Water Treatment," J. Am. Water Works Assoc., 77(8), pp. 66-73.

Manos, G.P., and C. Tsai, 1980. "Mechanisms of Humic Material Adsorption on Kaolin Clay and Activated Carbon," _Water, Air, and Soil Poll._, vol. 14, pp. 419-427.

Mantoura, R.F.C., and J.P. Riley, 1975. "The Analytical Concentration of Humic Substances from Natural Waters," _Analytica Chimica Acta_, 76(1), pp. 97-106.

Mattson, J.S., and H.B. Mark, 1971. _Activated Carbon: Surface Chemistry and Adsorption from Solution_, Marcel Dekker, Inc., New York, NY.

McCreary, J.J., and V.L. Snoeyink, 1980. "Characterization and Activated Carbon Adsorption of Several Humic Substances," _Water Res._, vol. 14, pp. 151-160.

Myers, A.L., and J.M. Prausnitz, 1965. "Thermodynamics of Mixed-Gas Adsorption," _AIChE J._, 11(1), pp. 121-127.

Narkis, N., and M. Rebhun, 1977. "Stoichiometric Relationship Between Humic and Fulvic Acids and Flocculants," _J. Amer. Water Works Assoc._, 69(6), 325-328.

Neukrug, H.M., M.G. Smith, S.W. Maloney, and I.H. Suffet, 1984. "Biological Activated Carbon - At What Cost?" _J. Am. Water Works Assoc._, 76(4), pp. 158-167.

Norwood, D.L., J.D. Johnson, R.F. Christman, and D.S. Millington, 1981. "Chlorination Products from Aquatic Humic Material at Neutral pH," in _Water Chlorination: Environmental Impact and Health Effects_, vol. 4, no. 1, pp. 191-200.

Prakash, A., and D.J. MacGregor, 1983. "Environmental and Human Health Significance of Humic Materials: An Overview," in _Aquatic and Terrestrial Humic Materials_, R.F. Christman and E.T. Gjessing, eds., Ann Arbor Science Publishers, Ann Arbor, MI, pp. 481-494.

Radke, C.J., and J.M. Prausnitz, 1972. "Thermodynamics of Multi-Solute Adsorption from Dilute Liquid Solutions," _AIChE J._, 18(4), pp. 761-768.

Randtke, S.J., and C.P. Jepsen, 1981. "Chemical Pretreatment for Activated-Carbon Adsorption," _J. Amer. Water Works Assoc._, 73(8), 411-419.

Randtke, S.J., and C.P. Jepsen, 1982. "Effects of Salts on Activated Carbon Adsorption of Fulvic Acids," _J. Am. Water Works Assoc._, 74(2), pp. 84-93.

Randtke, S.J., and V.L. Snoeyink, 1983. "Evaluating GAC Adsorptive Capacity," J. Amer. Water Works Assoc., 75(8), 406-413.

Roberts, P.V., P. Cornel, and R.S. Summers, 1985. "External Mass-Transfer Rates in Fixed-Bed Adsorption," J. Env. Eng., 111(6), 891-905.

Rook, J.J., 1974. "Formation of Haloforms During Chlorination of Natural Waters," J. Water Trtmnt. Exam., 23(2), pp. 234-243.

Semmens, M.J., and T.K. Field, 1980. "Coagulation Experiences in Organics Removal," J. Amer. Water Works Assoc., 72(8), 476-483.

Semmens, M.J., A.B. Staples, G. Hohenstein, and G.E. Norgaard, 1986. "Influence of Coagulation on Removal of Organics by Granular Activated Carbon," J. Am. Water Works Assoc., 78(8), pp. 80-84.

Sierka, R.A., and G.L. Amy, 1985. "Catalytic Effects of Ultraviolet Light and/or Ultrasound on the Ozone Oxidation of Humic Acid and Trihalomethane Precursors," Ozone Sci. and Eng., 7(1), 47-62.

Singer, P.C., J.J. Barry, G.M. Palen, and A.E. Scrivner, 1981. "Trihalomethane Formation in North Carolina Drinking Waters," J. Amer. Water Works Assoc., 73(8), 392-401.

Smisek, M., and S. Cerny, 1970. Active Carbon: Manufacture, Properties, and Applications, Elsevier Publishing Co., Amsterdam, The Netherlands.

Somiya, I., H. Yamada, E. Nozawa, and M. Mohri, 1986. "Biodegradability and GAC Adsorbability of Micropollutants by Preozonation," Ozone Sci. and Eng., 8(1), 11-26.

Sontheimer, H., B.R. Frick, J. Fettig, G. Hörner, C. Hubele, and G. Zimmer, 1985. Adsorptionsverfahren zur Wassereinigung, Engler-Bunte-Inst. der Univ. Karlsruhe, Karlsruhe, Fed. Rep. of Germany (in German).

Standard Methods for the Examination of Water and Wastewater, 1975. Amer. Water Works Assoc., Water Poll. Control Fed., and Amer. Public Health Assoc., eds.

Steinberg, C., and U. Muenster, 1985. "Geochemistry and Ecological Role of Humic Substances in Lakewater," in Humic Substances in Soil, Sediment, and Water, G.R. Aiken, D.M. McKnight, R.L. Wershaw, and P. MacCarthy, eds., pp. 105-146.

Stephenson, P., A. Benedek, M. Malaiyandi, and E.A. Lancaster, 1979. "The Effect of Ozone on the Biological Degradation and Activated Carbon Adsorption of Natural and Synthetic Organics in Water. Part I: Ozonation and Biodegradation," Ozone Sci. and Eng., 1(3), 263-279.

Summers, R.S., 1986. "Activated Carbon Adsorption of Humic Substances: Effect of Molecular Size and Heterodispersity," Ph.D. Dissertation, Stanford Univ., Stanford, CA.

Symons, J.M., T.A. Bellar, J.K. Carswell, J. DeMarco, K.L. Kropp, G.G. Robeck, D.R. Seeger, C.J. Slocum, B.L. Smith, and A.A. Stevens, 1975. "National Organics Reconnaissance Survey for Halogenated Organics," J. Am. Water Works Assoc., 67(11), pp. 634-647.

Tardiff, R.G., 1977. "Health Effects of Organics: Risk and Hazard Assessment of Ingested Chloroform," J. Am. Water Works Assoc., 69(12), pp. 658-661.

Trussell, R.R., and M.D. Umphres, 1978. "The Formation of Trihalomethanes," J. Am. Water Works Assoc., 70(11), pp. 604-612.

van Breeman, A.N., T.J. Nieuwstad, G.C. van der Meent-Olieman, 1979. "The Fate of Fulvic Acids During Water Treatment," Water Res., vol. 13, pp. 771-779.

Wang, C.K., 1986. "Dynamic Modeling of Fixed-Bed Adsorbers Using a Micro-Adsorbent-Diameter-Depth (MADD) System," Ph.D. Dissertation, Univ. of Michigan, Ann Arbor, MI.

Weber, W.J., T.C. Voice, and A. Jodellah, 1983. "Adsorption of Humic Substances: The Effects of Heterogeneity and System Characteristics," J. Amer. Water Works Assoc., 75(12), 612-619.

Werdehoff, K.S., 1986. "Effects of Chlorine Dioxide on THM and TOX Formation Potentials and on the Formation of Inorganic By-Products," Master's Thesis, Univ. of North Carolina, Chapel Hill, NC.

Wilke, C.R., and P. Chang, 1955. "Correlation of Diffusion Coefficients in Dilute Solutions," AIChE J., vol. 1, pp. 264-270.

Yamada, H., I. Somiya, and F. Inanami, 1986. "The Effect of Preozonation on the Control of Trihalomethane Formation," Ozone Sci. and Eng., 8(2), pp. 129-150.

Zabel, T.F., 1985. "The Application of Ozone for Water Treatment in the United Kingdom - Current Practice and Recent Research," Ozone Sci. and Eng., 7(1), pp. 11-30.